

THE ENTROPY OF DELTA - CODED SPEECH

by

Bruce Gillies Taylor

Thesis presented for the Degree of Doctor of
Philosophy of the University of Edinburgh in
the Faculty of Science.

May, 1968



Abstract

This thesis presents a study of the information properties of delta-coded speech and a derivation and evaluation of applications of the results to channel encoding and signal detection problems.

First, a signal analysis of the coding technique is given, and performance characteristics are presented for a message approximant of realistic power spectral density.

A speech processing facility based on SC247 analogue and PDP-8 digital computers is then described, and details are given of the software for transition probability matrix assembly and the hardware for message time-scaling and DM^{\dagger} interfacing. The results of computations of the entropy of Markov process approximations to the source of order 1 - 9 are detailed, and the redundancy is found to be typically about one half.

Linear prediction of the source sequence by Wiener estimation is considered, and a predictor success probability of 0.72 is found to be typical, while optimal group codes for block lengths 2 - 6 are determined and evaluated for comparison with predictive coding. The optimal non-linear predictor structures for orders 1 - 7 are established, and the entropies of the sequences generated by modulo-2 addition of the predictions and source elements are computed and found to be

[†] Delta Modulation

much closer to the process entropies than the corresponding performance characteristics for group encoding.

The form of a practical near-optimal 6th order predictive coder is treated in detail, and a TTL^{*} prototype which attains a typical success probability of 0.9 is described.

Encoding of the predictor error sequence to achieve bandwidth reduction is then considered, and 5 element group encoding, attaining a compression factor of 0.48, is found to be superior to run-length encodings. The combination IP[†] transformation achieves this compression with very considerably less hardware complexity than is required for equivalent performance by direct exact coding of blocks of source elements.

To determine the channel buffer requirements for transmission at uniform data rate, the statistical properties are analysed by an application of queueing theory, and a capacity of 270 words is shown to be sufficient for a 2 to 1 bandwidth compression.

Finally, it is shown that the redundancy of the message source can alternatively be exploited at a DM receiver, and a typical 40% error probability reduction is found to result from an easily implemented application of non-linear prediction to optimisation of the signal detection process.

* Transistor - Transistor Logic

† Information - Preserving

Table of contents

<u>Abstract</u>	ii
<u>List of figures</u>	vii
<u>List of symbols</u>	ix
<u>Chapter 1</u> <u>Introduction</u>	1
<u>Chapter 2</u> <u>Signal analysis</u>	10
2.1 Message power spectral density	10
2.2 Information rate	13
2.3 Message autocorrelation	15
2.4 Quantisation noise	17
2.5 Message derivative	22
<u>Chapter 3</u> <u>Delta - coded speech processor</u>	25
3.1 FM system	25
3.2 Analogue filter	26
3.3 Delta - coder	28
3.4 Computer interface	30
<u>Chapter 4</u> <u>Linear prediction</u>	37
4.1 Entropy	37
4.2 Predictive coding	38
4.3 Estimator function	41
4.4 Estimator error	45
4.5 Implementation	49

<u>Chapter 5</u>	<u>Relative entropy</u>	54
5.1	Transition matrix assembly	54
5.2	Markov process entropy	56
5.3	Parameter variation	57
5.4	Transform sequence entropy	59
<u>Chapter 6</u>	<u>Group encoding</u>	64
6.1	Group entropy	64
6.2	Optimal group codes	65
6.3	Code evaluation	67
<u>Chapter 7</u>	<u>Non-linear prediction</u>	72
7.1	Predictor function	72
7.2	Processor form	75
7.3	IC predictive coder	76
7.4	Data errors	78
<u>Chapter 8</u>	<u>Error sequence encoding</u>	82
8.1	Direct error transmission	82
8.2	Error sequence entropy	84
8.3	Run-length encodings	85
8.4	Group error encoding	90
<u>Chapter 9</u>	<u>Channel buffer</u>	96
9.1	Queue organisation	96
9.2	Codeword length distributions	98
9.3	Buffer capacity	101

<u>Chapter 10</u>	<u>DM signal detection</u>	105
10.1	Optimal receiver structure	106
10.2	Decision boundary loci	107
10.3	Error rates	111
<u>Chapter 11</u>	<u>Conclusion</u>	118
11.1	Transmitter applications	118
11.2	Receiver applications	119
11.3	Further work	120
<u>Appendices</u>	1 Message power spectral density	121
	2 Analogue filter	122
	3 Transition probability matrix assembler	124
	4 4th order matrix for DM speech	138
<u>Acknowledgements</u>		139
<u>References</u>		140

List of figures

Fig.	1.1	Delta modulation	4
	1.2	Channel encoding	7
Fig.	2.1	Message and quantisation noise spectra	12
	2.2	Information rate	14
	2.3	Message autocorrelation	16
	2.4	Quantiser characteristic	18
	2.5	Characteristic shift function	20
	2.6	Quantisation noise autocorrelation	23
	2.7	Sampling frequency	27
Fig.	3.1	FM speech demodulator	29
	3.2	Precision deltamodulator	31
	3.3	Analogue interface	33
	3.4	MB register interface, data error control	34
	3.5	MA register interface, data transfer control	36
	3.6	SC247 and PDP-8 computers	40
	3.7	Delta - coded speech interface	46
Fig.	4.1	DM predictive coding	48
	4.2	Optimal weighting functions	50
	4.3	Linear prediction success probability	
	4.4	Relative estimator error	

Fig. 5.1	Relative entropy characteristics	58
5.2	Process entropy for constant overload probability	60
5.3	Predictive coding sequence entropy (zero order)	62
Table 5.4	Optimal predictors for delta-coded speech	63
Fig. 6.1	Delta-coded speech entropies	66
6.2	State subset tree	68
Table 6.3	Optimal codebooks for delta-coded speech	70, 71
Fig. 7.1	N = 6 predictor Karnaugh map	74
7.2	Predictive coder configuration	77
7.3	TTL encoder for DM speech	79
7.4	N = 6 predictor error performance	81
Fig. 8.1	Error sequence entropies	86
8.2	Run-length distributions	88
Table 8.3	Run-length codebook	91
8.4	Optimal error sequence codebooks	93, 94
Fig. 9.1	Codeword length distributions	99
9.2	Average queue length	102
9.3	Channel buffer characteristic	104
Fig. 10.1	Optimal receiver structure	108
10.2	Signal probability density distributions	110
10.3	Decision boundary loci	112
10.4	Detector bias characteristics	114
10.5	Error probabilities	114
Fig. A2.1	Analogue message filter	123

List of symbols

Principal symbols in order of use.

$m(t)$	- Message waveform
$\Phi(\omega)$	- Power spectral density
Δ	- DM increment
f_s	- Sampling frequency
R	- Information rate
$\phi(\tau)$	- Auto- or cross-correlation function
q	- Quantiser interval
$E[\]$	- Expected value of variant
$n(t)$	- Noise waveform
S_i	- Source state vector
N	- Markov process order
H	- Process entropy
B_i	- Element block
G_N	- Group entropy
F_N	- Conditional entropy
T	- Transformed element
S	- Source element
E	- Predictor element
P_s	- Predictor success probability
H_T	- Mod - 2 adder sequence entropy
η	- Transmitter power saving

$E(s)$	- Estimator transfer function
$e(t)$	- Estimator impulse response
$m_i(t)$	- DM echelon signal
$w(\tau)$	- Optimal weighting function
λ	- Signal generation time
$\epsilon(t)$	- Error waveform
σ_e	- Rms estimator error
$m_e(t)$	- Estimate of message
$f(\tau)$	- Integral weighting function
N_i	- Codeword length
R_B	- Group encoder compression factor
R_M	- Upper bound for group encoding
P_b	- Element error probability
TH_T	- Error sequence mod-2 adder output entropy
r	- Run-length
P_{gr}	- Geometric distribution run-length probability
H_g	- Geometric distribution entropy
L_g	- Geometric distribution sequence length
H_{gr}	- Geometric distribution relative entropy
P_r	- Run probability
H_r	- Relative entropy for run-length encoding
TG_N	- Error sequence group entropy
TR_M	- Upper bound for error sequence group encoding
TH	- Error sequence entropy
TR_B	- Error sequence group encoding compression factor
N_c	- 5 element error sequence group encoding word length

N_m	- Number of sources multiplexed
N_q	- Buffer capacity
f_c	- Channel data rate per source
N_a	- Average codeword length
N_b	- Average queue length
P_{ov}	- Buffer overflow probability
Θ_i	- Signal transmitted for symbol i
$\Lambda(x)$	- Likelihood ratio
K	- Decision threshold
ρ	- Signal cross-correlation coefficient
x_c	- Correlator output
b	- Detector bias level
δ	- Rms noise level
M	- Mean signal power
x_d	- Decision boundary
α, β	- Component error probabilities
P_{Tf}	- Fixed bias error probability
P_{Tv}	- Variable bias error probability
x_n	- Envelope detector output
x_{dn}	- Decision boundary for noncoherent signalling
T	- Transition probability matrix

Chapter 1

Introduction

With the continuing expansion of world demand for interpersonal telecommunications facilities at a rate more than twice that of world population - and that is a growth described by demographers as an explosion - research activity is profitably directed to the development of improved ways of encoding messages, new methods of signalling the codes, new media for transmission of the signals, and new schemes for the detection and processing of the received information. In the field of circuit technology, the progress of the microelectronic era is altering profoundly the results of cost-effectiveness evaluations of complex digital signal processing systems, and motivates the further application of information theoretic principles to the study of specific message generating and transmitting situations in order to exploit these advances to augment the effective communications capability of existing links and ensure efficient utilisation of those envisaged.

Today, most speech communication traffic is transmitted by channels carrying signals which are frequency-division-multiplexed analogue transforms of the source messages, generated from them by the application of filtering for bandwidth restriction and frequency translation to spectrally adjacent

locations in the passband of the channel. But for several reasons it may be expected that in future an increasing proportion of this traffic will be transmitted by digital signals. First, a very rapid growth in the volume of machine-originated data communication is envisaged as a result of developments in computer science which allow multiple-access to large processors by many dispersed users, and it is economically unattractive to provide separate channel facilities for digital and analogue signals. Second, the switching process by which a channel is routed involves discrete signal processing, and hence can be conveniently integrated with the message signals if both are digital in form. Also, the conversion of many existing communications circuits to digital signal operation results in valuable increases in channel capacity, because proper decoding of these signals is less disturbed by the high attenuation and distortion which previously restricted the usable circuit bandwidth. Further, when applied to long multi-stage speech circuits, digital techniques result in improved and consistent transmission quality because with the use of regeneration at intermediate repeaters the effects of noise are not cumulative. Finally, in military applications, it is known that the encyphering of speech messages to preserve secrecy is most readily and effectively accomplished when the messages are in digital coded form.

Delta modulation (DM) is an analogue - digital conversion

scheme, with properties particularly appropriate to speech message encoding, first described by Libois⁽¹⁾ and since studied extensively in theory and practice in basic and variant forms*. The principle of DM is illustrated in Fig. 1.1.

In the encoder, the analogue message waveform $m(t)$ is compared continuously with the output of an integrator connected to the channel line. The error signal amplitude is hard limited by a non-linear network, and the output of this clipper is sampled periodically to generate a train of positive and negative impulses for transmission. At the decoder, the impulse train is integrated as by the local integrator in the encoder, and the resultant echelon approximation to $m(t)$ is then filtered to remove noise outside the spectrum of the message. Since in practice the channel signals are not impulses but have finite amplitude and duration, the encoder incorporates delaying gates or a master-slave flip flop at the output of the comparator in order that changes in error signal polarity during their transmission are inhibited.

As a delta-coder is logically simple, and does not require a precision divider network, nor a reference voltage supply, it can be readily realized by present techniques as a single-chip low-cost integrated microcircuit and is therefore an attractive solution to the source encoder problem in a digital speech communications network. Because the scheme is

*For a comprehensive bibliography, see Reference (2).

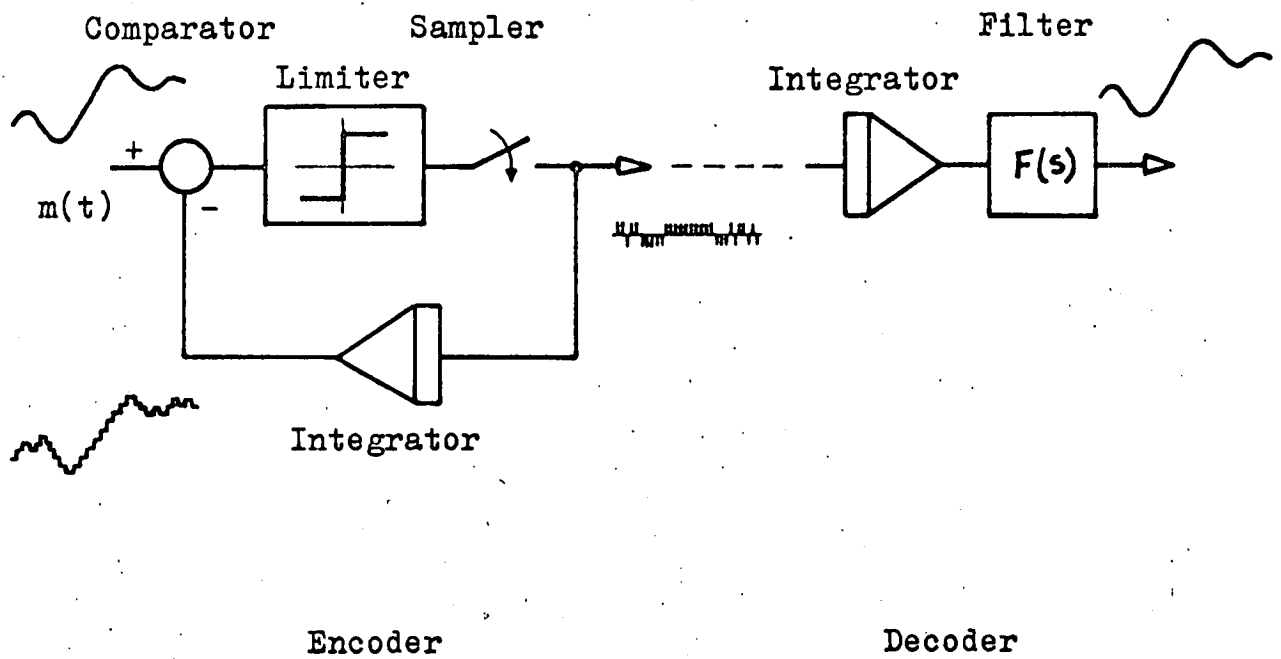


Fig. 1.1 Delta modulation

essentially a single-bit form of differential pulse code modulation (PCM), no word synchronisation is required between senders and receivers connected to the network, a feature which results in a valuable hardware simplification at multiplexing nodes and terminals.

It is known^{(3),(4)} that for applications in which the required quality of speech transmission is not high, DM is a relatively efficient encoding scheme in the sense that the channel bit rate required is lower than that necessary for the same transmitted speech quality by other systems such as conventional PCM*. Where the speech quality required is high, however, the channel bit rate in the case of DM is greater, so that in this case if channel capacity is at a premium a requirement for more complex coding is indicated. Now the anticipated properties of the promising new media for overland channels provide inexpensive broad but dispersive bandwidths appropriate to the transmission of time-division-multiplexed digital signals. The channel bandwidth of an overmoded circular waveguide under development, for example, is 35 GHz, while the inherent capacity of a single laser beam exceeds that required for the total of present day telephone, radio and television world communications. Interest in DM for source encoding therefore parallels progress in the development of

* Conventional PCM refers to a system of ADC whereby the message is bandlimited, then sampled at the Nyquist rate and the sample amplitudes are quantised and encoded as groups of binary digits.

these media.

But in typical communications situations it is necessary to integrate with the network circuits of a kind such that either the medium itself is expensive, as with submarine telephony, or the terminal facilities, as in troposcatter links, and intermediate hardware, as in satellite relays, are much more costly than average. Since the traffic volume carried by these links is only a small proportion of the total originated, it is economically inappropriate to equip every message source with a complex encoder whose greater efficiency is justified only during infrequent communication events involving high-cost channel capacity.

This problem can be solved in the manner shown in Fig. 1.2 if it is possible to provide, as part of the terminal equipment which processes signals for transmission over expensive major links, channel encoders which perform an information-preserving (IP) transformation* on incoming digital signals from source encoders. The output transform sequences, from which the original signals can be reconstructed by an inverse operation in the channel decoders, are generated at a lower bit rate and hence utilize the available channel capacity more efficiently. In conventional analogue telephony practice, the concept of employing special coding to achieve more efficient circuit

* IP transformations are such that the entropies of the operand sequence and its transform are the same. This is sometimes called 'exact coding'.

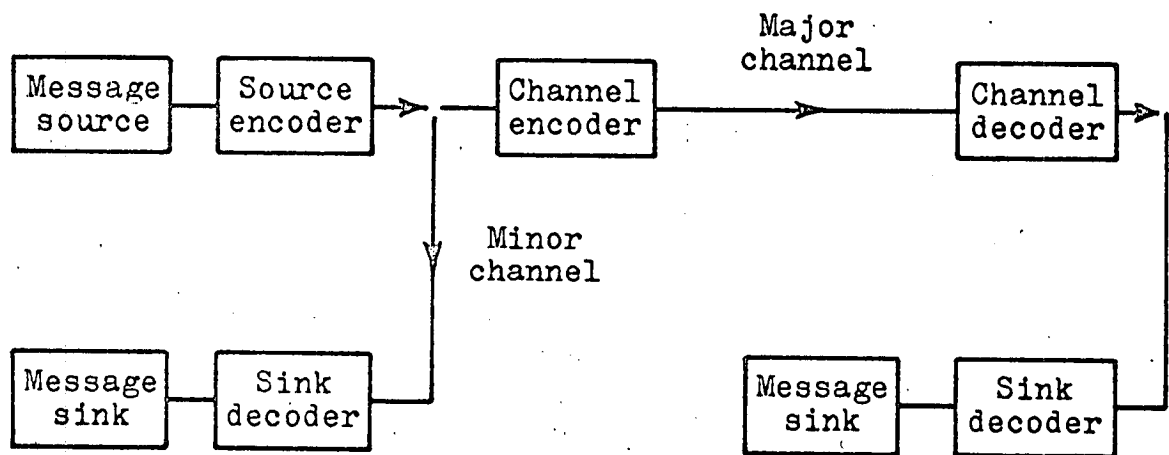


Fig. 1.2 Channel encoding

utilisation is well known and is applied extensively at the terminals of major channels. Such schemes are primarily of the TASI^{*(5)} generic type which exploit individual source inactivity, because the application of transformations to active channels in the analogue case suffers the limitation that since in general the operations are not IP they incur an irrevocable degradation in fidelity, and this must be held to a level which is perceptually tolerable. The magnitude of the bandwidth compression attainable by IP transformation in a digital speech communication system is determined by the extent to which the source encoder sequences exhibit redundancy as a result of the nature of the encoding scheme and constraints on the properties of the message generating process.

This thesis presents a new study of the information properties of delta-coded speech with a derivation and evaluation of signal processing procedures which may be exploited in channel encoders to effect redundancy removal for the reduction of the channel capacity required for transmission. Coding systems for reducing the entropy of the distribution of the average signal element in the sequence generated by DM are described, and compared with computations of the relative entropy of the message generating process for orders up to 9. Linear prediction using Wiener estimation, and non-linear

*TASI is an acronym. Time assignment speech interpolation.

prediction by optimal and practically convenient sub-optimal functions, is presented. Optimal group encoder structures are determined, and their performance compared with that of the predictive coding procedures. The compression of the transformed signal sequences generated by modulo-2 addition of the predictor outputs and source messages by run-length codings and group encoding is studied, and the effect on system performance of errors due to channel noise is determined. The buffer capacity required to allow transmission of the variable length code at a uniform data rate is then examined and operating characteristics are derived. Finally, the related problem of exploiting the redundancy of the source sequences at a DM receiver is treated, and a further application of non-linear prediction to optimise the signal detection process is presented.

Chapter 2

Signal analysis

The study of a continuous message generating process, and of connected information coding and transmission systems, involves a marriage of two major areas of statistical communication theory. There is first the field explored by Wiener⁽⁶⁾ in his work on the spectral analysis of random processes and the theory of optimal filtering of signals and noise. In this approach, which is applied here to the problems of message analysis, linear estimation and signal/detection, integral transform techniques are used extensively and primary manipulations are developed in the frequency domain. Complementing Wiener's correlation methods is the body of knowledge originated by Shannon⁽⁷⁾ which deals quantitatively with the concept of information production and transmission rather than the analysis of the signals by which it is accomplished, and it is on this work that the major contributions of this thesis, the analyses of the relative entropies of delta-coded speech and redundancy-removing encoding systems, are based.

2.1 Message power spectral density

A non-deterministic approach to the signal analysis of DM speech commences with the selection of a rational function approximation $\hat{\Phi}_{mm}(\omega)$ to the power spectral density of the exciting

speech message. For conversational speech, Dunn and White⁽⁸⁾ have reported power spectral density measurements which indicate a maximum at 300 - 450 Hz and a fall of about 6 dB/octave over the following decade, while bandpass filtering is employed in communication practice to achieve concentration of the power in the range 300 - 3000 Hz as this results in improved intelligibility at the expense of an acceptable loss of naturalness. Since DM slope overload occurs when $|m'(t)| > \Delta \cdot f_s$, the inverse square power spectrum contributes to the relative efficacy of the scheme for encoding speech, the transmitted power[†] for a given overload probability being greatest for a message with this spectral characteristic.

Tschebycheff polynomials may be employed to derive for the system function

$$H(s) = \frac{k s^6}{\prod_{i=1}^7 (s^2 + 2\delta_i s + r_i^2)} \quad (2.1.1)$$

a pole distribution which results in a denominator real coefficient set (Appendix 1) for

$$\Phi_{mm}(\omega) = \frac{k^2 \omega^{12}}{\sum_{i=0}^{12} A_{2i} \omega^{2i}} = |H(j\omega)|^2 \quad (2.1.2)$$

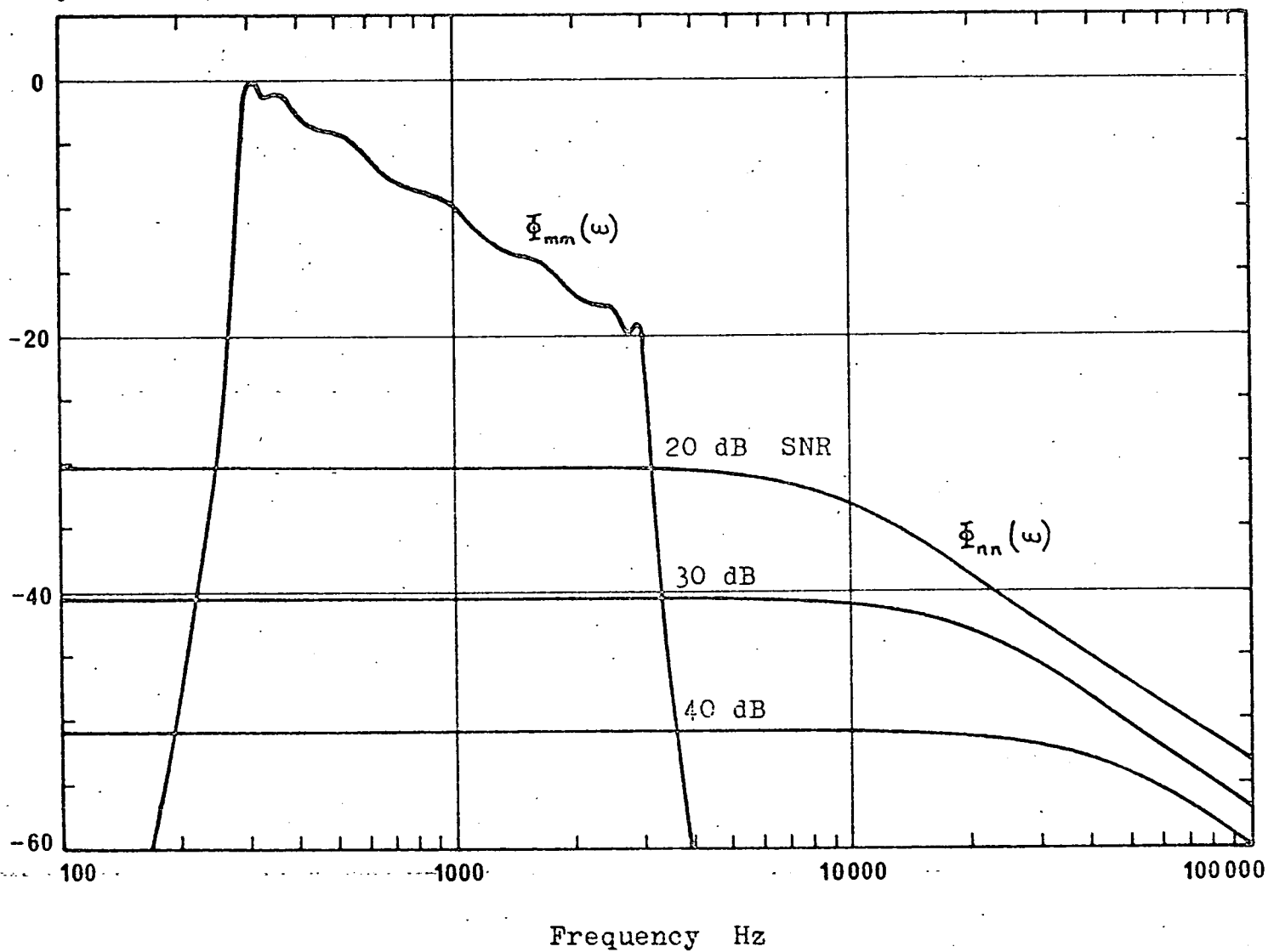
such that the function is a 1 dB equi-ripple approximant in the message band and has rapid cut-off at upper and lower band limits, while k^2 is computed such that the message power

$\overline{m^2(t)} = \int_{-\infty}^{\infty} \Phi_{mm}(\omega) d\omega = 1$. The power spectral density is shown in Fig. 2.1.

[†] i.e. the reproduced message power at a decoder.

Normalised
Power spectral
density dB

Fig. 2.1 Message and quantisation noise spectra



2.2 Information rate

Shannon⁽⁹⁾ has demonstrated that a message with Gaussian amplitude probability distribution has higher entropy than those generated by other processes of the same power. Hence by considering excitation by a stationary Gaussian message an upper bound for the information transmission rate capability of DM for the derived $\Phi_{mm}(\omega)$ may be found. For if the power spectral density of the error due to coding is $\Phi_{nn}(\omega)$, the information rate⁽¹⁰⁾

$$R = \frac{1}{2\pi} \int_0^\infty \log \frac{\Phi_{mm}(\omega)}{\Phi_{ss}(\omega)} d\omega \quad (2.2.1)$$

$$\text{where } \Phi_{ss}(\omega) = \begin{cases} \Phi_{nn}(\omega) & \text{for } \Phi_{nn}(\omega) \leq \Phi_{mm}(\omega) \\ \Phi_{mm}(\omega) & \Phi_{nn}(\omega) > \Phi_{mm}(\omega) \end{cases}$$

Because the contribution to the information rate of spectral components of the message power outside the region $\Phi_{nn}(\omega) \leq \Phi_{mm}(\omega)$ is precisely zero, the boundaries ω_1, ω_2 of this region will be termed the information band limits, and the signal-to-noise ratio is defined as the ratio of total message power to total noise power in the information band

$$\text{SNR} = \frac{\int_{\omega_1}^{\omega_2} \Phi_{mm}(\omega) d\omega}{\int_{\omega_1}^{\omega_2} \Phi_{nn}(\omega) d\omega} \quad (2.2.2)$$

It will later be shown that the power spectrum of the quantisation noise introduced by delta-coding the message is flat within 0.3 dB over the information band for an SNR of

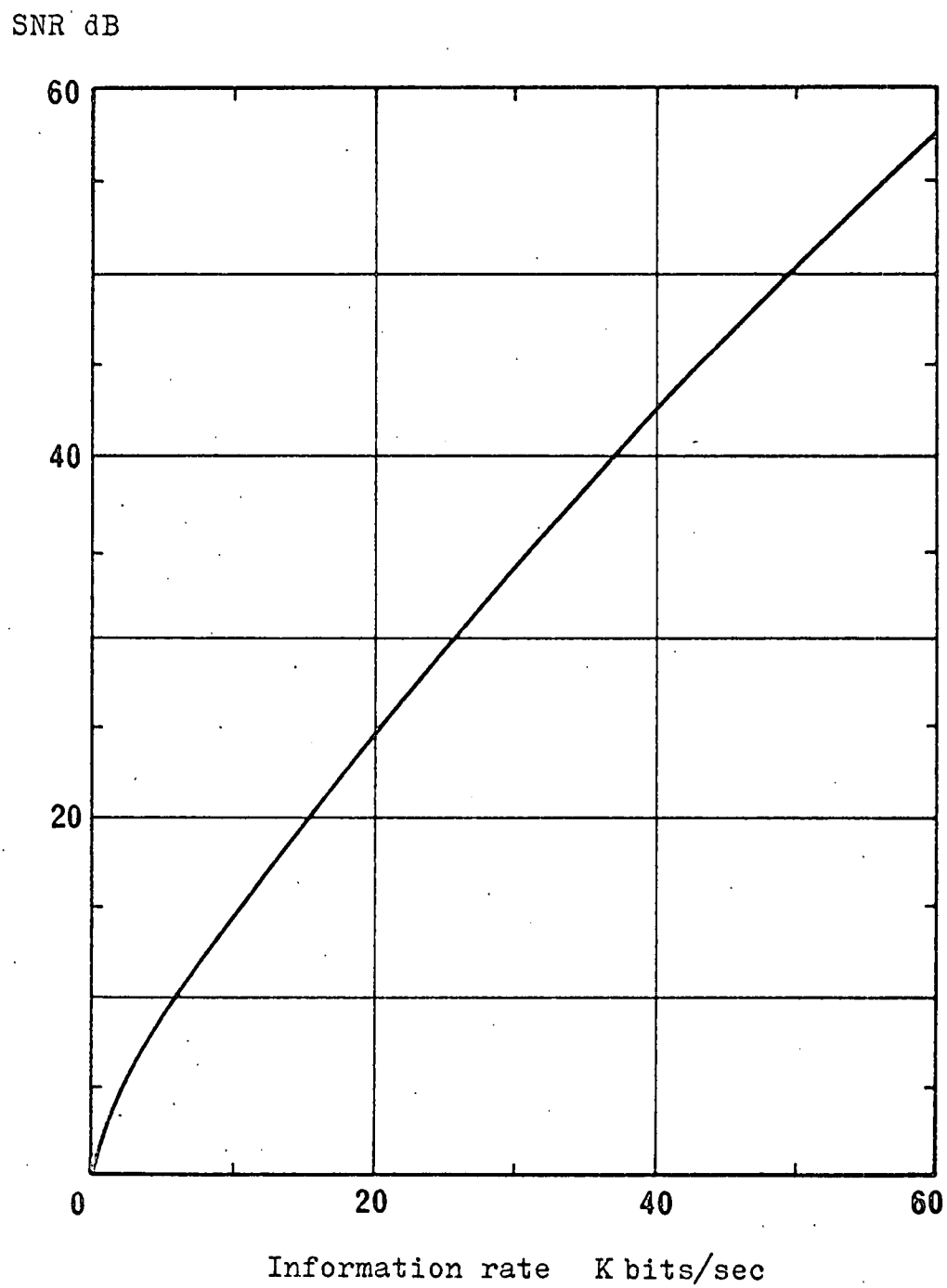


Fig. 2.2 Information rate

20 dB, and more nearly uniform for higher SNR, so that a white noise approximation may be taken. At an SNR of 20 dB, less than 0.05% of the message power lies outside the information band. It then becomes convenient to iteratively adjust ω_1 and ω_2 to determine Φ_{nn} for a range of SNR and evaluate the corresponding information rates, shown in Fig. 2.2. This establishes the theoretical minimum channel bit rate required for the transmission of the message with a given SNR if the coding efficiency were 100%, and allows the appraisal of possible improvements in known practical systems for which the actual channel bit rates necessary are significantly greater.

2.3 Message autocorrelation

Computation by inverse Fourier transformation of the message autocorrelation function

$$\begin{aligned}\phi_{mm}(\tau) &= \frac{1}{2\pi} \int_{-\infty}^{\infty} \Phi_{mm}(\omega) e^{j\omega\tau} d\omega \\ &= \frac{1}{\pi} \int_0^{\infty} \frac{k^2 \omega^{12}}{\sum_{i=0}^{14} A_{2i} \omega^{2i}} \cos \omega\tau d\omega\end{aligned}\quad (2.3.1)$$

is fundamental to evaluation of the characteristics of DM quantisation noise and indicates also the temporal extent of the constraint on the message source output. Fig. 2.3 shows that, for a typical $f_s = 96$ KHz, there is strong correlation ($\phi_{mm}(\tau) > 0.9$) over 7 consecutive samples and significant correlation over intervals of several milliseconds (hundreds of

Message autocorrelation
function $\rho_{mm}(\tau)$

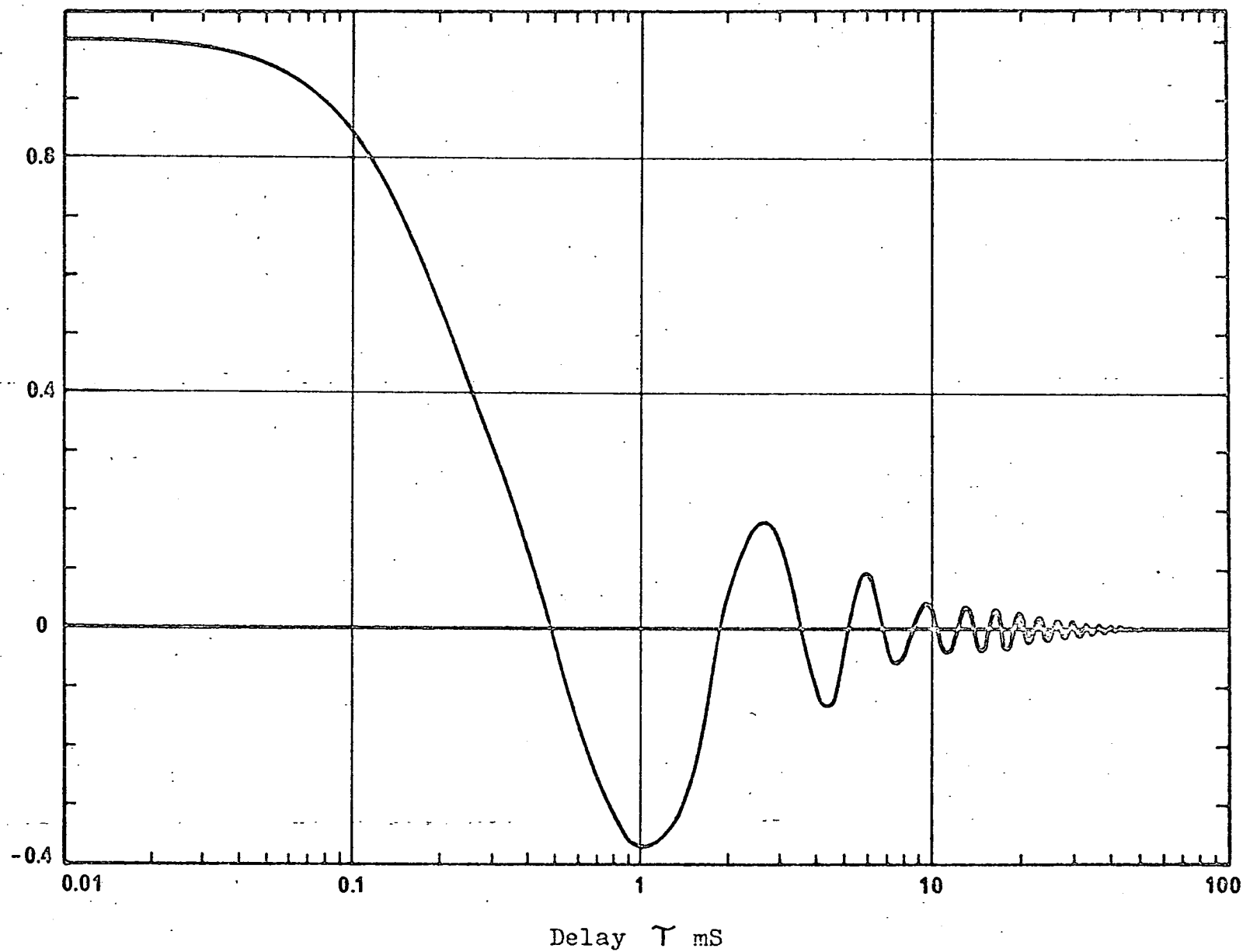


Fig. 2.3 Message autocorrelation

samples). The indicated statistical dependence of the message amplitude at any sampling instant on the amplitudes of many previous samples is evidence of redundancy in the message sequence, but it should be noted that Δ increment and sampling frequency for DM are such that there is sufficient correlation between successive sample amplitudes for their difference to be in general less than Δ and they are not encoded independently.

2.4 Quantisation noise

Typically, an equi-interval quantiser with step size q has a transfer characteristic such that it delivers an output kq for inputs x in the range $q(k-\frac{1}{2}) \leq x < q(k+\frac{1}{2})$; i.e. the input is approximated by the nearest integer multiple of the quantising interval. The echelon signal produced by delta-coding, however, has the special property that an increment $\pm \Delta$ occurs at every sampling instant, even when the new level is a poorer approximant to the message than the old. The process may therefore be represented as that of sampling and quantisation by the characteristic of Fig. 2.4, a unity gain quantiser with interval $q=2\Delta$ and clock-synchronised origin shift function

$$a(t) = \frac{\Delta}{2}(\cos \pi f_s t + 1) \quad (2.4.1)$$

shown in Fig. 2.5.

Applying Watts' ⁽¹¹⁾ analysis of a generalised quantiser, the joint moment between the quantisation noises n_x, n_y of two correlated unit power Gaussian signals x, y separately

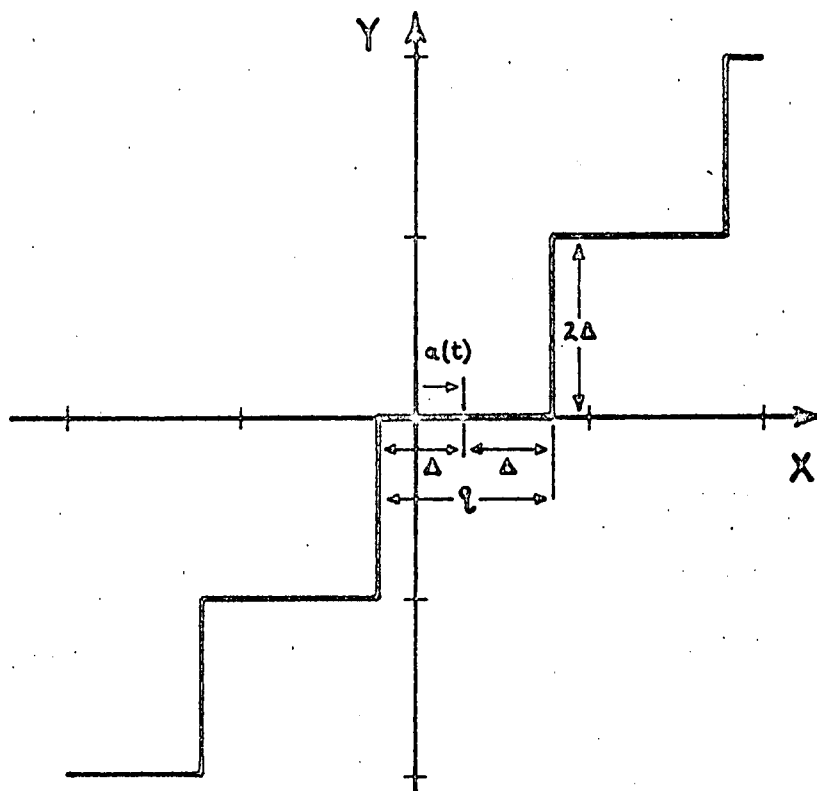


Fig. 2.4 Quantiser characteristic

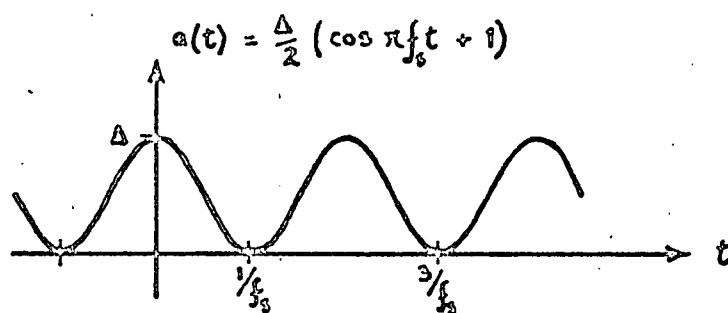


Fig. 2.5 Characteristic shift function

processed by the quantiser of Fig. 2.4 is found to be

$$E[n_x n_y] = \frac{1}{(-j2\pi)^2} \sum_{k \neq 0} \sum_{m \neq 0} e^{-j2\pi(k+m)a(t)} \cdot \frac{(-1)^{k+m}}{km} \cdot e^{-2\pi^2 \left[\left(\frac{k}{q} \right)^2 + \frac{2km}{q^2} E[xy] + \left(\frac{m}{q} \right)^2 \right]} \quad (2.4.2)$$

For $x = m(t)$, $y = m(t-\tau)$ (Fig. 2.6), the joint moment between x and y becomes the message autocorrelation function

$$E[xy] = \overline{m(t) \cdot m(t-\tau)} = \varphi_{mm}(\tau) \quad (2.4.3)$$

($m(t)$ ergodic)

and the quantisation noise autocorrelation function referred to the quantiser output

$$\varphi_{nn}(\tau) = -\frac{\Delta^2}{\pi^2} \sum_{k \neq 0} \sum_{m \neq 0} e^{-j2\pi(k+m)a(t)} \cdot \frac{(-1)^{k+m}}{km} \cdot e^{-\frac{\pi^2}{2\Delta^2} \left[k^2 + 2km\varphi_{mm}(\tau) + m^2 \right]} \quad (2.4.4)$$

Since $\varphi_{mm}(\tau) \leq 1$, the exponent of the last factor results in significant terms for $k = -m$ only, so that

$$\varphi_{nn}(\tau) = \frac{2\Delta^2}{\pi^2} \sum_{k=1}^{\infty} \frac{1}{k^2} \cdot e^{-\left(\frac{\pi k}{\Delta} \right)^2 (1 - \varphi_{mm}(\tau))} \quad (2.4.5)$$

and the same noise autocorrelation function is found for a single fixed quantiser with interval $q = 2\Delta$.

The total quantisation noise power by this derivation

$$\begin{aligned} \overline{n(t)^2} &= \varphi_{nn}(0) = \frac{q^2}{2\pi^2} \sum_{k=1}^{\infty} \frac{1}{k^2} \\ &= \frac{q^2}{12} \quad (\text{Jolley}^{(12)}) \end{aligned} \quad (2.4.6)$$

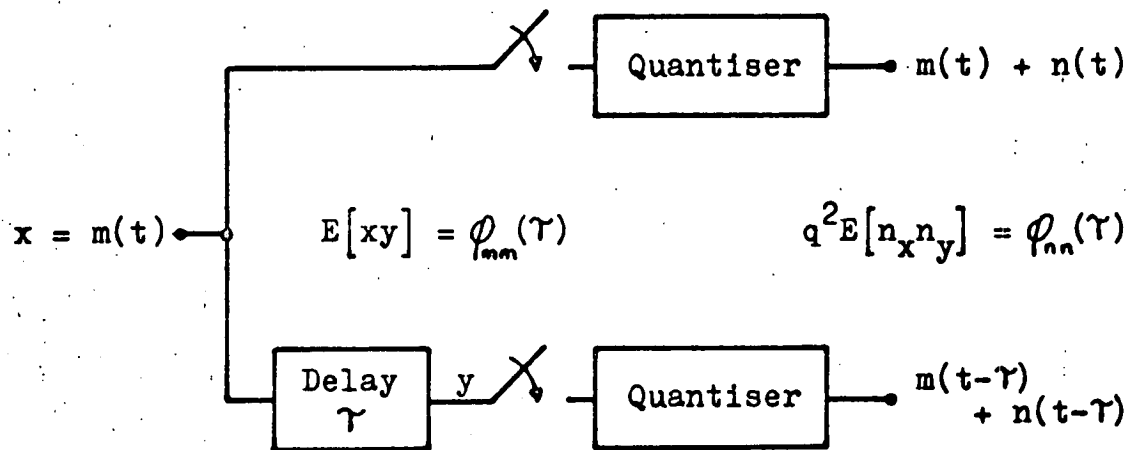


Fig. 2.6 Quantisation noise autocorrelation

which verifies a well known result. (13)

From (2.3.1) and (2.4.5) the quantisation noise power spectral density

$$\begin{aligned}\bar{\Phi}_{nn}(\omega) &= \int_{-\infty}^{\infty} \phi_{nn}(\tau) e^{-j\omega\tau} d\tau \\ &= \frac{4\Delta^2}{\pi^2} \int_0^{\infty} \sum_{k=1}^{\infty} \frac{1}{k^2} e^{-\left(\frac{\pi k}{\Delta}\right)^2 (1-\phi_{nn}(\tau))} \cos \omega\tau d\tau\end{aligned}\quad (2.4.7)$$

may be computed* for any increment Δ .

From the numerical results the relation

$$\log_{10} \bar{\Phi}_{nn} = -5.288 + 3 \log_{10} \Delta \quad (2.4.8)$$

has been derived and determines the power spectral density in the information band within 1% for the usual range of SNR.

The DM increments for $\bar{\Phi}_{nn}$ values corresponding to the range of SNR considered in section 2.2 are therefore readily evaluated and noise power spectra for SNR = 20, 30, 40 dB are shown in Fig. 2.1. The spectra are flat in the information band and have an asymptotic rate of fall of 6 dB/octave; but in the proximity of the break frequencies, which increase as the quantisation is made finer, they are sharper than for a first order characteristic. Because of the higher sampling frequencies employed in DM, aliasing of noise power into the information band is negligible for the spectra shown, in contrast to the

* Approximately 5 minutes central processor time per spectrum on an English Electric KDF9 computer.

large proportion of the total quantisation noise power which may be spectrally transposed downwards into the band as the lower sidebands of the fundamental and harmonic components of the sampling function in systems employing the Nyquist rate.

2.5 Message derivative

DM sampling frequencies are selected such that, for the Δ increment which satisfies the required SNR criterion, amplitude excursions of the message derivative exceeding $\Delta \cdot f_s$ are infrequent. For the power spectral density (2.1.2), the variance of the message derivative

$$\overline{(m'(t))^2} = 2 \int_0^\infty \omega^2 \Phi_{mm}(\omega) d\omega \quad (2.5.1)$$

is computed as $3.553 \times 10^7 \text{ S}^{-2}$

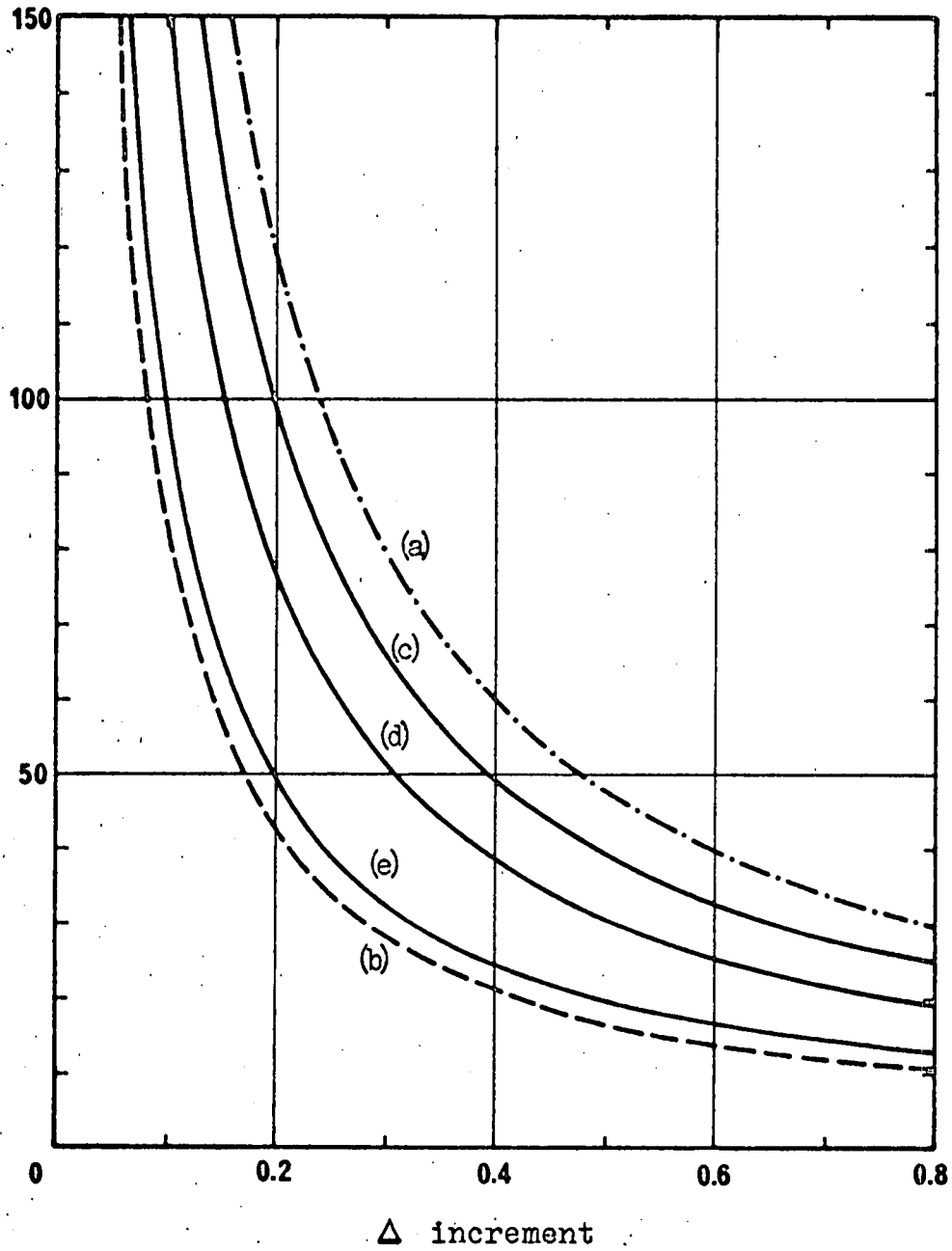
De Jager⁽¹⁴⁾ and others have found it convenient to test DM systems with a sine wave of reference frequency such that overloading occurs simultaneously in corresponding encoders with amplitude and slope limitation, significant overloading being avoided if the message does not exceed the maximum amplitude of this test tone. This reference frequency ω_r is here given by

$$\omega_r^2 = \overline{(m'(t))^2} \quad (2.5.2)$$

and is found to be 949 Hz, which compares with de Jager's observation of 800 Hz.

For a Gaussian message, $m'(t)$ is also Gaussian and

Sampling frequency
 f_s KHz



- | | |
|--------------------------------------|-------------------------------|
| (a) $d_d = \frac{1}{4}$ rms overload | (c) Overload probability 0.1% |
| (b) De Jager test tone 949 Hz | (d) " " 1% |
| | (e) " " 10% |

Fig. 2.7 Sampling frequency

writing $\sigma_d = \overline{m'(t)^2}^{\frac{1}{2}}$ one finds for this distribution

$$p\left(|m'(t)| > \Delta \cdot f_s\right) = 1 - \sqrt{\frac{2}{\pi}} \int_0^{\frac{\Delta \cdot f_s}{\sigma_d}} e^{-\frac{t^2}{2}} dt \quad (2.5.3)$$

from which the sampling frequencies required for a range of Δ are shown in Fig. 2.7.

Parameter values assumed in earlier studies^{(13), (15)} result in an rms overload level of $4\sigma_d$, which corresponds to rather light loading of the encoder and an overload probability of less than 0.007%.

Chapter 3

Delta - coded speech processor

Some of the properties of delta modulation are revealed by the performance of the encoder with a deterministic input⁽¹⁶⁾ (for which an excitation-dependent model is applicable), while the random signal analysis presented in chapter 2 determines the characteristics for an information-generating source of prescribed statistical properties. However, a detailed study of delta-coded speech requires the analysis, by a data processor with substantial rapid-access memory capacity, of the signal sequences generated when the exciting waveform is an actual speech message. Effective changes in processor structure, and also subsequent processing of results, are accomplished readily if the machine is a general purpose digital computer operating on the data by executing a stored instruction set. Such a facility has been established, based on the hybrid operation of Solartron SC247 analogue and DEC PDP-8 digital computers with an interface for delta-coded speech, and is described briefly in this chapter.

3.1 FM system

Frequency division of speech messages by a factor of 64 to the band 4.7 - 47 Hz scales the source spectrum appropriately for the analogue computer and with a PDP-8 core store cycle time of

1.5 μ S allows the execution of 150 to 220 memory reference instructions during a minimum period of 667 μ S for a real time sampling frequency of 96 KHz. Source message recordings prepared directly by Edinburgh University Phonetics Department are transferred with a frequency scale of $\frac{1}{2}$ to an Elliott Tandberg data recorder using a carrier frequency of 12 KHz. A transcription of this record with a scale of $\frac{1}{4}$ is replayed on an Akai M8 crossfield head machine with a final scale of $\frac{1}{8}$ and a tape speed of $1\frac{7}{8}$ i.p.s., so that the output carrier frequency is 375 Hz.

The FM signal is processed by the demodulator of Fig. 3.1, in which the message is extracted by the smoothing (by an FET 7th order Butterworth active LP filter with a rapid cut-off above 60 Hz) of an internally generated train of equi-energy pulses triggered by the input signal zero-crossings. Calibration tones at $\pm 50\%$ frequency deviation, corresponding to peak message excursion for the design deviation ratio of 4, are used with the SC247 digital voltmeter to set the DC amplifier gain for a range of effective values of Δ increment, the step size of the delta-coder being in fact fixed.

3.2 Analogue filter

Bandpass filtering of the message to the power spectrum of Fig. 2.1 is achieved by M-method synthesis of the transfer function $H(s)$ (Sec. 2.1) with the time-scaled frequency variable and one additional zero at the origin, giving

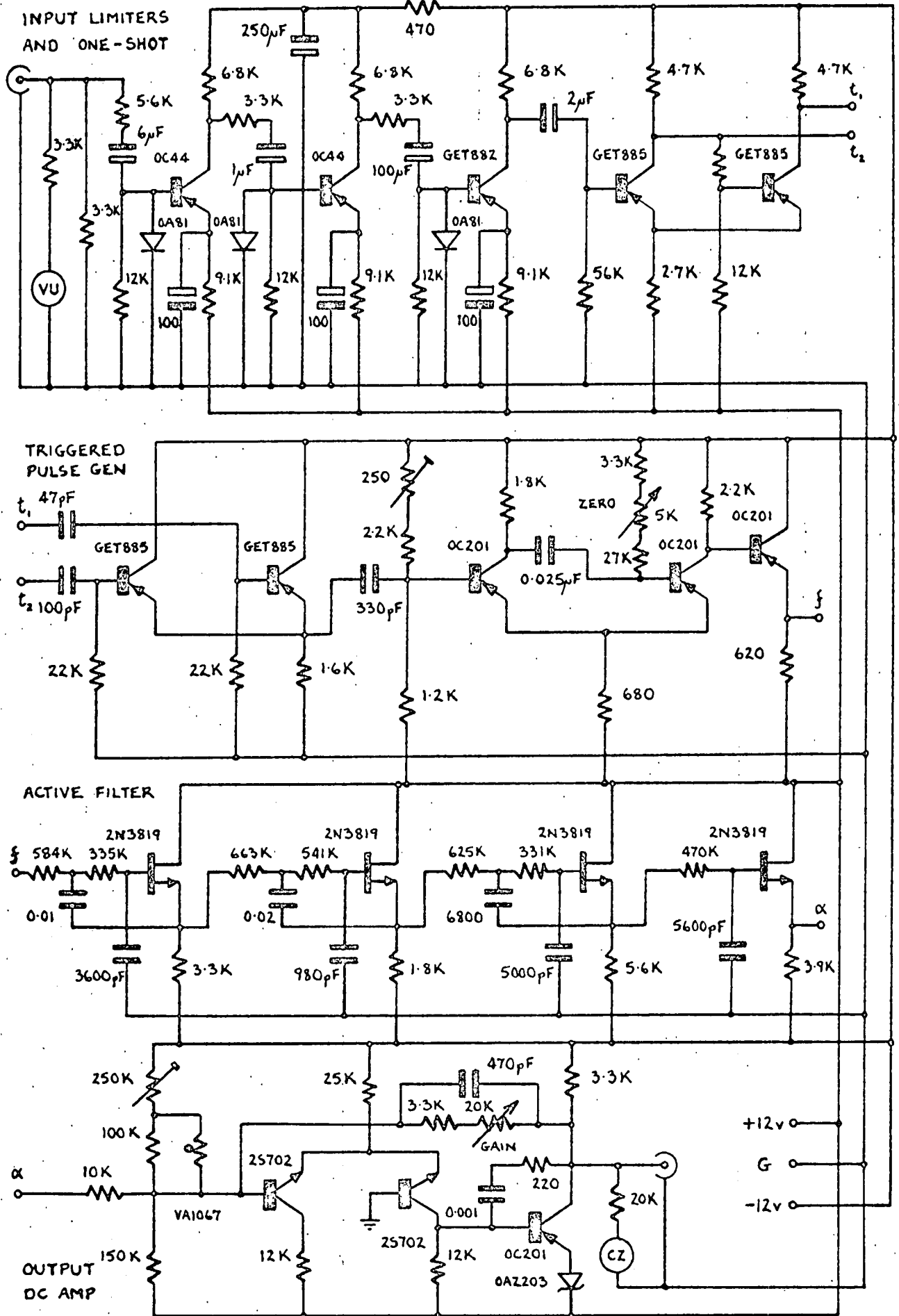


Fig. 3.1 FM speech demodulator

$$G(s) = \frac{Y}{X} = \frac{ks^7}{\sum_{i=0}^{14} Q_i s^i} \quad (3.2.1)$$

where the Q_i are computed from the product of quadratic factors in (2.1.1).

Letting

$$\frac{Y}{ks^7} = \frac{X}{\sum_{i=0}^{14} Q_i s^i} = M \quad (3.2.2)$$

and scaling for equal coefficients, appropriate computer variables are $(Q_i s^i M)$ so that the solution for the highest derivative is

$$Q_{14} s^{14} M = X - \sum_{i=0}^{13} Q_i s^i M, \quad (3.2.3)$$

which is synthesised by the configuration detailed in Appendix 2.

3.3 Delta - coder

The precision DM unit shown in Fig. 3.2 replaces a dual inverter module in the SC247. Diode - isolated positive and negative increment pulses transmitted from the computer interface are integrated by one unit of the associated twin operational amplifier and the error between the message and its sampled and quantised approximant is extracted and limited by the second amplifier.

The translated error signal operates an IC differential

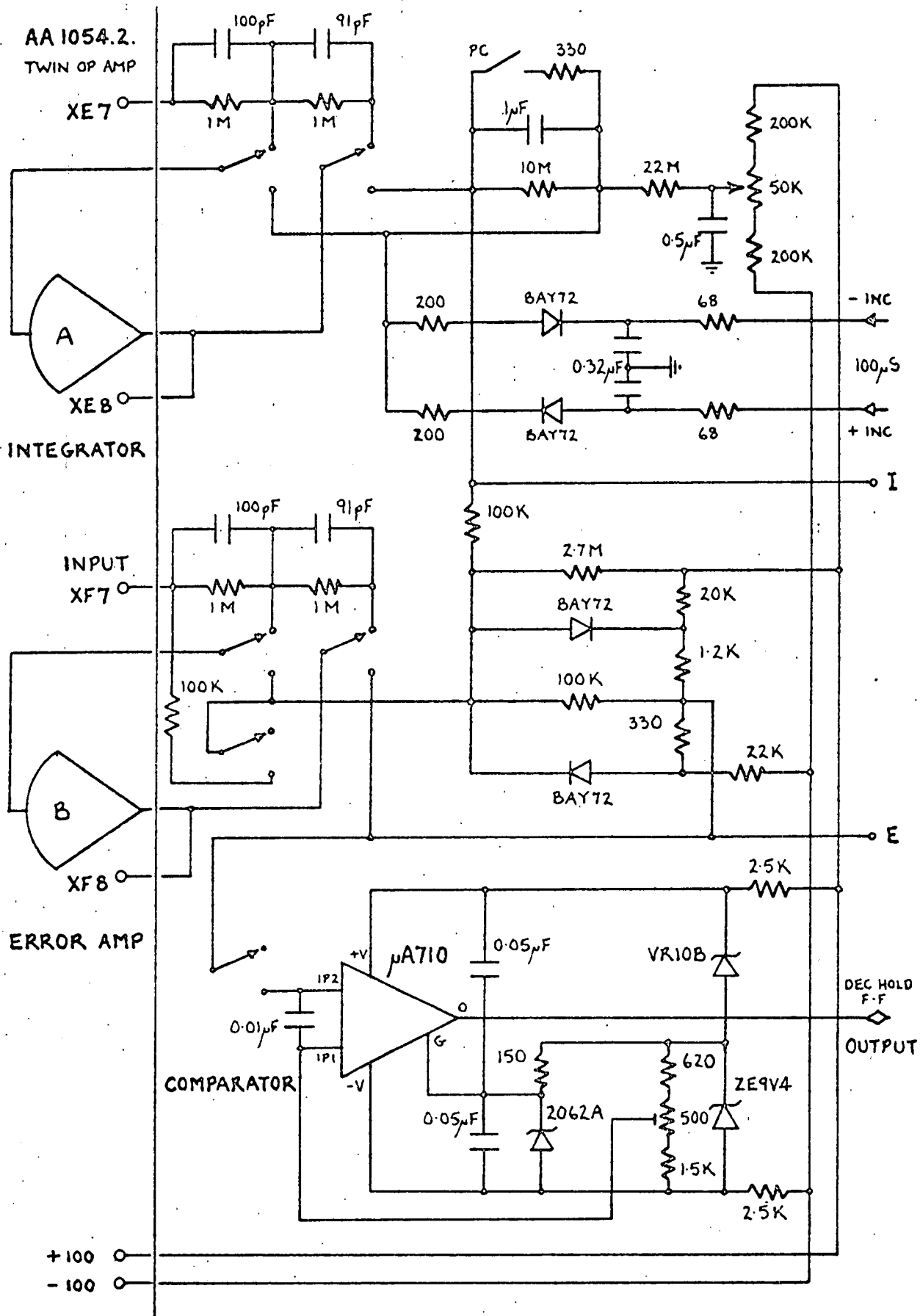


Fig. 3.2 Precision deltamodulator

comparator, an arrangement which ensures that the resolution of the comparator (3mV), whose input range is restricted, is effective over the whole of the 300 V echelon signal range at the integrator output, and therefore remains fine relative to the DM step size of 1 V. The comparator is biased to the logic threshold for zero message and integrator output and arranged to deliver the inverted levels required by the interface DEC modules.

3.4 Computer interface

The detailed configuration of the interface logic is determined by the processing operations with the most stringent computer time requirements, increased program volume compensating for the sub-optimal data organisation in other cases.

In the analogue interface (Fig. 3.3) the variable clock, which is the primary timing source for DM sampling and data transfers, pulses DCD gates enabled in complement by the status of the delta-coder comparator. The gates are internally conditioned by the associated flip flop which holds the comparator decision during the sampling periods and enables the one-shot multivibrators which generate increment pulses of the appropriate polarity for return transmission to the SC247.

At the same time as the selected one-shot is pulsed by the delayed clock signal, the flip flop status is transferred

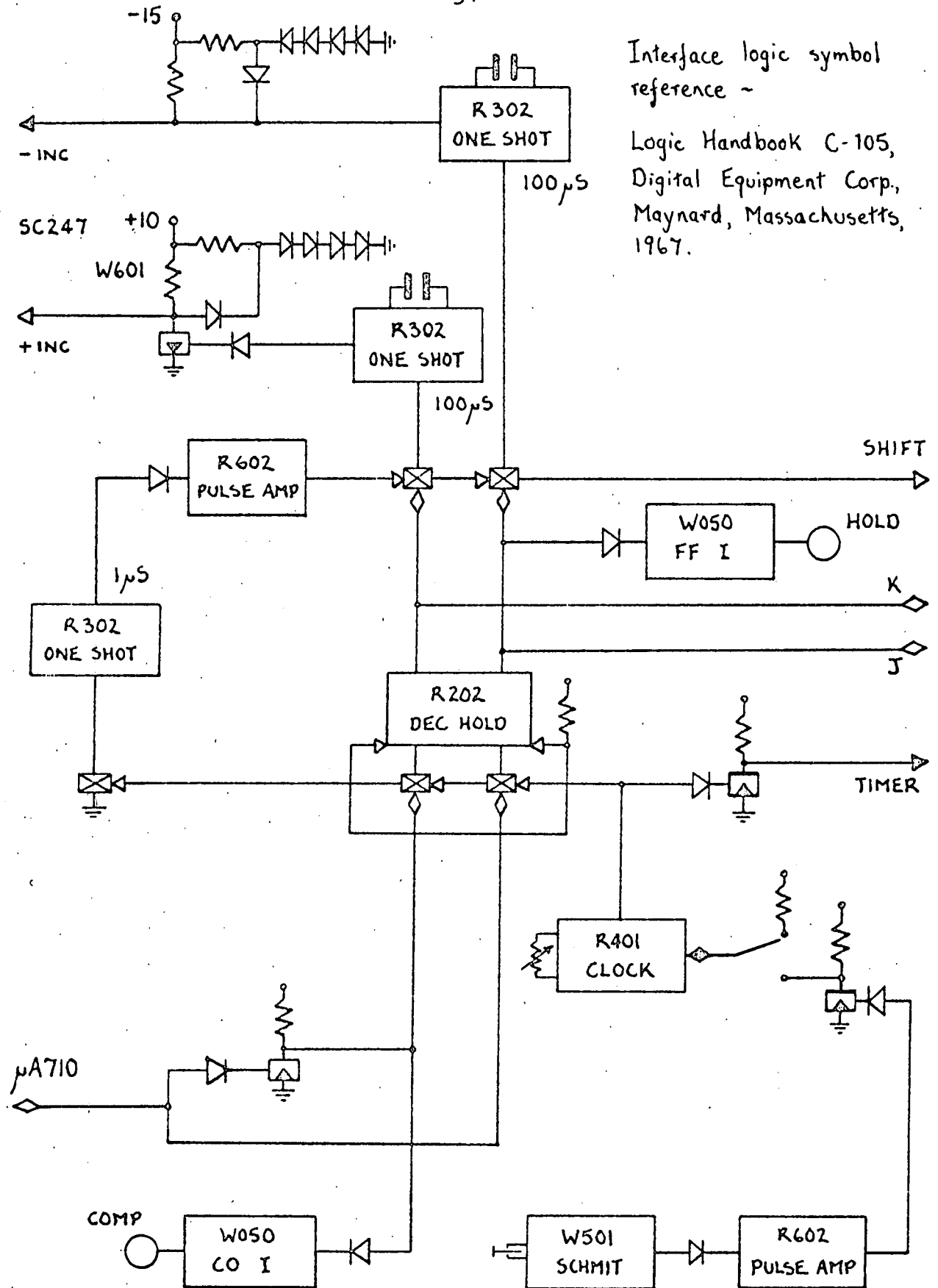


Fig. 3.3 Analogue interface

to the least significant slot of a 7 bit shift register parallel - connected to the PDP-8 memory buffer^(M8) (Fig. 3.4).

After this shift, but before a data transfer is initiated, two further input gates, enabled by a flip flop whose status is under program control, are pulsed to complement the least significant bit if an error is called for. During subsequent shift cycles the erroneous bit continues to propagate along the input buffer.

When data transfer is selected, the delayed complement pulse sets the break request flip flop (Fig. 3.5) which signals the computer to enter the break state after completion of the current instruction. The location in core memory for each transfer is specified by the content of the interface memory address register^(MA), the more significant 5 bits (selecting one of the available 32 pages of 128 words) being set by switch register and the remaining 7 bits by an up - counter.

When the break state has been entered, the address accepted pulse generated by the computer is used to clear the break request flip flop, increment the MA register and trigger a one - shot which grounds the program interrupt bus.

Synchronisation between program execution and the DM clock is thus achieved by arranging that the effective starting address of the instruction set is 0001* and after completion of the processing initiated at a sampling instant the machine cycles

* 12 bit computer words and memory addresses are written throughout as 4 digit octal numbers.

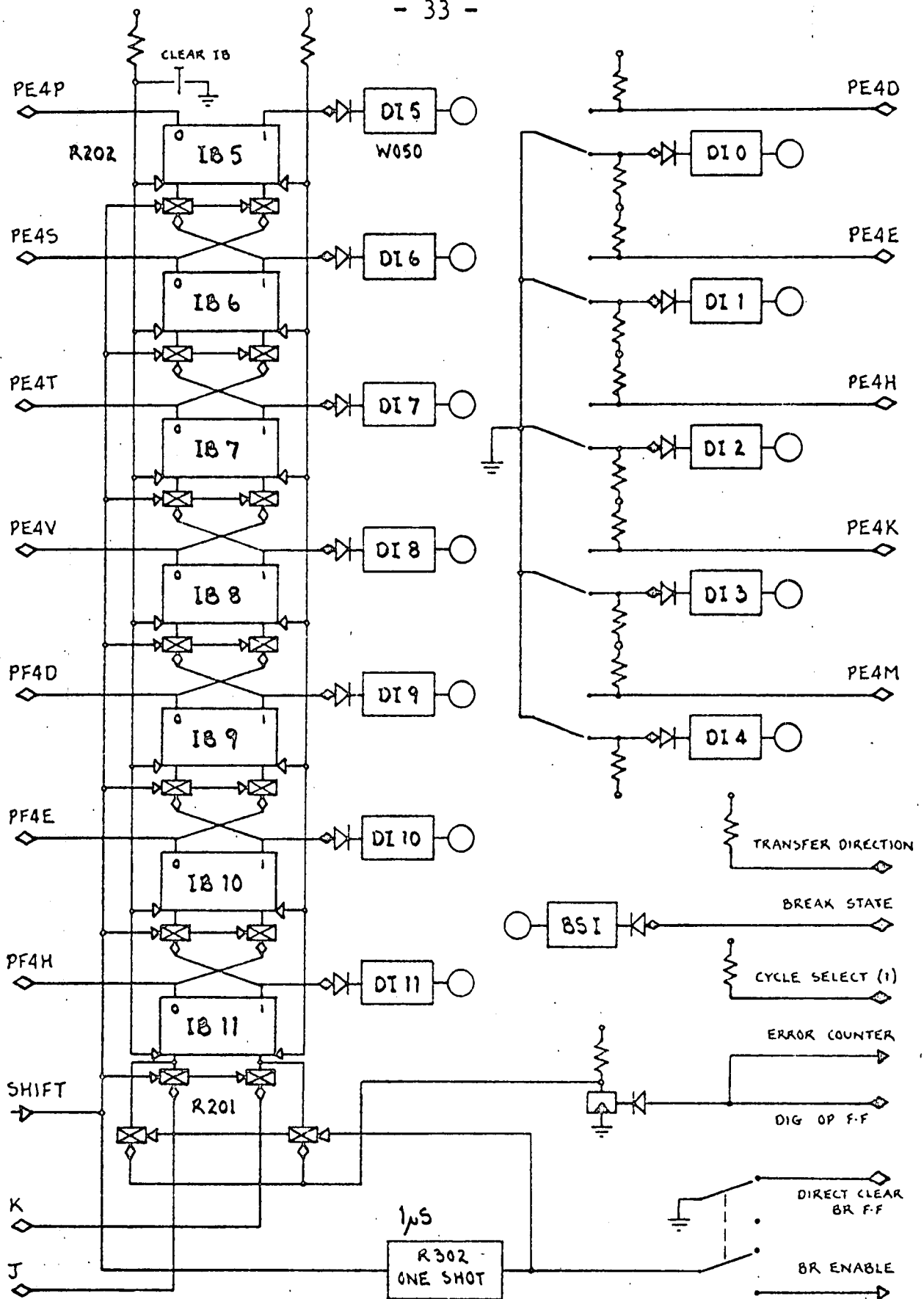


Fig. 3.4 MB register interface, data error control

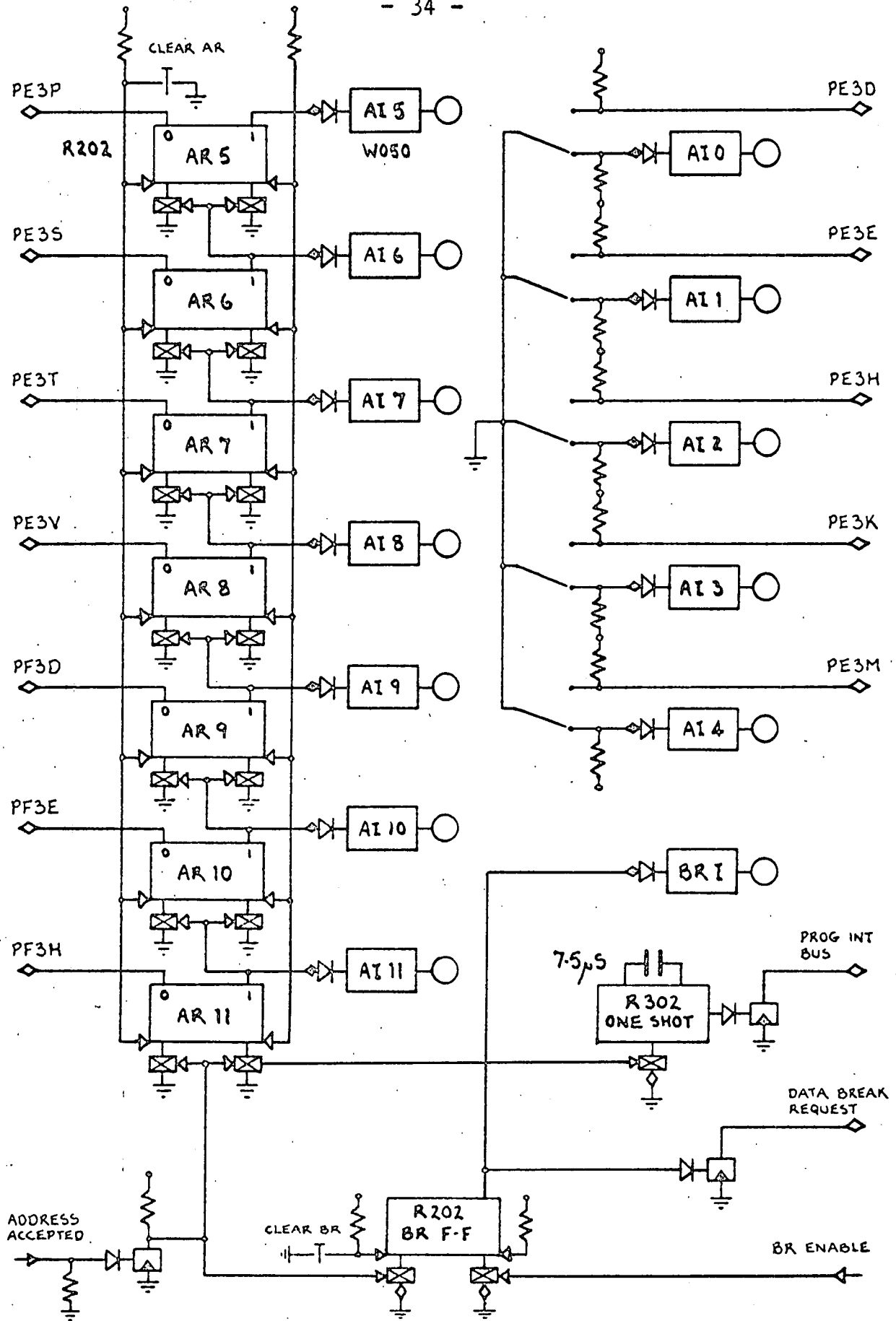


Fig. 3.5 MA register interface, data transfer control

in an instruction loop with the interrupt enabled until a data break is requested.

The interface thus allows any selected page of PDP-8 core memory to be operated as a continuously cycling data register in which can be accessed at any time the 134 most recent bits of the DM sequence. Each word on this page is composed of 5 preselected bits (the processing of which by program execution forms from the word an absolute machine address with data-specified within-page section) followed by 7 consecutive data bits of which the more significant 6 are written redundantly in the less significant locations of the next lower address, and the less significant 6 in the more significant locations of the group in the next higher, the last address of the page being followed functionally by the first of the same page rather than of the next page.

The delta-coded speech processor is shown in Figs. 3.6, 3.7.

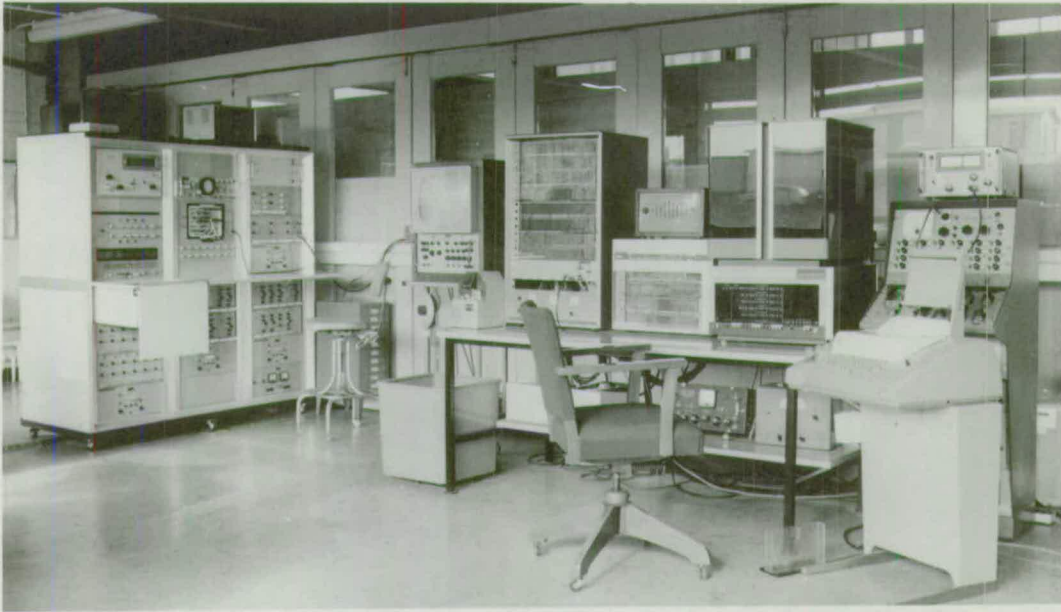


Fig. 3.6 SC247 and PDP-8 computers

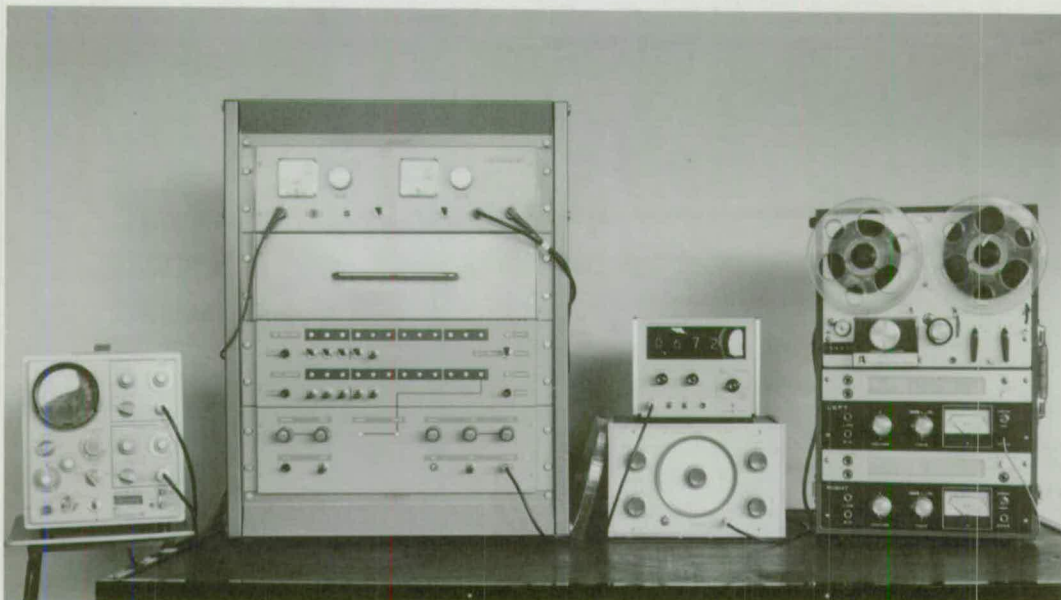


Fig. 3.7 Delta-coded speech interface

Chapter 4

Linear prediction

In introducing the discrete information source treatment of the signal generated by a delta-coder, the constituent 0 or 1 symbols of the binary output sequence are termed the elements of the message, while the state i of the source at any time is defined by a multi-dimensional vector whose components are a finite number of the symbols which have been generated prior to that time. Fig. 2.3 indicates that the significant dimensionality of the states exceeds 100, and N th order Markov process approximations to the source are studied for which an element is considered to have a statistical dependence limited to the preceding N symbols.

4.1 Entropy

The lemmas of Shannon identify three entropy measures relevant to a DM message. There is first the entropy* of the process

$$H = - \sum_i \sum_j p(i) p(j|i) \log p(j|i) \quad (4.1.1)$$

in which $p(j|i)$ is the conditional probability of occurrence of state j following state i .

Second, there is the entropy of blocks B_i of N elements of

* Apart from explicit exceptions, entropy measures are per element of the signal sequence.

the signal sequence,

$$G_N = -\frac{1}{N} \sum_i p(B_i) \log p(B_i) \quad (4.1.2)$$

And third, for an N th order approximation ($(N+1)$ th order in Shannon's terminology) to the source in which the N element block B_i determines the conditional distribution from which the next symbol S_j is drawn, the entropy

$$F_N = -\sum_i \sum_j p(B_i, S_j) \log p(S_j | B_i) \quad (4.1.3)$$

By the adoption of the finite state ($1 \leq i \leq 2^N$) representation of the signal source, F_N may be equated with the process entropy H and evaluated by (4.1.1) which involves the conditional rather than the joint probabilities.

As the channel capacity required for direct transmission of a delta-coded message is equal to the average element entropy*, relative entropies are referred to the $H = 1$ bit per element value for a source for which the S_j are equiprobable and independent of preceding elements.

4.2 Predictive coding

Procedures for redundancy† reduction by predictive

* 'Average element entropy' is used concisely throughout with the meaning 'entropy of the distribution of the average element' and should be clearly distinguished from the average of the entropies of the distributions of the elements, which is the entropy of the process.

† Redundancy is the complement of relative entropy.

coding⁽¹⁷⁾ lower the entropy of the average element distribution by a transformation utilising such information about the conditional probability $p(S_j|B_i)$ as it is economically viable to compute at sender and receiver for limited size blocks B_i of past elements. For a delta-coded message, an estimator processing N previous elements can make a binary prediction of the next element in sequence and the transformation effected as shown in Fig. 4.1 by modulo-2 addition of the element and its prediction.

$$T = \bar{S} \cdot E + S \cdot \bar{E} \quad (4.2.1)$$

At the receiver, the same prediction is generated by an identical estimator processing the same elements and the new element is determined by processing inversely.

For by De Morgan's laws

$$\bar{T} = (\overline{\bar{S} \cdot E}) \cdot (\overline{S \cdot \bar{E}}) = (\bar{E} + S \cdot E) \cdot (\bar{S} + S \cdot E)$$

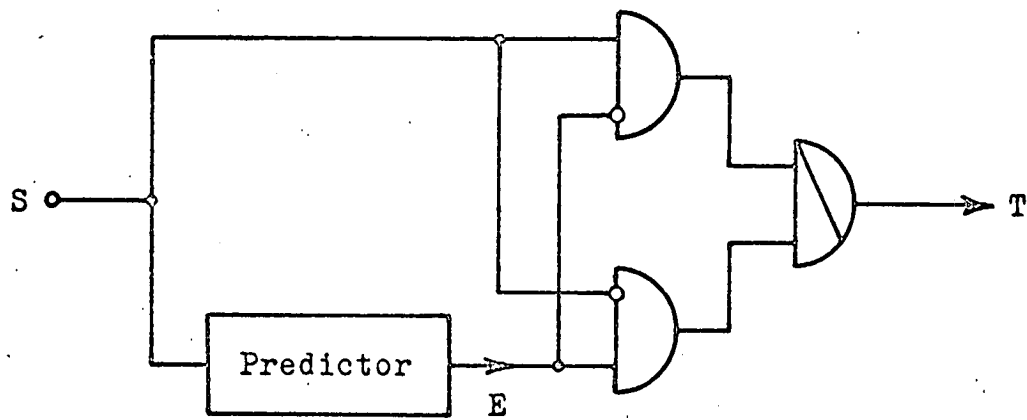
So that

$$\begin{aligned} \bar{T} \cdot E + T \cdot \bar{E} &= (\bar{E} + S \cdot E) \cdot (\bar{S} + S \cdot E) \cdot E + (\bar{S} \cdot E + S \cdot \bar{E}) \cdot \bar{E} \\ &= S \end{aligned} \quad (4.2.2)$$

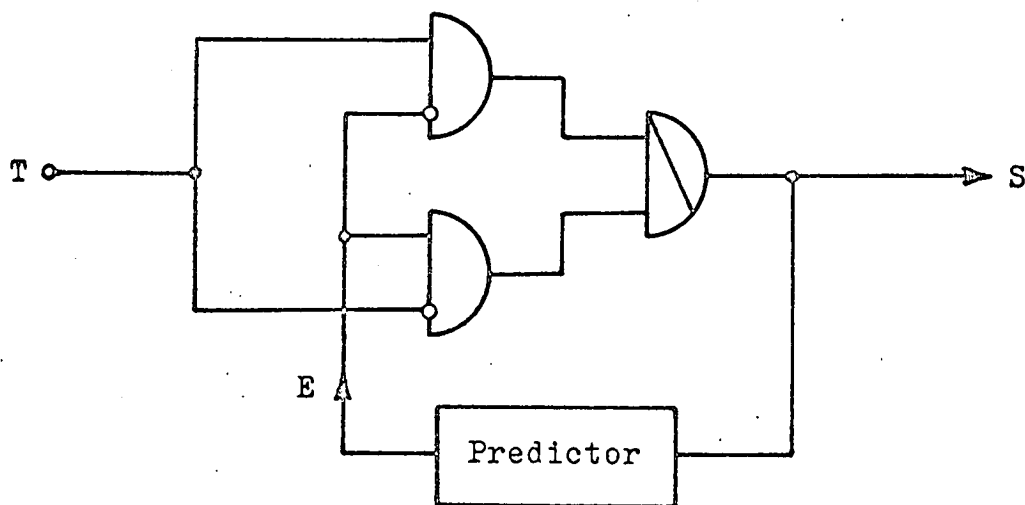
In words, the binary symbols which previously had the direct significance :

$$(a) \quad \begin{cases} 0: & \text{Decrement approximant by } \Delta \\ 1: & \text{Increment} \quad \quad \quad " \quad \quad \quad " \end{cases}$$

then assume the indirect function :



Transformation



Inversion

Fig. 4.1 DM predictive coding

- 0: Estimator output correct, interpret it as (a)
 1: " " wrong, complement it and interpret as (a)

As the transformations are one - one the process entropy computed by (4.1.1) for $N \rightarrow \infty$, the weighted average of the entropies of the conditional distributions for all possible states, is the same for operand and transform sequences, but for a predictor success probability $P_s > 0.5$, the entropy

$$H_T = - [P_s \log P_s + (1 - P_s) \log (1 - P_s)] \quad (4.2.3)$$

of the average element of the new sequence is lower. While schemes for encoding the transformed sequence to achieve a reduction in channel bit rate are described later (chapter 8), it is noted here that direct transmission of the sequence in an application in which binary 1 is signalled by an output pulse, binary 0 by pulse absence, results in a transmitter power economy of

$$\eta = 100 (2P_s - 1) \% \quad (4.2.4)$$

4.3 Estimator function

Although processing of the same number of elements by a predictor function without a linearity constraint is in general advantageous for other than stationary Gaussian messages, linear prediction by a Wiener estimator is first described, for the hardware requirement increases exponentially with N in the former case but in direct proportion for the latter. Of course the linear predictor can also be synthesised without data

truncation as an analogue network rather than a digital circuit, but in this case errors due to component tolerances would be expected between encoder and decoder predictions when the estimates are near the binary decision threshold. The estimator, with transfer function $E(s)$, corresponding impulse response $e(t)$, is assumed to be excited by the echelon signal $m_i(t)$ formed at the integrator output and is required to produce an optimal estimate of the message with zero lag (i.e. neither delayed nor advanced) for comparison with the echelon signal itself as in a standard delta-coder to generate the logical prediction E for processing as shown in Fig. 4.1.

The method of spectrum factorisation⁽¹⁸⁾ is first applied to the input message plus noise power spectral density

$$\Phi_{ii}(\omega) = \Phi_{mm}(\omega) + \Phi_{nn}(\omega), \quad (4.3.1)$$

with corresponding autocorrelation function $\phi_{ii}(\tau)$, to compute factors

$$\Phi_{ii}^+(s) \cdot \Phi_{ii}^-(s) = \Phi_{ii}(s) \quad (4.3.2)$$

such that $\Phi_{ii}^+(s)$ contains the 28 left half plane singularities, while $\Phi_{ii}^-(s)$ has poles and zeros in the right half plane only*.

*For most SNR, a combination procedure involving a modification of the Bernoulli method for approximate location and an extension of the Birge-Vieta algorithm to the complex plane for refinement of the estimate has been found to ensure certainty of convergence while avoiding the rapid growth of the numbers involved from iteration to iteration.⁽¹⁹⁾

The inverse transform of $\Phi_{ii}^+(s)$ is therefore zero for $t < 0$, so that

$$\Gamma_{ii}^+(s) = \frac{1}{\Phi_{ii}^+(s)}$$

(which also has singularities confined to the left half plane, the poles and zeros of $\Phi_{ii}^+(s)$ becoming the zeros and poles of its reciprocal) is a physically realizable transfer function which would convert the coded message to white noise.

For the case of desired estimator output equal to the message without lag or lead, the Wiener-Hopf* equation⁽²⁰⁾, derived by the application of a variational method to minimise the mean square error, takes the form

$$\phi_{im}(\tau) = \int_{-\infty}^{\infty} e(\delta) \phi_{ii}(\tau - \delta) d\delta, \quad \tau \geq 0 \quad (4.3.3)$$

so that writing

$$\Psi(s) = \frac{\Phi_{im}(s)}{\Phi_{ii}^-(s)} \quad (4.3.4)$$

the transform

$$R(s) = \Phi_{ii}^-(s) \left[E(s) \cdot \Phi_{ii}^+(s) - \Psi(s) \right] \quad (4.3.5)$$

has no left half plane singularities.[†]

The input signal - message cross power spectral density

* The analyses of Wiener and Lee are developed in the λ plane, $\lambda = \omega + j\delta$, while the standard complex variable $s = \delta + j\omega$ is retained in this thesis. Hence functions with poles and zeros in the left half plane have the time domain properties of those with upper half plane singularities in the literature referenced.

[†] Note that the restriction $\tau \geq 0$ in (4.3.3) allows $R(s)$ right half plane poles.

in (4.3.4), which corresponds to the cross correlation function $\phi_{im}(\tau)$ in (4.3.3), becomes

$$\begin{aligned}\Phi_{im}(\omega) &= \Phi_{mm}(\omega) + \Phi_{nm}(\omega) \\ &= \Phi_{mm}(\omega)\end{aligned}\quad (4.3.6)$$

on the assumption that Δ is sufficiently fine for the message - quantisation noise cross power spectral density to be zero.

There results some pole - zero cancellation with the right half plane input spectrum factor in (4.3.4) and the complex residues at the remaining 14 left half plane message spectrum poles are evaluated to allow the partial fraction expansion

$$\Psi(s) = \Psi^+(s) + \Psi^-(s) \quad (4.3.7)$$

in which $\Psi^+(s)$ contains the terms with left half plane poles.

Inspection of

$$\frac{R(s)}{\Phi_{ii}^-(s)} = E(s) \cdot \Phi_{ii}^+(s) - \Psi^+(s) - \Psi^-(s) \quad (4.3.8)$$

shows that for the estimator function to be physically realizable (left half plane poles only)

$$E(s) = \frac{\Psi^+(s)}{\Phi_{ii}^+(s)} \quad (4.3.9)$$

Although the message is sharply bandlimited, $|E(j\omega)|$ does not decrease more rapidly than $1/\omega$ at high frequencies. This

characteristic necessarily results if the corresponding impulse response, formally

$$e(t) = \frac{1}{2\pi j} \int_{c-j\infty}^{c+j\infty} \frac{\Psi^+(s)}{\Phi_{ii}^+(s)} e^{st} ds, \quad (4.3.10)$$

has its maximum at $t = 0$, so that the weighting function $w(\Upsilon) = e(\Upsilon)$, where $\Upsilon = t - \lambda$ is the age at time t of the signal generated at time λ , weights the new datum most strongly.

(4.3.10) represents tandem processing by systems with the impulse responses

$$\psi^+(t) = \frac{1}{2\pi} \int_{-\infty}^{\infty} \Psi^+(\omega) e^{j\omega t} d\omega \quad (4.3.11)$$

and

$$\gamma_{ii}^+(t) = \frac{1}{2\pi} \int_{-\infty}^{\infty} \frac{1}{\Phi_{ii}^+(\omega)} e^{j\omega t} d\omega \quad (4.3.12)$$

Thus

$$w(\Upsilon) = \int_{-\infty}^{\infty} \psi^+(\lambda) \gamma_{ii}^+(\Upsilon - \lambda) d\lambda \quad (4.3.13)$$

Optimal weighting functions are shown in Fig. 4.2, in which the steeper initial slope of $w(\Upsilon)$ for higher SNR corresponds in the frequency domain to the use, in generating the estimate, of the information in the upper spectral components of the message which are less severely impaired than when the quantisation noise power is greater.

4.4 Estimator error

The estimator error distribution and DM quantising

Weighting function
 $w(\tau)/10^4$

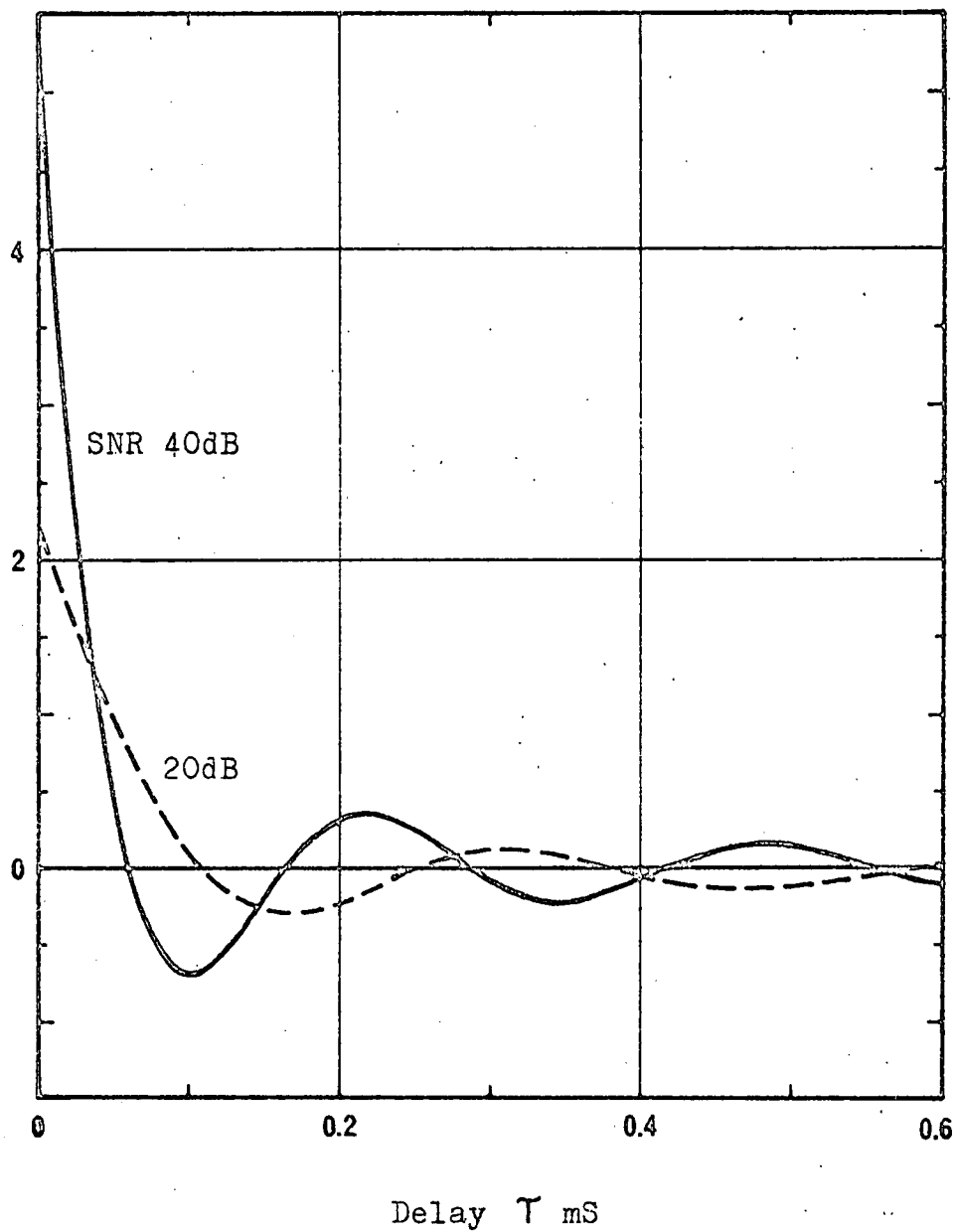


Fig. 4.2 Optimal weighting functions

interval determine the probability of successful binary prediction. For the estimate $m_e(t)$ whose value at the sampling instants has the probability density function $p(\epsilon)$ with mean (which is $m(t)$) displaced δ from the last quantised level, the probability of an individual prediction being correct is

$$p_s = \int_{-\delta}^{\infty} p(\epsilon) d\epsilon^{\dagger} \quad (4.4.1)$$

For reasonably fine quantisation, the distribution of δ over the set of $p(\epsilon)$ at the sampling instants may be considered uniform over the range $-\Delta < \delta < \Delta$, so that the predictor success probability is

$$P_s = \frac{\int_{\delta=-\Delta}^0 \int_{\delta}^{\infty} p(\epsilon) d\epsilon d\delta}{\int_{\delta=-\Delta}^0 d\delta} \quad (4.4.2)$$

For $m(t)$ Gaussian, $\epsilon(t)$ is also normally distributed, and writing $\sigma_e^2 = \overline{\epsilon^2(t)}$,

$$P_s = \frac{1}{\Delta} \int_{\delta=-\Delta}^0 \left[\frac{1}{2} + \frac{1}{\sqrt{\pi}} \int_0^{-\frac{\delta}{\sqrt{2}\sigma_e}} e^{-u^2} du \right] d\delta \quad (4.4.3)$$

$$= \frac{1}{2} + \frac{1}{2} \operatorname{erf} \frac{1}{\sqrt{2}} \left(\frac{\Delta}{\sigma_e} \right) + \frac{1}{\sqrt{2\pi}} \left(\frac{\sigma_e}{\Delta} \right) \left[e^{-\frac{1}{2} \left(\frac{\Delta}{\sigma_e} \right)^2} - 1 \right] \quad (4.4.4)$$

$$\text{For } \left(\frac{\Delta}{\sigma_e} \right) > 4, \quad P_s \approx 1 - 0.399 \left(\frac{\Delta}{\sigma_e} \right) \quad (4.4.5)$$

Fig. 4.3 shows how the predictor success probability, and corresponding average element entropy, vary with the

[†] In which $p(\epsilon)$ is the probability density function of the error $\epsilon(t) = m_e(t) - m(t)$

Predictor success probability P_s
 Entropy of average element H_T

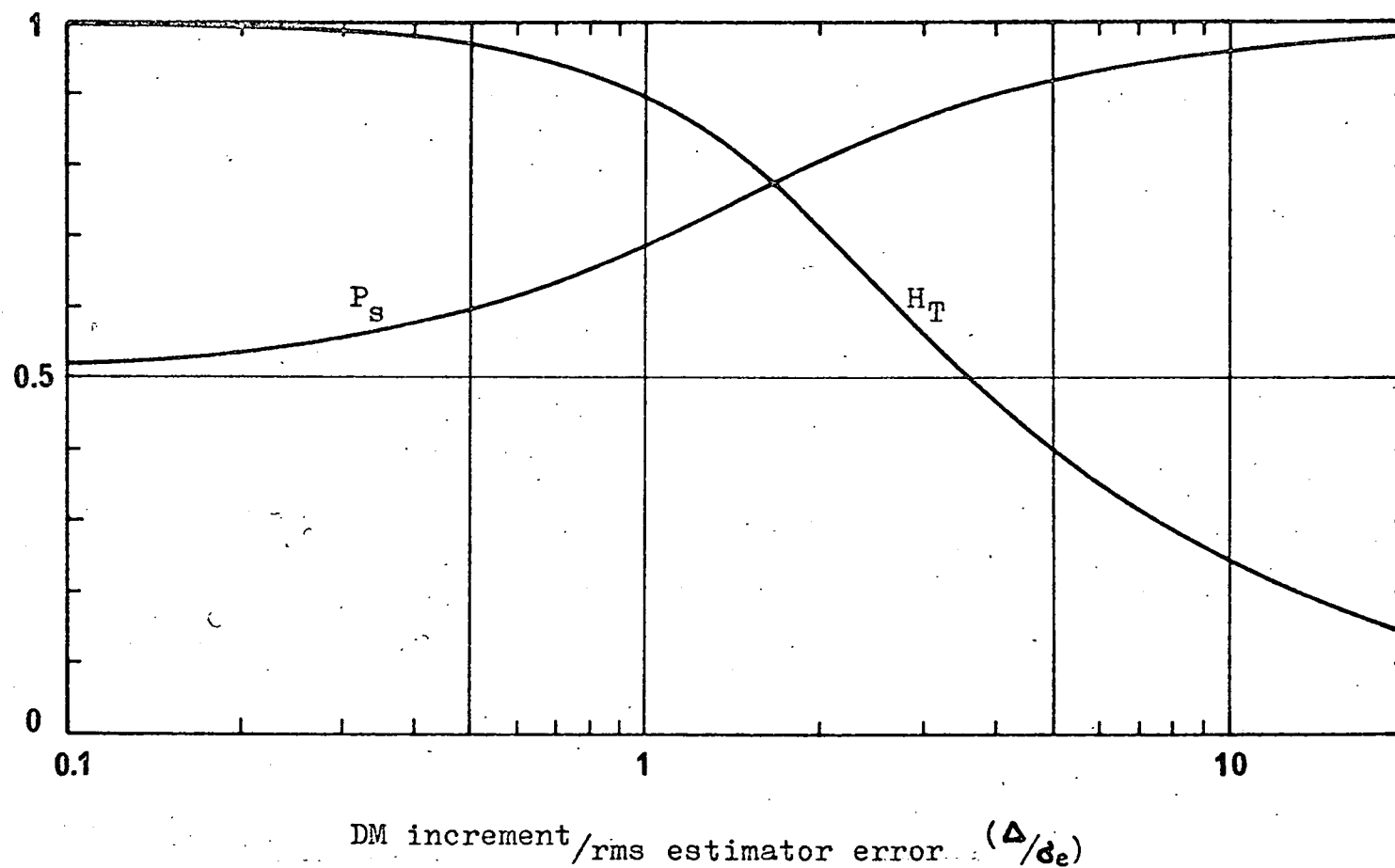


Fig. 4.3 Linear prediction success probability

relative magnitudes of Δ increment and rms estimator error.

For the estimator with the optimum transfer function given by (4.3.9), the error power is determined from (4.3.5), (4.3.7) and (4.3.11) by computing the integral square of the inverse transform of $\Psi^+(\omega)$ over an adequate time range

$$\overline{\epsilon^2(t)} = \varphi_{mm}(0) - \frac{1}{2\pi} \int_0^\infty [\psi^+(\tau)]^2 d\tau \quad (4.4.6)$$

in which $\varphi_{mm}(0) = 1$ for unit message power.

The relation between relative estimator error and SNR is then determined from (2.2.2), (2.4.7) and (4.4.6) and shown in Fig. 4.4, from which it is found that the corresponding power saving η (4.2.4) indicated by the characteristics as attainable by predictive coding ranges from 59% at low SNR for which DM is relatively satisfactory to over 70% where the quality required is high and the inefficiency of conventional DM is greater.

4.5 Implementation

Convolution of the input signal and the weighting function given by (4.3.13) yields the estimate

$$m_e(t) = \int_0^\infty w(\tau) m_i(t-\tau) d\tau \quad (4.5.1)$$

For a digital implementation with a finite duration signal sequence, $w(\tau)$ is truncated at $\tau = \theta$ and scaled to retain

$$\int_0^\theta w(\tau) d\tau = 1.$$

$\frac{\text{DM increment}}{\text{rms estimator error}} \quad (\Delta/\delta_e)$

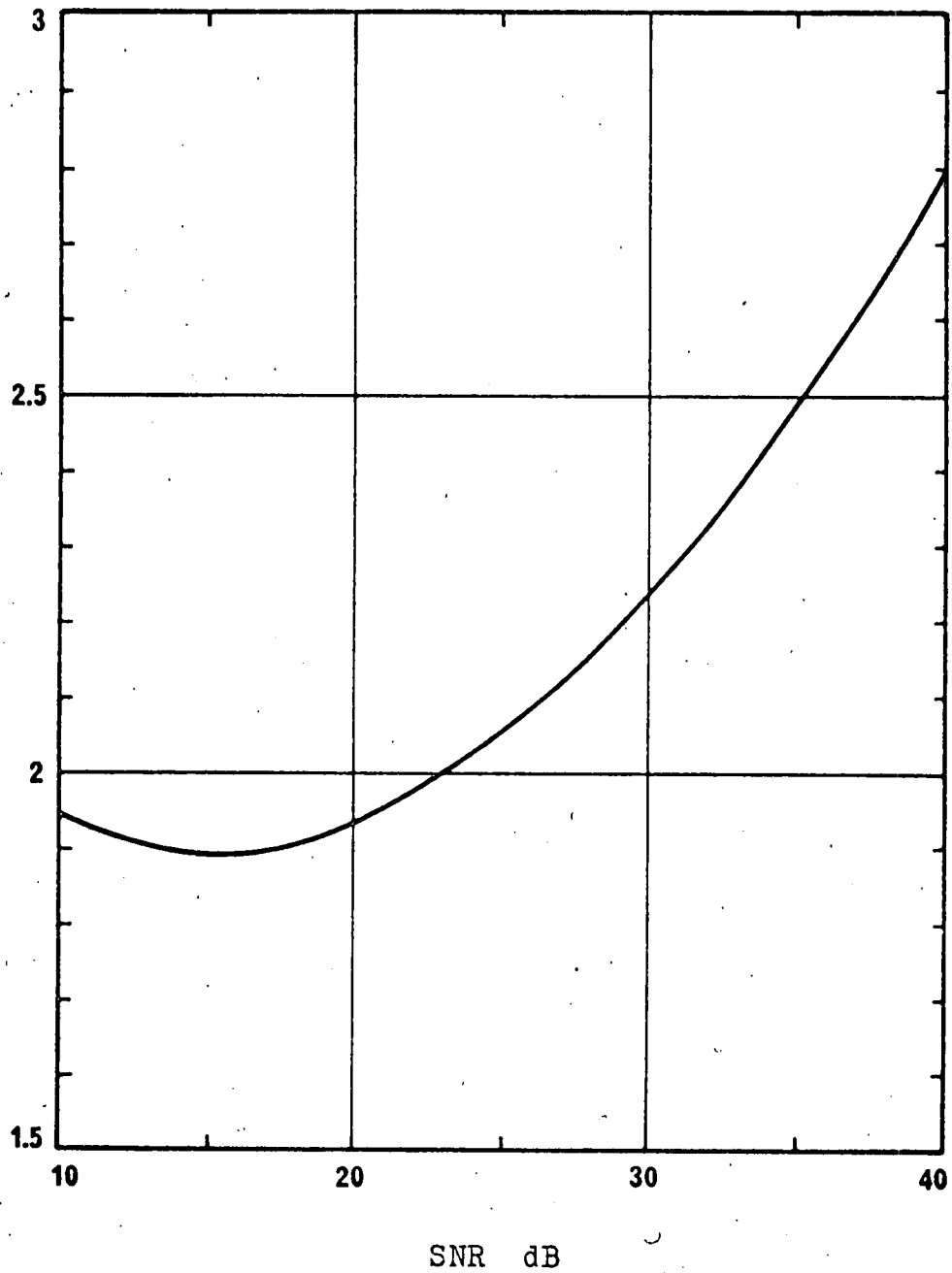


Fig. 4.4 Relative estimator error

Then approximately

$$m_e(t) = \int_0^{\theta} w_i(\tau) m_i(t - \theta + \tau) d\tau \quad (4.5.2)$$

in which $w_i(\tau) = w(\theta - \tau) \quad (4.5.3)$

The multiply time of a digital computer (for PDP-8 360 μ S by software; or 21 μ S with extended arithmetic unit) is too great for real time evaluation of (4.5.2), so we proceed by calculating the integrand product by parts.

$$\begin{aligned} m_e(t) &= \left[m_i(t - \theta + \tau) \int_0^{\theta} w_i(\tau) d\tau \right]_0^{\theta} - \int_0^{\theta} \left[\frac{d}{d\tau} m_i(t - \theta + \tau) \right] \left[\int_0^{\theta} w_i(\tau) d\tau \right] d\tau \\ &= m_i(t) - \int_0^{\theta} \left[\frac{d}{d\tau} m_i(t - \theta + \tau) \right] [f(\tau)] d\tau \end{aligned} \quad (4.5.4)$$

where the integral weighting function

$$f(\tau) = \int w_i(\tau) d\tau \quad (4.5.5)$$

The logical prediction E being determined by the sign of $[m_e(t) - m_i(t)]$, we have

$$\begin{aligned} E &= 1, \quad \int_0^{\theta} \left[\frac{d}{d\tau} m_i(t - \theta + \tau) \right] [f(\tau)] d\tau \leq 0 \\ &= 0, \quad \quad \quad > 0 \end{aligned} \quad (4.5.6)$$

At any time t, the function $\frac{d}{d\tau} m_i(t - \theta + \tau)$ is a signal sequence which is the time derivative of that portion of the input signal from $\lambda = t - \theta$ to the immediate datum $\lambda = t$. The sequence is a bipolar impulse train with value zero between the sampling instants, so that the relevant values of $f(\tau)$ form



a fixed ordinate set. Implementation of (4.5.6) by a data processor therefore involves for each prediction only the fast summation ($3\mu\text{S}$ per addition in two's complement arithmetic with directly addressed operand) of the members of the set with sign gated by the polarity of the corresponding impulses of the derivative sequence.

This procedure has been tested with PDP-8 for a speech message* of 43 sec. duration and parameters $f_s = 48\text{ KHz}$, $\text{SNR} = 25\text{ dB}$, and yields a predictor success probability of 0.72, increased to 0.75 with a refinement by which after an error the decision threshold is adjusted for subsequent data to a level such that the estimate would just have resulted in the complement prediction. Program organisation trades processor memory size for arithmetic capability by arranging that the appropriate 19 DM code blocks of 7 bits selected from the data page during a sampling period each address locations in core store containing the corresponding integral contributions for one segment of the weighting function, so that only 18 additions are executed although a 133 bit sequence is processed.

The integral contribution set is calculated by a larger KDF9 computer and converted in tape code and by the addition of

*The reading of 'The North Wind and the Sun' which is the source message for the University of Edinburgh's PAT speech synthesiser and can also be generated by the Atlas computer of Manchester University.

pseudo instructions by PDP-8 to a source language program for translation by Macro-8 assembler to the binary format data sequence actually loaded into core memory. As the optimum weighting function $w(\tau)$ for $\tau > 0$ is less than 1% of $w(0)$ and the quantisation of the ordinates of $f(\tau)$ is fine (12 bit), an analogue estimator would be expected to have a similar performance.

Chapter 5

Relative entropy

Following the introduction of chapter 4, the signal information properties of delta-coded speech are now determined in detail. A stochastic state transition probability matrix source representation is used throughout, the matrix being 2^N square for an Nth order approximation and containing two non-zero complementary elements per operand state column vector. Of course, all the matrix elements for an unconstrained symbol source have value 0.5, while greater and lesser transition probabilities from high probability operand states will correspond to significant redundancy in the sequences generated.

5.1 Transition matrix assembly

The matrix assembly software, a combined octal/symbolic listing of part of which is given in Appendix 3 (but treatment of some features is deferred), has the characteristics briefly described in the following.

With a typical test signal sequence in excess of 4 million bits (a 42 sec. duration message sampled at 96 KHz), the high probability states are entered more frequently than the maximum count which can be stored by one word of core memory, so that two consecutive locations are utilised per counter to store the

parts of upper and lower significance. Additionally, for each state entered, two counts are required to total the transition frequencies to both of the possible subsequent states, so that a memory allocation of 2^{N+2} words is required for an Nth order approximation. Computations for $N \leq 9$ may therefore be performed by the 4096 - word PDP-8, and one half of the core memory is available for program instructions, literals, temporary registers, loading, initializing, list processing, code conversion and output routines and the one page cycling data register.

On entry, the counter and temporary storage registers and transfer flags are cleared, the data register is loaded with an alternate sequence of binary digits and the data and state address registers are initialized. The program interrupt is enabled and the machine cycles in an instruction loop until the interface generates the first data break request at the commencement of the speech message on magnetic tape. During the clock-synchronised program execution which is then initiated, the appropriate data page addresses are referenced to determine the current state and the subsequent transition, and the corresponding counters are incremented using the link as a carry register following accumulator overflow.

At the termination of a 46 minute test run, PDP-8 scans the pages of counters in sequence and generates the 9 element states corresponding to the addresses of the groups of 4 registers

which they have been allocated. A listing is produced by high speed paper tape punch of the state vectors, represented as 3 - digit octal numbers, followed by the transition totals for each of the possible following states, the double precision binary counts being converted to BCD before output in ASCII code. The counters are then scanned again and each state is masked to 8 elements only, the transitions from and to states which then become identical being summed and the limit of the output, but not of the register scan, being reduced by one half. This procedure continues repetitively with appropriate masks and limits to generate blocks of data for all Markov process orders $N = 9 - 0$, and the total bit count for the run is also accumulated and punched. A representative transition probability matrix for a 4th order approximation and typical DM parameters is given in Appendix 4.

5.2 Markov process entropy

To proceed with relative entropy computations based on the matrix element listings, the previous data and instruction set is over-written in core memory by the Fortran object time system by which are loaded interpretive code programs which operate on the data punched at the end of the test run for a range of analyses. For each process order N the entropy for every state is first computed and then the average H of all the entropies, each weighted in proportion to the probability of occurrence of the corresponding state, is determined in

accordance with (4.1.1).

Fig. 5.1 presents the results of five test runs with $f_s = 48$ KHz and values of Δ increment ranging from coarse quantisation to that causing frequent overloading. We find that in all cases, the redundancy of the delta-coded message exceeds one half for $N \geq 4$. The characteristics define the lower bounds of the channel capacity required for transmission of the DM signal after IP transformation by an encoder processing N elements only.

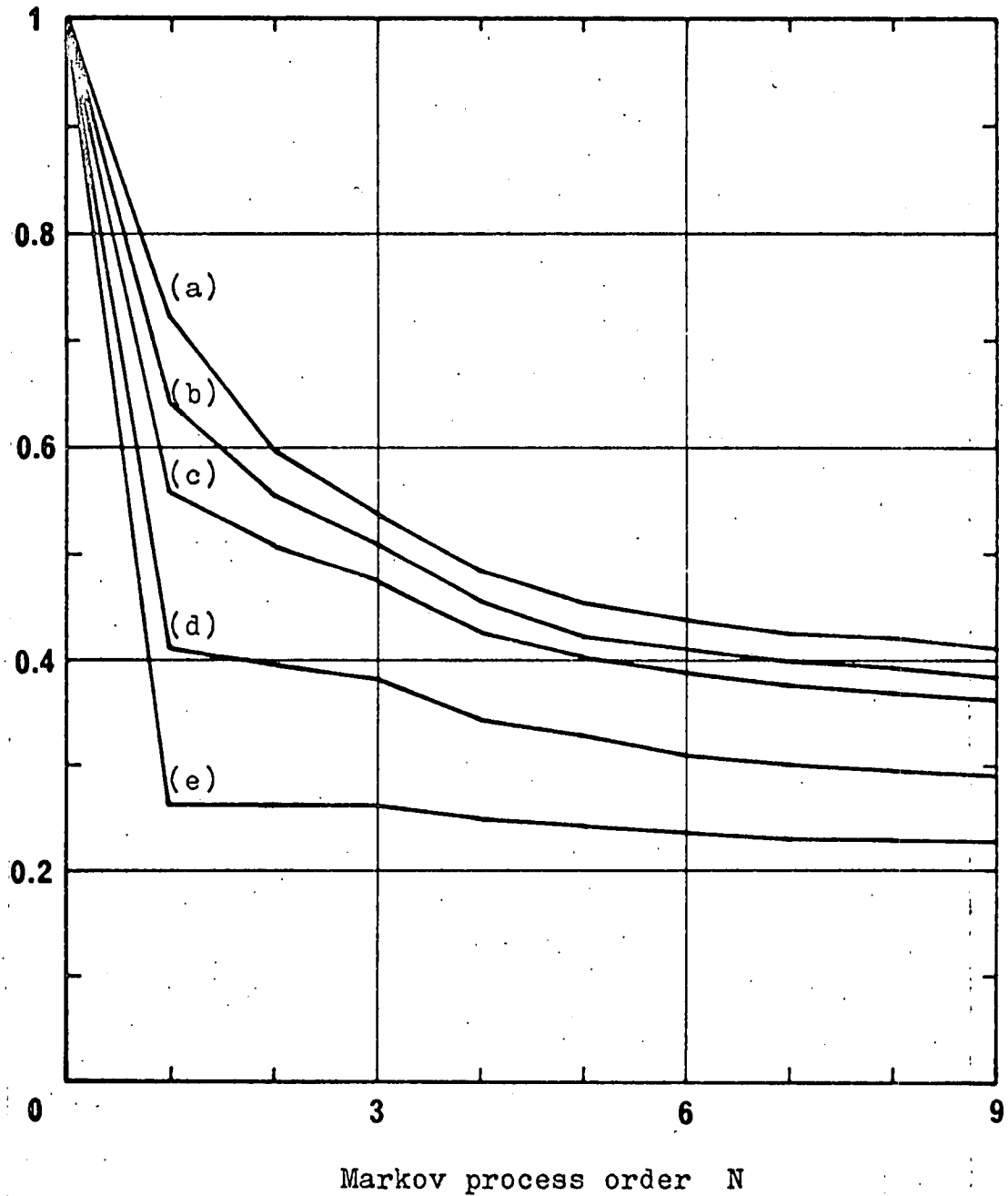
Redundancy reduction studies endeavour to determine practically convenient schemes which achieve performance approaching the bound with acceptable hardware complexity. Were the entropy computation continued for large N , a value for the total message information could be obtained by the procedure described, and this might correspond to a rather low value of relative entropy per element. But the result would be more apposite to a study of phonetic constraint than communications engineering since the memory requirement of an encoder capable of processing many elements increases in proportion with that of the computer required for the investigation.

5.3 Parameter variation

Information properties found to be subject to wide variation with choice of DM design parameters would entail

Relative
entropy

H



Pk - pk message amplitude (a) 70Δ (b) 56Δ (c) 42Δ
(d) 28Δ (e) 14Δ

Sampling frequency f_s 48 KHz

Fig. 5.1 Relative entropy characteristics

elaborate presentation and be of limited application.

Fortunately the relative entropy characteristics prove to be substantially independent of changes in sampling frequency and Δ increment provided their choice is appropriate (i.e. they are altered in inverse proportion). This invariance is shown by the constant overload probability groups of Fig. 5.2, which contain members for $f_s = 32, 48, \text{ and } 96 \text{ KHz}$, and comparison of the corresponding transition probability matrices shows that this property extends to the detailed predictor structures also. In general, parameter values $f_s = 96 \text{ KHz}$, peak-peak message amplitude 128Δ are considered, these being typical for good communications quality with infrequent overloading. Agreement between repeat test runs is better than 0.1%, and adequate test message duration is indicated by differences of less than 0.5% between results for the complete passage and its halves processed separately.

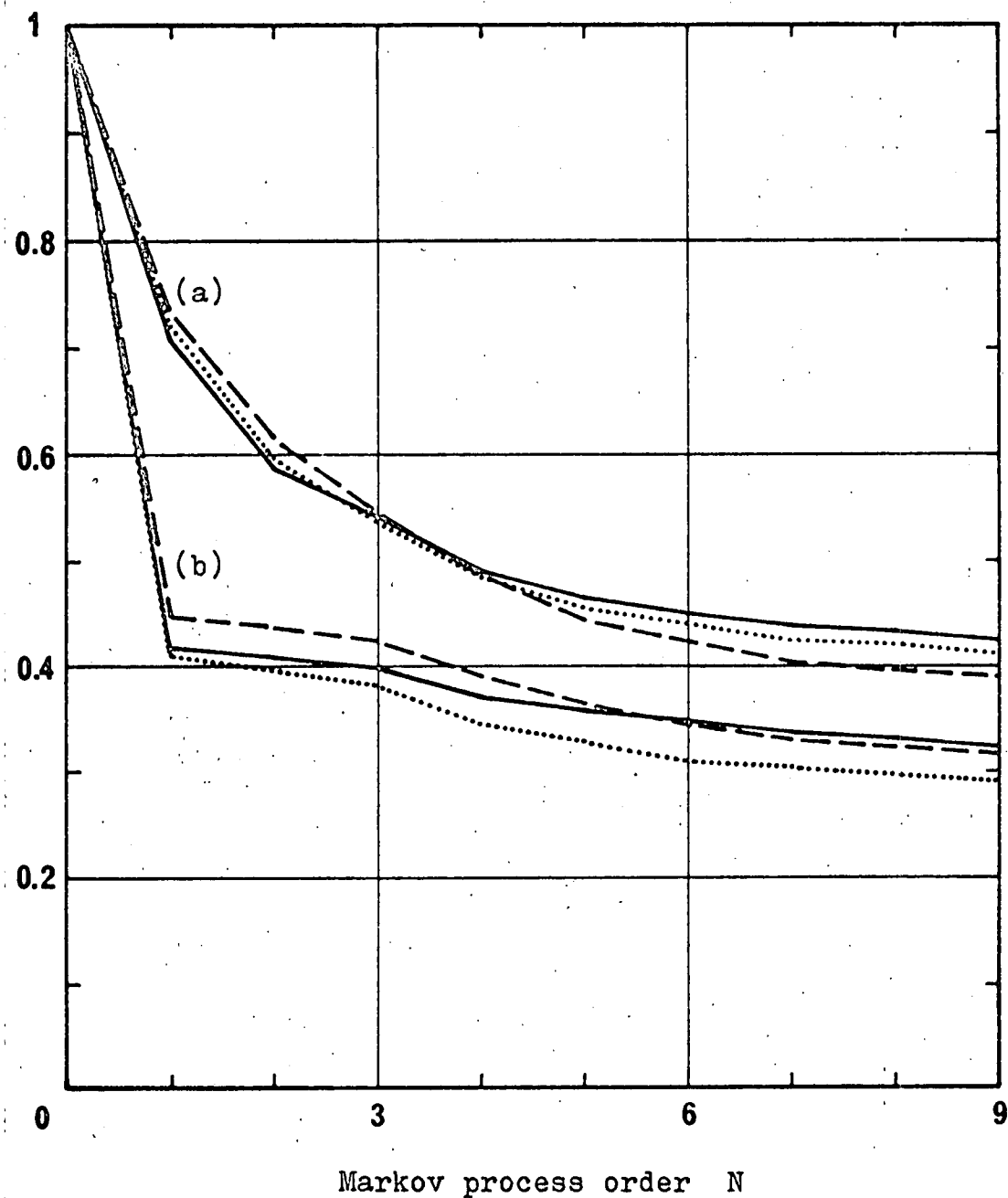
5.4 Transform sequence entropy

In generating a complete element listing for all vector source states, the transition matrix assembler implicitly defines the forms of the optimal discrete fixed-structure predictors operating on blocks of signal elements of length N .
† On identification of the current state, the next element is predicted by these functions such that the subsequent state is that for which the transition probability is known to be a maximum.

† The attention of the reader is drawn to this statement, which defines the non-linear prediction procedure. An example is given in Appendix 4.

Relative
entropy

H



Constant $\Delta f_s =$ Pk message amplitude $\times \begin{cases} 1.39 & \text{group (a)} \\ 3.48 & \text{" (b)} \end{cases}$

Sampling frequency $f_s \begin{cases} \text{---} & 32 \\ \text{.....} & 48 \\ \text{---} & 96 \end{cases} \text{ KHz}$

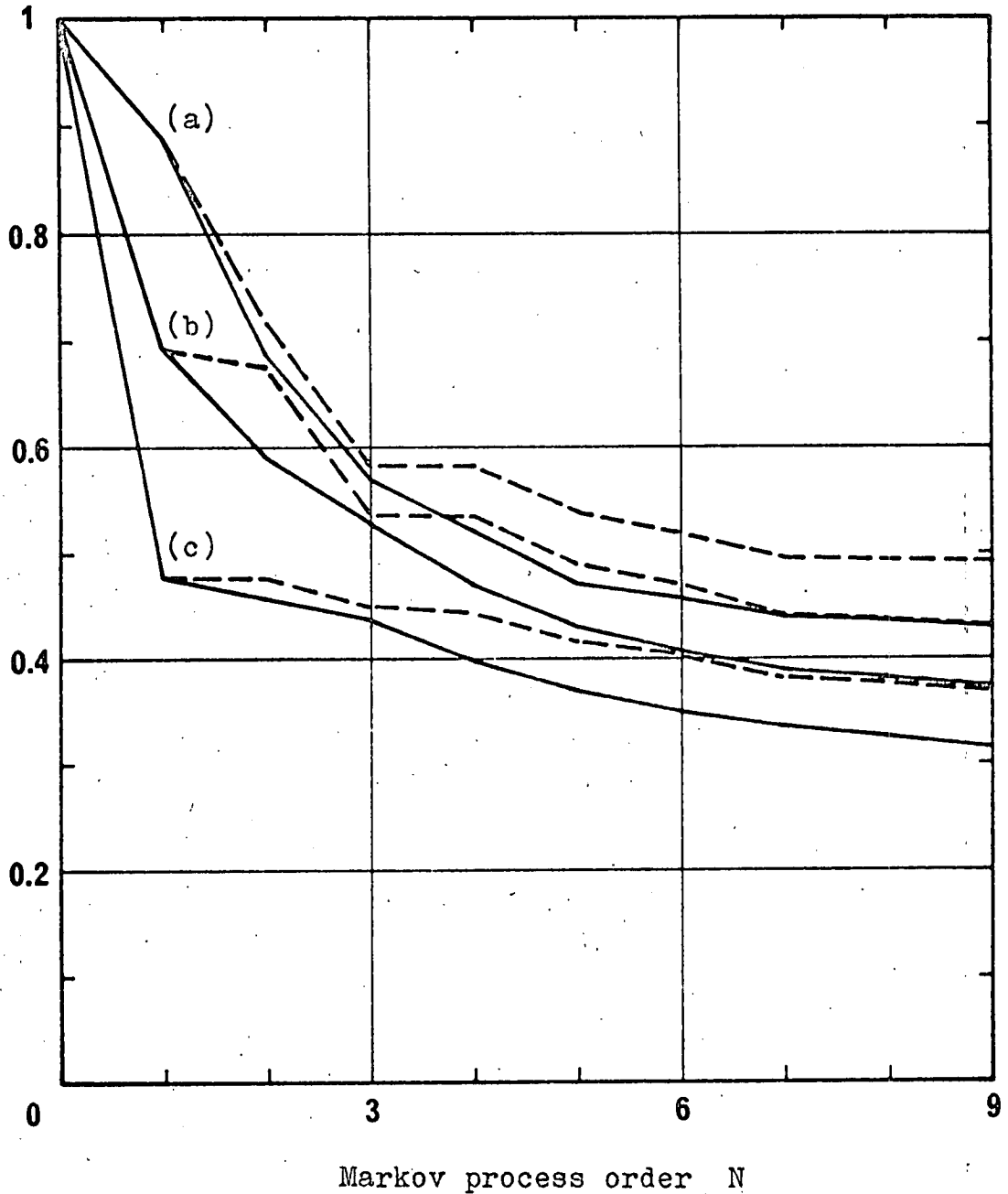
Fig. 5.2 Process entropy for constant overload probability

Since the transformation of Fig. 4.1 is IP, the asymptotic process entropies for the DM source signal and modulo-2 adder output sequence are the same, but the entropy of a zero order approximation to the latter, computed for three test runs and shown by the characteristics of Fig. 5.3, is much less than that of a zero order representation of the former. For a range of N and Δ , the average element entropy of the transformed sequence for N element prediction does not greatly exceed the process entropy of an N th order approximation to the delta-coded message source and for the typical median characteristic, an $N = 6$ predictor achieves $P_g = 0.9$, corresponding to a power economy $\eta = 80\%$. The average element entropy is within 14% of the 6th order process entropy, and the redundancy in both cases exceeds one half. The optimal predictors for this characteristic for $N = 1 - 7$ are given in Table 5.4.

While increase of N by one order doubles the number of distinguishable states, the optimal predictor structure and performance changes only if the transition probability distributions for two or more of the states previously considered together have maxima for complementary next elements. In the cases of characteristic (a) for $N = 3 - 4$ and (c) for $N = 1 - 2$ in Fig. 5.3, for example, this does not occur so that predictors operating on the shorter signal sequences are as effective as those processing the longer.

Relative
entropy

H, H_T



————) Relative entropy of process (order N)
 - - - - -) Half adder output sequence entropy (zero order)
 with N element optimum predictor

Pk - pk message amplitude (a) 256Δ (b) 128Δ (c) 64Δ

Sampling frequency f_s 96 KHz

Fig. 5.3 Predictive coding sequence entropy (zero order)

TABLE 5.4 OPTIMAL PREDICTORS FOR DELTA CODED SPEECH

SAMPLING FREQ 96 KHZ PK-PK MESSAGE AMP 128 DELTA
(VECTOR STATES IN OCTAL)

N = 1

STATE	PRED
0	1
1	0

N = 2

0	0
1	0
2	1
3	1

N = 3

0	0	4	1
1	0	5	0
2	1	6	1
3	0	7	1

N = 4

00	0	10	1
01	0	11	0
02	1	12	1
03	0	13	0
04	1	14	1
05	0	15	0
06	1	16	1
07	0	17	1

N = 5

00	0	10	1	20	0	30	0
01	0	11	0	21	0	31	0
02	0	12	1	22	1	32	1
03	1	13	0	23	0	33	0
04	1	14	1	24	1	34	0
05	0	15	0	25	0	35	1
06	1	16	1	26	1	36	1
07	1	17	1	27	0	37	1

N = 6

00	0	10	1	20	0	30	1	40	0	50	1	60	0	70	0
01	0	11	0	21	0	31	0	41	0	51	0	61	0	71	0
02	0	12	1	22	1	32	1	42	0	52	1	62	1	72	1
03	1	13	0	23	0	33	0	43	0	53	0	63	0	73	1
04	0	14	1	24	1	34	1	44	1	54	1	64	1	74	0
05	0	15	0	25	0	35	1	45	0	55	0	65	0	75	1
06	1	16	1	26	1	36	1	46	1	56	1	66	1	76	1
07	0	17	1	27	0	37	1	47	0	57	1	67	0	77	1

N = 7

000	0	020	0	040	0	060	0	100	0	120	0	140	0	160	0
001	0	021	0	041	0	061	0	101	0	121	0	141	0	161	0
002	0	022	0	042	0	062	1	102	0	122	1	142	0	162	0
003	1	023	0	043	0	063	0	103	1	123	0	143	0	163	0
004	0	024	1	044	1	064	1	104	0	124	1	144	0	164	0
005	0	025	0	045	0	065	0	105	0	125	0	145	0	165	0
006	1	026	1	046	1	066	1	106	1	126	1	146	1	166	1
007	1	027	1	047	0	067	0	107	0	127	0	147	0	167	1
010	0	030	1	050	1	070	1	110	1	130	1	150	0	170	0
011	0	031	0	051	0	071	0	111	0	131	0	151	0	171	0
012	1	032	1	052	1	072	1	112	1	132	1	152	1	172	1
013	1	033	1	053	0	073	1	113	0	133	0	153	0	173	1
014	1	034	1	054	1	074	0	114	1	134	1	154	1	174	0
015	1	035	1	055	0	075	1	115	0	135	1	155	1	175	1
016	1	036	1	056	1	076	1	116	1	136	1	156	1	176	1
017	1	037	1	057	1	077	1	117	1	137	1	157	1	177	1

Chapter 6

Group encoding

Instantaneous group encoding procedures considered by Shannon⁽⁷⁾, Fano⁽²¹⁾ and Huffman⁽²²⁾ effect redundancy reduction by the assignment, to N element blocks B_i of the signal sequences generated by a source, of uniquely decipherable N_i element codewords in a manner determined by their occurrence probability set. For all procedures, the average channel capacity required for transmission of the encoded signal, expressed per element of the source output, approaches G_N (4.1.2) as N increases, while G_N converges to H for large N , so that the coding schemes are asymptotically completely efficient. But for finite N the Huffman approach yields group codes with optimal efficiency, and its application to delta-coded speech is therefore studied for a comparative evaluation with predictive coding.

6.1 Group entropy

To compute the relative entropy of groups of signal elements, the transition matrix element listings are again processed by a PDP-8 Fortran program. For each listing for source approximation order N , the occurrence frequencies of $N+1$ element blocks are simply the separate transition totals from every state. The entropy contributions for each such group are totalled and

divided by $N+1$ to obtain the relative entropies per element of the encoded sequence and the results are shown in Fig. 6.1. The group entropies are compared with the Markov process and modulo-2 adder output sequence entropies based on the same total number of signal elements, including the immediate elements in the last two cases, direct transmission corresponding to a zero order approximation or encoding in groups of one element. The characteristic defines a lower bound to the required channel capacity for signal transmission after group encoding by any procedure.

By optimal coding it is always possible to establish a transformation resulting in an average codeword length $\sum_i p(B_i) N_i$ within one element of the average block total entropy NG_N , so that an upper bound, also shown in Fig. 6.1, is set by

$$NR_B \leq NG_N + 1 = NR_M \quad (6.1.1)$$

in which the ratio of the channel capacity required for the encoded signal to that for direct transmission

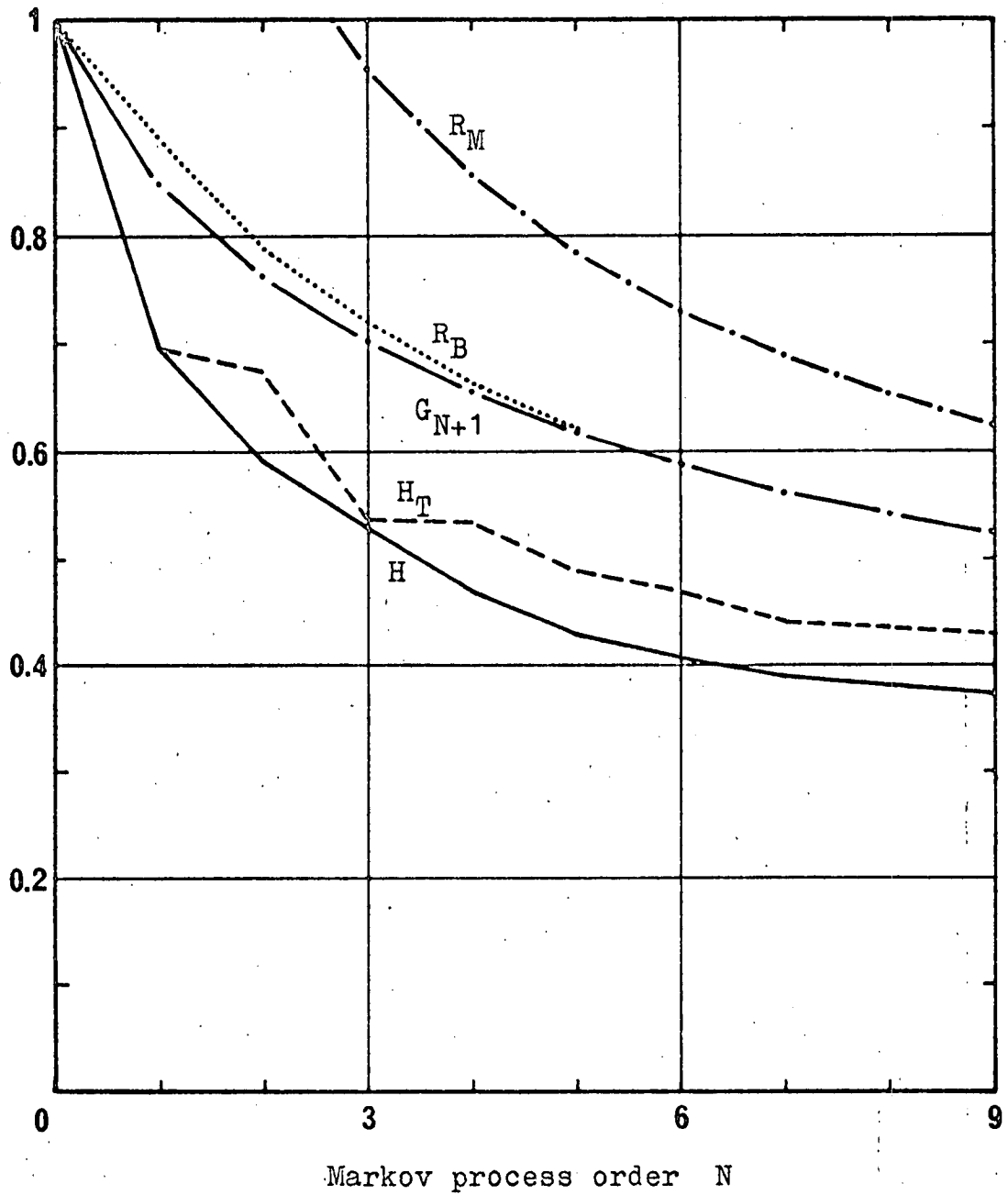
$$R_B = \sum_{i=1}^{2^N} \frac{p(B_i) N_i}{N} \quad (6.1.2)$$

indicates the redundancy reduction produced.

6.2 Optimal group codes

Limited computer memory capacity dictates a two stage computational - topological technique for the determination of

Relative
entropy



- R_M Upper bound for group encoding
- R_B Huffman encoder characteristic
- G_{N+1} N+1 element group entropy
- H_T Mod - 2 adder sequence entropy
- H Process entropy

Fig. 6.1 Delta coded speech entropies

the optimal codes. First the structures of the trees of successive state subsets are defined by processing the matrix element listings; then the trees are constructed and the codewords generated by the manual assignment of symbols to the intermediate branches.

For each group length, PDP-8 is programmed to initially scan the terminal nodes and locate the two states for which the sums of the transition probabilities to subsequent states are least. These states are printed and combined as a subset, described by the numerically lower and having probabilities equal to the sums of those of its member pair. After elimination of the higher state from the scan the process is repeated until the final two subsets are combined as the root. Then the state subset trees, of which Fig. 6.2 for 5 element groups is representative, are drawn from the intermediate node locations indicated by the state print-outs and the codewords are determined by tracing the unique path to each state via the annotated branches.

The optimal group codebooks for 2 to 6 signal elements are given in Table 6.3. Codes for larger blocks are unlikely to be of practical interest because of their complexity and the long word lengths associated with low probability states.

6.3 Code evaluation

To evaluate the efficiencies of the group codes, the codeword lengths N_i elements, indicated for each block by

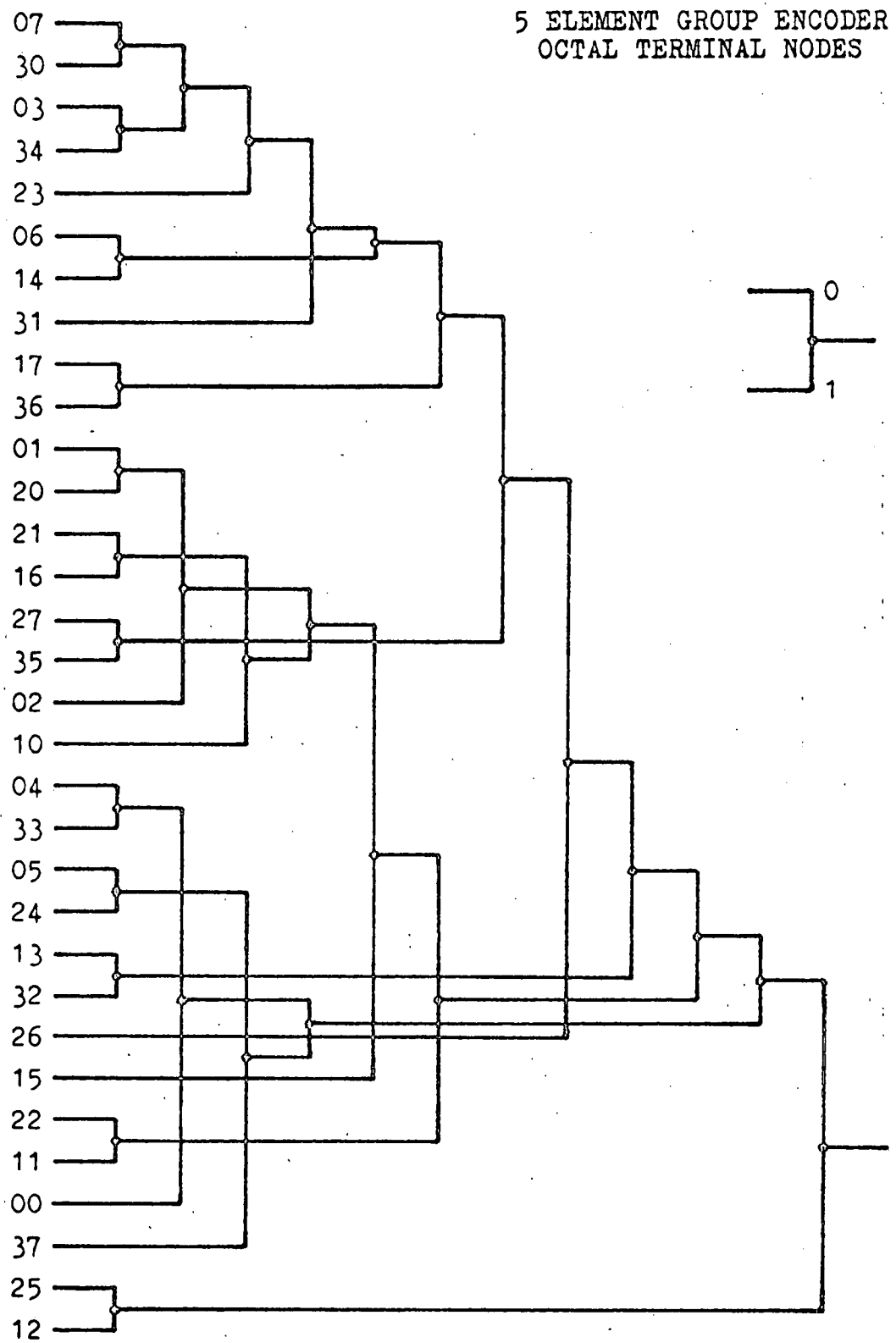


Fig. 6.2 State subset tree

Table 6.3, are loaded by a program which assigns them to the appropriate groups B_i of the source sequence. Each element is considered to be the first of a following group, so that the evaluation for each group length N is the average for N effective test runs with time origins at each of the elements of the leading DM code block. The element numbers for the effective runs are totalled and compared directly with the corresponding total message bit counts and values of R_B are shown in Fig. 6.1.

In appraising the group encoding results, it is noted that even for small N , the codes are efficient in the sense that R_B is near the lower bound set by the relative entropy of groups of $N + 1$ elements of the source sequences, and the performance characteristic converges to G_{N+1} much faster than does the upper bound R_M . But the convergence of G_N to the process entropy H is slow, so that large blocks must be encoded to achieve a high overall coding efficiency.

In comparison, the relative entropy (zero order) H_T of the modulo-2 adder output sequence for an N element optimum predictor remains much closer to H for all N , so that a predictive coding approach is found to be superior to optimal group encoding for delta-coded speech. H_T for a 3 element predictor for example, which has a quite elementary structure (Table 5.4), is lower than the attainable R_B for blocks of 8 elements, although the group encoder for the latter is complex in form and generates very long codewords.

TABLE 6.3 OPTIMAL CODEBOOKS FOR DELTA CODED SPEECH

BLOCK LENGTH N+1 ELEMENTS

N = 1

0 001
1 1
2 01
3 000

N = 2

0 001 1
1 000 10
2 1
3 000 00
4 000 11
5 01
6 010 01
7 001 0

N = 4

00 010 1
01 001 000 00
02 001 000 1
03 000 000 000 010
04 010 00
05 011 00
06 000 000 010
07 000 000 000 000
10 001 001 1
11 001 11
12 11
13 000 10
14 000 000 011
15 001 01
16 001 001 01
17 000 000 10

N = 5

00 000 11
01 001 010 010
02 000 001 00
03 001 000 100 001
04 000 000 1
05 001 000 100 01
06 001 000 100 000 001
07 001 000 000 001

N = 3

00 000 1
01 000 001
02 010 1
03 000 000 01
04 011 0
05 10
06 010 01
07 000 011
10 000 010
11 010 00
12 11
13 011 1
14 000 000 00
15 001 0
16 000 000 1
17 001 1

20 001 000 01
21 001 001 00
22 001 10
23 000 000 000 1
24 011 01
25 10
26 000 01
27 000 001 0
30 000 000 000 001
31 000 000 001
32 000 11
33 010 01
34 000 000 000 011
35 000 001 1
36 000 000 11
37 011 1

10 001 001 1
11 001 011 0
12 010 11
13 000 000 001 0
14 001 000 100 000 1
15 001 000 100 1
16 001 000 100 000 000 01
17 000 000 000 100

(N = 5 CODEBOOK CONTINUED)

20	000	000	01				
21	001	000	01				
22	001	11					
23	000	000	001	1			
24	010	01					
25	10						
26	011	10					
27	000	000	000	01			
30	001	000	100	000	000	001	
31	001	010	000	0			
32	011	00					
33	001	011	1				
34	001	000	100	000	000	000	01
35	001	001	00				
36	000	010	001				
37	001	010	001				
40	001	010	011				
41	000	010	000				
42	001	000	11				
43	001	000	100	000	000	000	1
44	000	011					
45	011	01					
46	001	010	000	1			
47	001	000	100	000	000	000	00
50	000	000	000	11			
51	011	11					
52	11						
53	010	10					
54	001	000	000	1			
55	000	10					
56	001	001	01				
57	000	001	01				
60	000	000	000	001			
61	001	000	100	000	000	1	
62	001	000	001	1			
63	000	000	000	000			
64	001	000	001	0			
65	010	00					
66	001	010	1				
67	000	001	1				
70	000	000	000	101			
71	001	000	100	000	01		
72	001	000	000	01			
73	000	010	1				
74	001	000	000	000			
75	000	010	01				
76	001	000	101				
77	001	10					

Chapter 7

Non-linear prediction

In developing the application of the general results of chapter 5 to the realization of a practical predictive coding procedure, attention is now restricted to a single typical case. Hardware complexity estimates based on Table 5.4 and attainable performance data indicated by Fig. 6.1 suggest that for delta-coded speech with peak-to-peak amplitude 128Δ and sampling frequency 96 KHz a 6th order predictor offers substantial encoding gains ($\eta = 80\%$, or $H_T = 0.48$) for a small investment per channel and the form of such an encoder is now considered in detail.

7.1 Predictor function

As a consequence of the information source asymptotic equipartition property fundamental to Shannon's central theorems, the source state ensemble for N large comprises a 2^{NH} member set of high probability and a remaining set of low probability. While a distinct set boundary does not occur for $N = 6$, $H = 0.41$, it may be inferred that a number of the 64 states of the ensemble will have quite low probabilities, and this is confirmed by the transition matrix listing. Eight states have occurrence probabilities less than 0.01%, and in a chain of over 4 million states, there are no occurrences at all

of 34_8 , all transitions to 70_8 and 71_8 being from 74_8 . This property may be exploited to derive practically convenient predictor functions which represent worthwhile simplifications at the expense of negligible performance degradation from that of the optimal structure.

If the predictor is implemented as a codebook with addressable memory, it is possible without seriously affecting the success probability to group together states with low probabilities of occurrence, and those with high occurrence probabilities but near equiprobable transition probabilities (high state entropies), and assign them an arbitrary prediction collectively. Alternatively, a more efficient simplification may be effected by the study of a Veitch-Karnaugh map representation of the optimal predictor function, which distinguishes those states for which allowing non-optimal prediction results in a direct logic hardware saving, and this is shown in Fig. 7.1. Correlation of the transition matrix with this approach indicates the numerous low probability states for which the simplest factoring is in fact achieved by optimal prediction.

Assertion of the 6 code elements processed is indicated in Fig. 7.1 by binary variables A, B, . . . F in order of generation time and the two dimensional array of predicted elements within the map is formatted to exhibit combinatorial symmetry for variable elimination about the central axes shown

N = 6 PREDICTOR
KARNAUGH MAP

ROW = 1ST 3 BIT GROUP
COL = 2ND 3 BIT GROUP

	000	001	011	010	110	111	101	100			
000	0	0	X	0	1	X	0	0	\bar{A}	\bar{B}	\bar{C}
001	1	0	0	1	1	1	0	1			C
011	1	0	0	1	1	1	1	1			\bar{C}
010	0	0	0	1	1	0	0	1			\bar{C}
110	0	0	0	1	1	0	0	1	A	B	\bar{C}
111	X	0	1	1	1	1	1	X			C
101	1	0	0	1	1	1	0	1			\bar{B}
100	0	0	0	0	1	0	0	1			\bar{C}
\bar{D}					D						
\bar{E}		E					\bar{E}				
\bar{F}	F		\bar{F}		F		\bar{F}				

Fig. 7.1

LOGIC FUNCTION

$$\begin{aligned}
 &A \cdot B \cdot C \cdot E + C \cdot \bar{F} + D \cdot E \cdot \bar{F} + B \cdot E \cdot \bar{F} + C \cdot D \cdot E + B \cdot C \cdot D + B \cdot D \cdot \bar{E} \cdot \bar{F} + A \cdot D \cdot \bar{E} \cdot \bar{F} \\
 &= A \cdot B \cdot C \cdot E + C \cdot \bar{F} + E \cdot \bar{F} \cdot (D + B) + C \cdot D \cdot (E + B) + D \cdot \bar{E} \cdot \bar{F} \cdot (A + B)
 \end{aligned}$$

as well as within the 16 element quadrants. For the map area corresponding to each state, there are six 'adjacent' areas corresponding to states differing in one element only, and between which it may be eliminated by grouping; four from the same quadrant and two images in the opposite parity quadrants.

By assigning 'don't care' predictions X to certain areas, the 1's factoring may be carried out as shown in groups of four or fewer variables by combining four or more elements per term and the sub-optimal predictor function becomes

$$A \cdot B \cdot C \cdot E + C \cdot \bar{F} + E \cdot \bar{F} \cdot (D + B) + C \cdot D \cdot (E + B) + D \cdot \bar{E} \cdot \bar{F} \cdot (A + B) \quad (7.1.1)$$

7.2 Processor form

The predictor function is compactly programmed for computer evaluation as the sequential application to the current state of a set of masks and tests based on the following properties implied by (7.1.1).

Prediction F: 4 states with $C - F = 0$, 4 with $C - F = 1$;
02 and its 5 element equivalent 42;
their 6 element complements 75 and 35;
04 and its complement 73.

Prediction \bar{F} : Remaining states, including 4 assigned 'don't cares'.

By prefixing the information analysis program by this test sequence as shown in Appendix 3, and incorporating modulo-2 addition of the prediction and source sequence before the

assembly routines, transition matrix element listings for the predictive coded message are generated which can be processed in the same way as those for the DM signal direct.

The results show that P_s for the former case and $N = 0$ is less than for the latter and $N = 6$ by 0.14%, which only slightly exceeds the variation between repeat runs. So the performance of the sub-optimal predictor described is little degraded from that of the optimal structure by the simplifications allowed in its derivation.

7.3 IC predictive coder

Existing expertise in monolithic semiconductor technology permits the fabrication of the predictive coder as a single functional array integrated circuit, and to establish the logic configuration for such an array a high speed saturated transistor-transistor encoder design has been evolved as shown in Fig. 7.2.

The encoder gates the outputs of the shift register of three dual J-K master-slave flip flops which store the signal elements to be processed. Complement outputs drive triple 2-input positive NAND gates which OR element 5 with 2, 3 and 6 and then dual 4-input and triple 3-input units effecting logical AND, the outputs of which are OR'd by a single 5-input gate to generate the prediction. While a small logic simplification could be achieved by the integration of the mod-2

adder with the prediction gating, it is convenient for system testing to preserve its separate identity and it is therefore assigned a distinct quad 2-input unit. The output of the adder conditions the encoder output flip flop on the arrival of the shift pulse which clocks into slot 1 of the shift register the most recent signal element with which the prediction has been compared. Obvious modifications of the structure form the corresponding decoder, in which the input signal drives the mod-2 adder but the output sequence enters the shift register.

The IC predictive coder is shown in Fig. 7.3. As PDP-8 is a negative logic system, it is powered from the positive bias channel and used in conjunction with level converting modules to exchange signals with the computer interface.

7.4 Data errors

In direct DM transmission, signal detection errors due to channel noise result in an output SNR reduction which has been found by Braun et al⁽²³⁾ to range from 1 dB for error probability $P_e = 0.001$ to 15 dB for $P_e = 0.1$. When the redundancy of the signals generated by an information source is reduced, the susceptibility of the message to mutilation by noise is increased. For the predictive coding of delta-coded speech, incorrectly detected elements cause the same immediate signal reconstruction errors on reception, but in addition P_s is reduced by the impairment of the decoder predictor's assessment

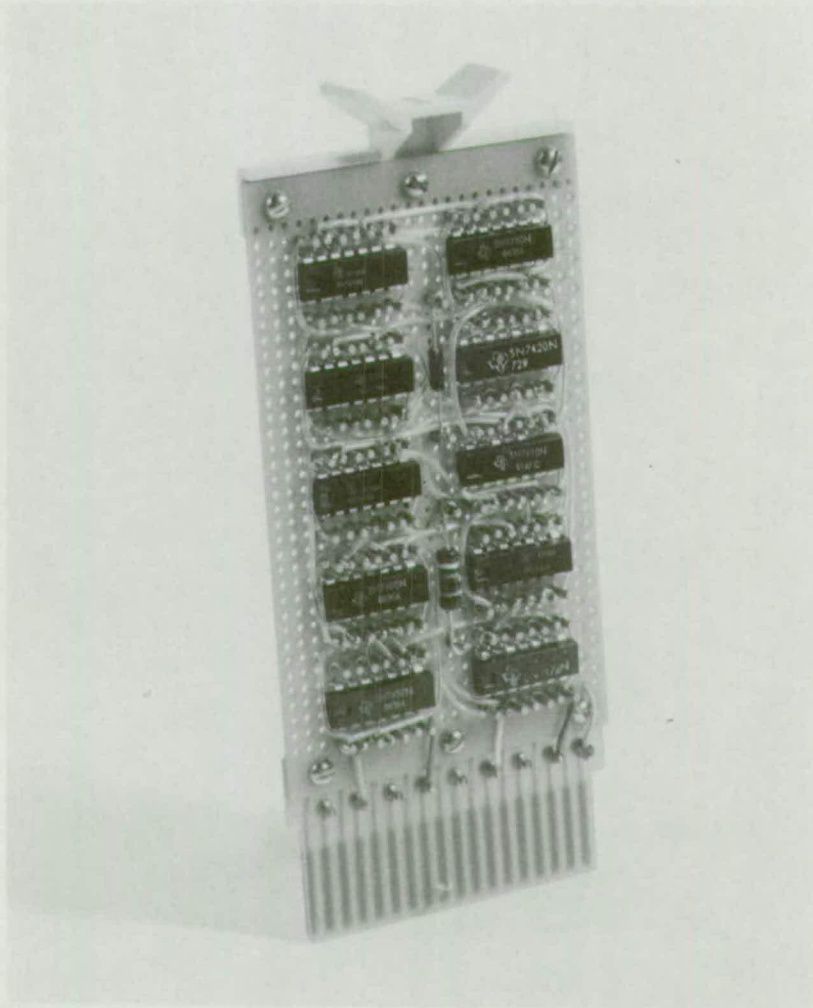


Fig. 7.3 TTL encoder for DM speech

of the subsequent N states and the increased entropy of the data sequence.

The sensitivity of the 6th order predictor performance to data errors is determined by a series of processor runs in which random element errors are introduced with a range of controlled probabilities P_b by facilities included in the software listing Appendix 3. Routines generate members of a random number set uniformly distributed over 0000-7777 during each sampling interval and cause the transmission of complement pulses to the interface when the samples exceed a switch register specified threshold which is P_b as an octal fraction.

The degradation of P_s with increasing data error rate is shown in Fig. 7.4, with the corresponding rise in H_T as the sequence properties change from the constrained statistics of delta-coded speech to those of binary random noise. The predictor remains effective for error rates up to that causing a considerable reduction in output SNR. However, as with all differential transmission systems, it is advisable to inhibit error accumulation by the periodic clearing of encoder and decoder memories, in this case conveniently to 12_8 or 25_8 .

Predictor success probability P_s

Entropy of average element H_T

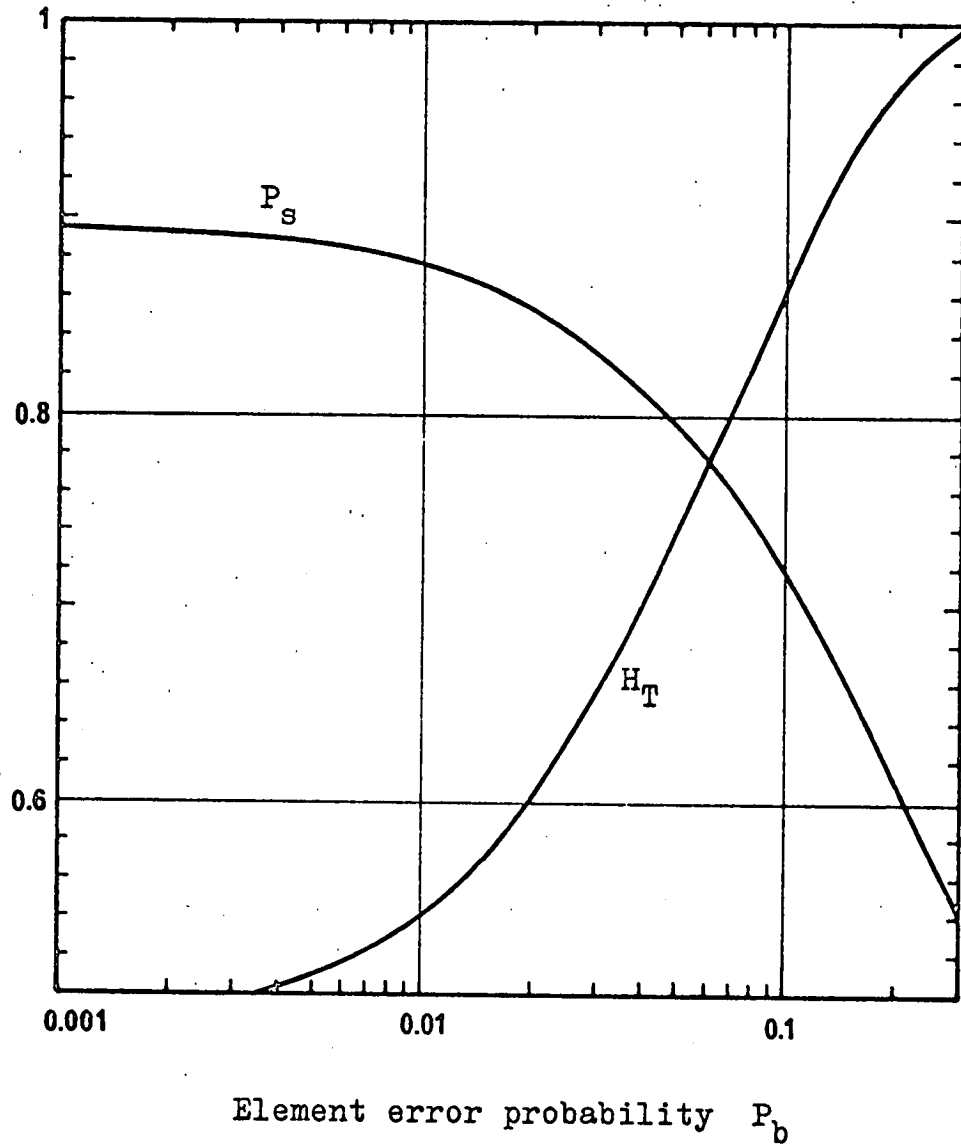


Fig. 7.4 $N=6$ predictor error performance

Chapter 8

Error sequence encoding

Having established that the realization of a 6th order near - optimal predictive coder capable of reducing the average element entropy of a delta-coded speech message by one half is practical, we now explore applications to channel encoding and transmitter power economy. The binary signal sequence generated by modulo-2 addition of the DM message and predictor output is termed the encoder error sequence, for as detailed in Sec. 4.2 it has the function of indicating the errors in the decoder predictions. Three methods of variable length coding the error sequence to achieve channel bandwidth compression are evaluated and compared.

8.1 Direct error transmission

As was noted earlier, a transmitter power saving is achieved by direct transmission of the predictive coded sequence instead of the original DM message, and for the 6th order predictor with $P_g = 0.9$ this has value $\eta = 80\%$. In a pack set application in which low level circuits are microminiaturized and the power input to the final transmitter stages is a large proportion of the total, operational life from a primary power source is therefore extended by a factor of several times.

In addition, use of this mode extends to pulse systems the operational advantages brought to analogue communications by suppressed carrier VOX working. For both techniques result in there being no output from a sender except during speech utterances, so that single channel conversational mode operation becomes possible among the contributing members of a communications net, bit synchronisation being established by the transmitting member and no frame synchronisation being required to decode the transmitted sequences.

The entropy characteristics of Fig. 6.1, and the corresponding predictor performances, were computed by processing a speech message generated by the continuous reading of a prepared text. In the case of duplex communications, the power saving (and also the detection immunity) compared with direct delta-coding are therefore further enhanced by the occurrence of intervals during which the transmitter output of a listening operator is zero, although his talk channel remains active for interruption of the sender at any time. The power saving for this case becomes

$$\eta = 100(1 - 2P_t + 2P_sP_t)\% \quad (8.1.1)$$

in which P_t is the channel activation probability, so that an extension of operational life by a factor of 10 is indicated in this service for $P_t = 0.5$.

At fixed stations, primary power consumption is generally a minor consideration and for a transmitter limited by output device

mean dissipation the encoding gains are more usefully exploited to allow an increase in channel signal power. The thermal time constants of the dissipating structures of high-power tubes and semiconductors are typically sufficient to smooth the fluctuations during speech and allow close to a factor of $1/2(1 - P_s)$ increase (7 dB for the 6th order predictor), but they are not sufficient to average the dissipated power over active and inactive periods in duplex working. For the case of a peak power limited sender, and for other ways of exploiting the redundancy of delta-coded speech, we must consider further processing of the encoder error sequence.

8.2 Error sequence entropy

In the channel encoder situation, it is required to translate the attainable average element entropy reduction to a decrease in bit rate*, either to increase the size of the TDM group or (pursuing a total coding philosophy advocated in the literature) to cascade the operation of removal of the inefficient source redundancy with that of substitution by the check digits of an error-correcting code chosen specifically for the particular channel noise properties encountered.

By processing the transition matrix listings produced by the software predictive coder of Sec. 7.2 by the Fortran programs outlined in Sec. 5.2, the error sequence information properties

* This may be termed a 'bandwidth compression' although the component digital signals are not associated with distinct spectral segments of their multiplex.

The TDM group situation is considered because the buffer requirement it demands is moderate.

summarized in Fig. 8.1 are determined. The process entropy characteristic given indicates the reduction of the statistical interdependence of sequential elements resulting from the coding, for the invariant distribution for the zero order case with element probabilities P_s , $1 - P_s$, has entropy not exceeding those computed from the sets of conditional distributions for $N = 1 - 9$ by more than 16%. The variation with N of TH_T , the average element entropy of the sequences generated by a second application of predictive coding, using optimal predictors of order N , to the error sequence for coding with the near-optimal 6th order predictor, is even less over this range. In fact an extension of the initial predictor order by 1 achieves an entropy reduction which it requires a second application predictor order $N > 9$ to match.

8.3 Run-length encodings

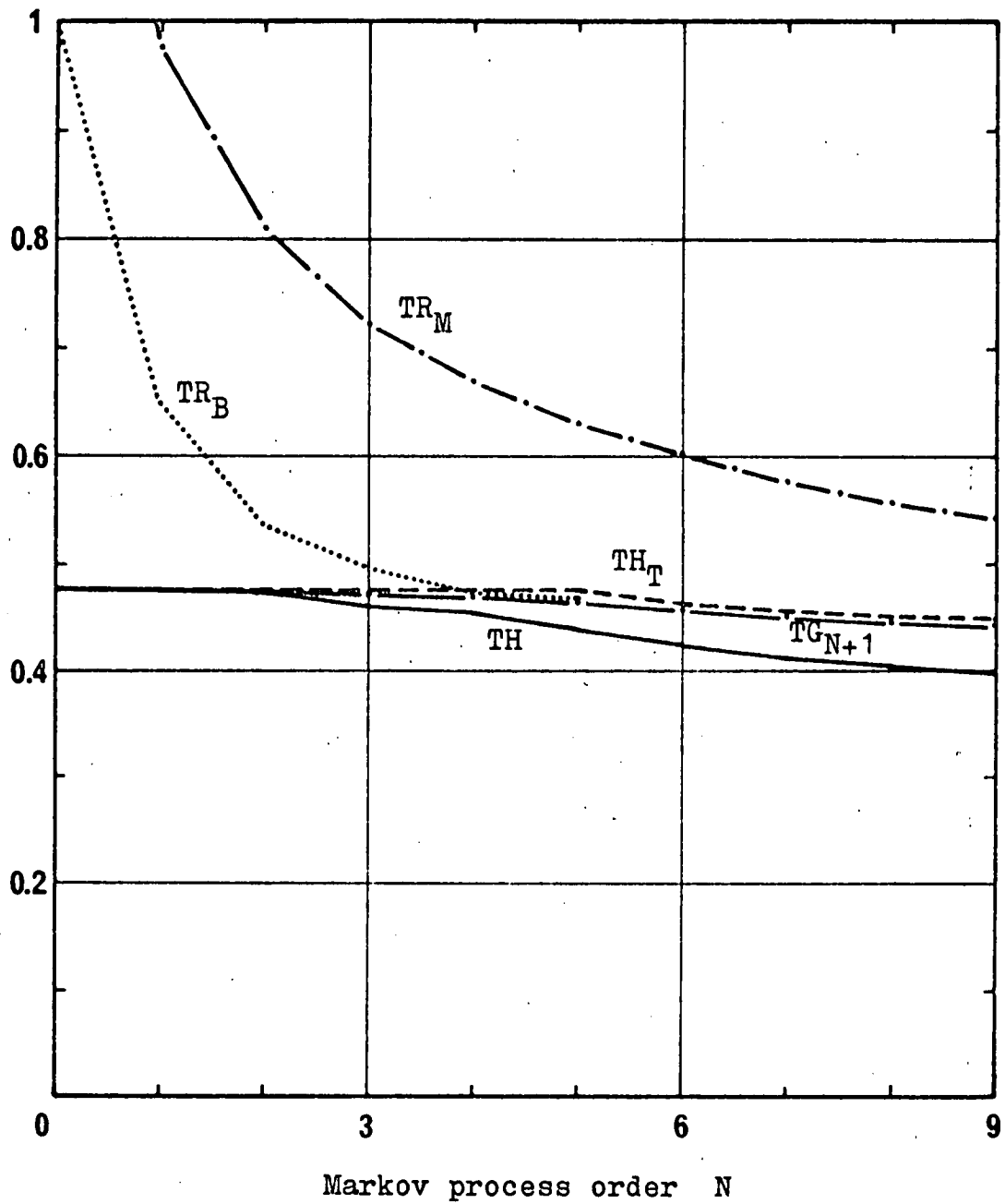
The zero order approximation to the error sequence suggested by the entropy results of Fig. 8.1 implies a geometric probability distribution for the lengths of runs of consecutive 0 symbols in the sequence. The probability of a run of length r ($r \geq 0$, so that every symbol 1 both terminates and starts a run) is

$$P_{gr} = P_s^r (1 - P_s) \quad (8.3.1)$$

and the entropy per selection from the distribution,

$$H_g = \sum_{r=0}^{\infty} P_{gr} \log P_{gr}, \quad (8.3.2)$$

Relative
entropy



TR_M Upper bound for group encoding
 TR_B Huffman encoder characteristic
 TG_{N+1} $N+1$ element group entropy
 TH_T Mod - 2 adder sequence entropy
 TH Process entropy

Fig. 8.1 Error sequence entropies

has value 4.66 bits for the 6th order predictor.

The average sequence length per run,

$$L_g = \sum_{r=0}^{\infty} P_{gr}(r+1) \quad (8.3.3)$$

is 9.83 elements and the relative entropy per element

$$H_{gr} = H_g/L_g = 0.474, \text{ corresponding to } TH_T \text{ for } N=0.$$

Similar form relations derive from the actual run probabilities P_r .

Error sequence run-length distributions are determined by processor tests with a program assembled by Macro-8 which executes predictive coding of the DM speech input and, on termination of all run-lengths $r < 256$, increments the appropriate registers of double precision occurrence counts assigned to 4 pages of core memory. The run occurrence frequencies are punched out on paper tape and subsequently processed by Fortran programs. Fig. 8.2 compares the run-length distribution for the typical DM parameter case with the geometric distribution for the same P_g , and distributions for other cases are similar. Deviations for small r are caused by the previous element dependence of the error element distribution remaining after coding, and for $r \geq 7$, P_r is always less than P_{gr} .

From the run probability results, the average entropy per run is computed as 4.31 bits and the average sequence length per run as 9.75 elements so that the relative entropy per element $H_r = 0.442$ is rather lower than for the geometric distribution.

Run probability P_r, P_{gr}

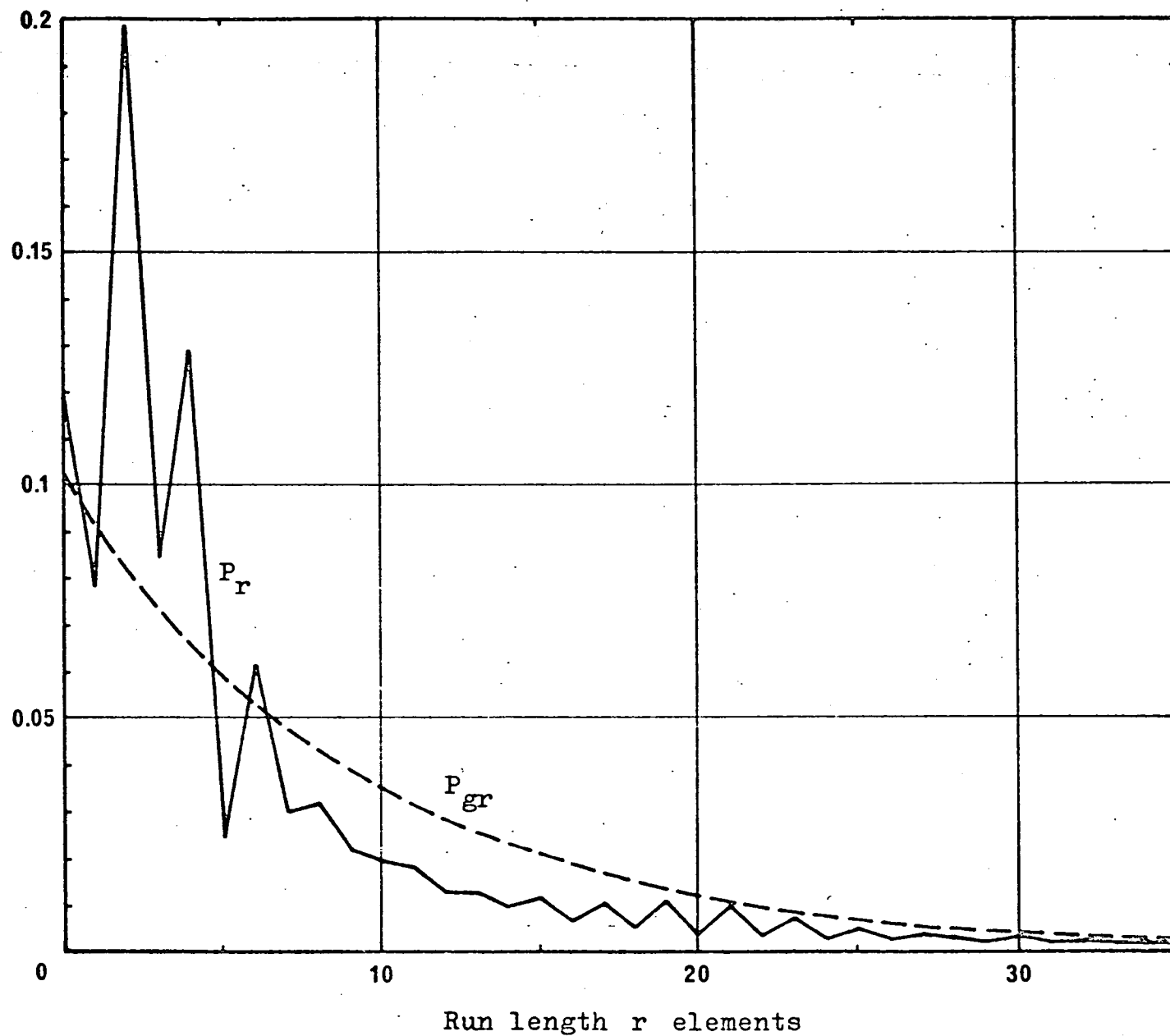


Fig. 8.2 Run length distributions

While Huffman encoding of the run-lengths in accordance with their occurrence probabilities, allows this compression to be closely attained, the codebook is quite large (64 entries to include 98% of the run-lengths) and the encoder, although very much simpler than that which would be required to achieve the same compression by a direct application to the source sequence (over 32K entries), is still unattractively complex.

Considering only comma-free codes for direct transmission through binary channels, a first practical alternative is fixed length binary number coding of the run-lengths, which of course is still a variable rate encoding procedure overall because of the distribution of element sequence lengths selecting each number. For this approach 6 bit coding yields a compression of 0.615, while encoding only run-lengths 0 - 31 (which includes 94% of the total) by 5 bits results in a ratio of 0.513. The occurrence of the longest runs, which are associated with quiet intervals between spoken words, is a function of the system noise and reverberation prior to source encoding and is likely to be less frequent in the average communications situation than for the studio environment in which the test message is prepared and the precision laboratory equipment by which it is processed.

For a second procedure of intermediate complexity, the set of P_r may be approximated by a geometric distribution which Golomb⁽²⁴⁾ has noted is favourable to Huffman encoding for

integer values of

$$m = - \frac{\log 2}{\log P_s} \quad (8.3.4)$$

For the 6th order predictor, $m = 6$ is appropriate and the initial entries for the run-length codebook are given in Table 8.3, examination of the structure of which reveals the following encoding rule for a run-length of r elements:

By division of r by 6, obtain $6A + R$. (integers $A \geq 0$,
 $0 \leq R \leq 5$)

Encoding rule: Output A binary 1's, followed by

$\left\{ \begin{array}{l} \text{for } 0 \leq R \leq 1, \text{ the 3 bit binary representation of } R \\ \text{for } 2 \leq R \leq 5, \text{ the 4 bit binary representation of } R+2 \end{array} \right.$

An equally straightforward decoding rule applies.

Evaluation of this encoding procedure for the actual run-length distribution of Fig. 8.2 indicates an average relative entropy (per element of the error sequence) of 0.486, reduced to 0.406 by truncation of the codebook at 32 entries. The approximation of the run-length statistics by a geometric distribution, and of P_s by a value giving m integer, thus yields a practical run-length encoding scheme with performance within 10% of H_r .

8.4 Group error encoding

While predictive coding has been considered in earlier sections as an IP transformation lowering the source sequence

TABLE 8.3

RUN LENGTH CODEBOOK

M = 6 GEOMETRIC DISTRIBUTION

<u>R</u>	<u>CODEWORD</u>
0	000
1	001
2	010 0
3	010 1
4	011 0
5	011 1
6	100 0
7	100 1
8	101 00
9	101 01
10	101 10
11	101 11
12	110 00
13	110 01
14	110 100
15	110 101
16	110 110
17	110 111
18	111 000
19	111 001
20	111 010 0
21	111 010 1
22	111 011 0
23	111 011 1
24	111 100 0
25	111 100 1
26	111 101 00
27	111 101 01
28	111 101 10
29	111 101 11
30	111 110 00
31	111 110 01

average element entropy, significant reductions are effected in the entropies of blocks of N elements for $N \geq 2$ also. The group entropy characteristic TG_{N+1} and upper bound for the optimal coding TR_M shown in Fig. 8.1 are obtained for the encoder error sequence by the processing method described in chapter 6 for the DM signal prior to coding. In the present case, TG_{N+1} remains much closer to TH , even for N small, and is actually slightly less than TH_T .

As a third approach, the group codes are therefore constructed by the application, to the encoder error sequence transition matrix element listings, of the computational - topological procedure described earlier, and the optimal codebooks are given in Table 8.4. Evaluation of these codes yields the characteristic TR_B shown in Fig. 8.1 for the reduction in required channel capacity. Convergence to the lower bound occurs rapidly, an average bit rate reduction of one half being obtained with groups of 4 only, and TR_B being less than TH_T for block length ≥ 5 . An attractive case, compromising considerations of coding efficiency and hardware complexity, is the 5 element group code which achieves $TR_B = 0.479$.

Comparison of the most practical case performance for each of the three error sequence encoding procedures described is now possible and the compression factors attainable are summarized below.

TABLE 8.4 OPTIMAL ERROR SEQUENCE CODEBOOKS

BLOCK LENGTH $N+1$ ELEMENTS

N = 1

0 1
1 01
2 000
3 001

N = 2

0 1
1 010
2 001
3 000 10
4 011
5 000 00
6 000 11
7 000 01

N = 4

00 1
01 011 1
02 010 1
03 010 000 00
04 001
05 010 000 1
06 000 000 1
07 000 001 010
10 011 0
11 000 01
12 010 001 1
13 000 001 011
14 010 001 0
15 000 000 000 000 00
16 000 001 000 1
17 000 000 010

N = 5

00 1
01 010 1
02 011 0
03 000 100 001
04 001 1
05 001 010 0
06 001 000 01
07 000 100 100 01

N = 3

00 1
01 010 0
02 011
03 000 010
04 001
05 000 101
06 000 001
07 000 000 10
10 010 1
11 000 11
12 000 011
13 000 000 01
14 000 100
15 000 000 001
16 000 000 11
17 000 000 000

20 000 1
21 010 010 0
22 010 011
23 010 000 01
24 000 001 1
25 000 000 000 1
26 000 000 001
27 000 000 000 010
30 010 010 1
31 000 001 000 0
32 000 000 000 011
33 000 000 000 000 01
34 000 001 001
35 000 000 000 001
36 000 000 011
37 000 000 000 000 1

10 011 1
11 000 101
12 001 000 1
13 000 100 100 1
14 001 001 1
15 000 100 000 000 000
16 000 100 100 00
17 000 000 000 1

(N = 5 ERROR SEQUENCE CODEBOOK CONTINUED)

20	010	0						
21	000	100	11					
22	000	011						
23	000	000	01					
24	001	010	1					
25	000	100	000	11				
26	000	000	101	1				
27	001	000	000	010				
30	001	001	0					
31	000	010	000	0				
32	000	100	000	000	001			
33	001	000	000	000	000	001	0	
34	000	100	000	01				
35	000	100	000	001	1			
36	000	000	100	1				
37	000	100	000	000	010			
40	000	11						
41	001	011						
42	000	010	1					
43	001	000	001					
44	000	001						
45	001	000	000	1				
46	000	100	101					
47	000	000	000	0				
50	000	100	01					
51	000	000	001					
52	000	100	000	10				
53	001	000	000	000	000	01		
54	000	000	101	0				
55	001	000	000	000	000	000	1	
56	001	000	000	000	01			
57	000	100	000	001	0			
60	000	000	11					
61	000	010	01					
62	000	010	000	1				
63	000	100	000	000	1			
64	001	000	000	011				
65	001	000	000	000	000	1		
66	001	000	000	000	000	001	1	
67	001	000	000	000	000	000	01	
70	000	010	001					
71	001	000	000	000	1			
72	001	000	000	001				
73	001	000	000	000	000	000	000	
74	000	000	100	0				
75	001	000	000	000	001			
76	000	100	000	000	011			
77	001	000	000	000	000	000	001	

(a)	6 element binary number coding of run-lengths	0.615
(b)	Geometric distribution run-length encoding	0.486
(c)	5 element group encoding of error sequence	0.479

Method (a) achieves simplicity at the cost of reduced efficiency, while speed considerations suggest that method (c), which attains the best performance with increased memory capacity, is preferable to obtaining a similar compression with greater arithmetic logic by method (b).

Chapter 9

Channel buffer

In speech communication, as opposed to telegraphy, the rate of reconstruction of the message for the recipient cannot be varied from its rate of generation without distortion of the intelligence conveyed, and this requirement is easily met in the case of conventional DM transmission for which the necessary channel capacity is the fixed maximum for $N = 0$. Where redundancy reduction is effected by a statistical encoding procedure, however, the required channel capacity is proportional to the information content of the source messages. At channel encoders and decoders, buffer stores are therefore necessary to smooth the fluctuating data rate for transmission and reconstruct its variation with time on reception. The analysis of the channel buffer situation presented in this chapter utilizes the theory of queueing (see Fry⁽²⁵⁾) developed by telephone traffic statisticians for considering trunking problems, and telephone switching system terminology is retained where it remains appropriate.

9.1 Queue organisation

For the specific numerical results, it is assumed that redundancy reduction is achieved by the 6th order predictor derived in chapter 7 followed by 5 element group encoding of the

error sequence by the code given in Table 8.4 ($N=4$). Each DM source, with data rate f_s , thus selects for transmission codewords of length $N_c = 1-14$ elements (excluding 2 and 11) at a rate $f_s/5$.

The sequence of codewords generated by successive selections by the members of the multiplex of N_m sources is held in the buffer store, of limited capacity N_q words, and this queue is serviced in order by the sender which transmits corresponding signals over the channel at a bit rate $N_m f_c$. For its complete transmission, each codeword requires a 'holding time' proportional to its length, after which the channel becomes available to service the next codeword in the buffer.

When a codeword is generated, it encounters a number w of codewords ahead of it awaiting or undergoing transmission. With a probability which is small, w is zero and the codeword is processed immediately; while more frequently it experiences a delay which will have duration $> \tau$ if $w-1$ or fewer codeword transmissions are completed during time τ . Buffer capacity and channel data rate require to be chosen such that τ rarely exceeds $5 N_q / f_s N_m$, so that the probability of buffer overflow* is small. The requirement for the receiver is

* Blasbalg and Van Blerkom⁽²⁶⁾ suggest degrading the source fidelity to maintain transmission when buffer overflow occurs. Short codewords which approximate the longer sequences selected may be sent until the overflow clears.

identical, codewords transmitted by the channel entering the buffer store which receives sequential service from the group decoder.

9.2 Codeword length distribution

From the information analysis of the predictor error sequence described in Sec. 8.2 the total occurrence frequency of each 5 element state is found and, by grouping those states for which the corresponding codewords from Table 8.4 are equal in length, the probabilities of all N_c are computed. The resultant integral distribution function $p(>N_c)$ is given in Fig. 9.1 and the average codeword length

$$N_a = \sum_{N_c=1}^{14} p(N_c) N_c \quad (9.2.1)$$

is 2.40 elements.

As shown, a negative exponential approximation to the distribution with the same average may be taken, for which

$$p(N_c) = \frac{1}{N_a} e^{-N_c/N_a} \quad (9.2.2)$$

For N_m large, successive codewords in the buffer queue may be considered to have lengths independently selected in accordance with this probability set.

The average channel holding time is $N_a/N_m f_c$, and the probability of a holding time exceeding t ,

$$p(>t) = e^{-t N_m f_c / N_a} \quad (9.2.3)$$

Probability of
length $> N_c$

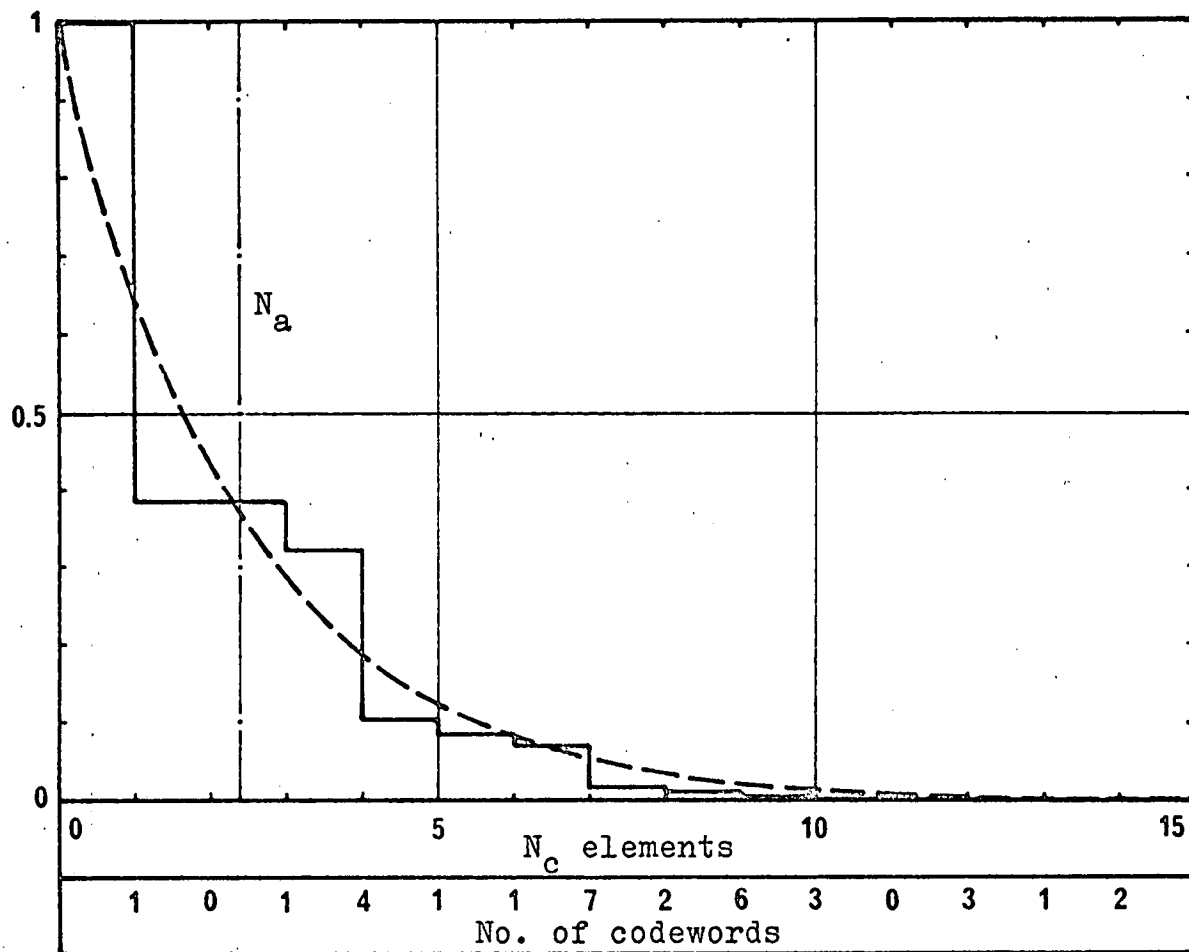


Fig. 9.1 Codeword length distributions

while a holding time between t and dt occurs with probability

$$p(t) dt = \frac{N_m f_c}{N_a} e^{-\frac{t N_m f_c}{N_a}} dt \quad (9.2.4)$$

Thus the probability of the transmission of a codeword ending during dt ,

$$\frac{p(t) dt}{p(>t)} = \frac{N_m f_c}{N_a} dt \quad (9.2.5)$$

independent of the time of commencement of transmission.

Now the probability p_1 that one codeword transmission ends during an interval τ is the probability that none ends between 0 and t ($t < \tau$), one ends between t and $t + dt$, and none ends in the remaining time up to τ . From (9.2.3) and (9.2.5),

$$\begin{aligned} p_1 &= \int_0^{\tau} e^{-\frac{t N_m f_c}{N_a}} \cdot \frac{N_m f_c}{N_a} \cdot e^{-\frac{(\tau-t) N_m f_c}{N_a}} dt \\ &= \left(\frac{\tau N_m f_c}{N_a} \right) \cdot e^{-\frac{\tau N_m f_c}{N_a}} \end{aligned} \quad (9.2.6)$$

Similarly for 2 codewords,

$$\begin{aligned} p_2 &= \int_0^{\tau} e^{-\frac{t N_m f_c}{N_a}} \cdot \frac{(\tau-t) N_m f_c}{N_a} \cdot e^{-\frac{(\tau-t) N_m f_c}{N_a}} \cdot \frac{N_m f_c}{N_a} dt \\ &= \left(\frac{\tau N_m f_c}{N_a} \right)^2 \frac{1}{2} e^{-\frac{\tau N_m f_c}{N_a}} \end{aligned} \quad (9.2.7)$$

Extending this approach, the probability that transmission of $w-1$ codewords is completed during time τ has the Poisson distribution

$$p_{w-1} = \left(\frac{\gamma N_m f_c}{N_a} \right)^{w-1} \frac{1}{(w-1)!} e^{-\frac{\gamma N_m f_c}{N_a}} \quad (9.2.8)$$

9.3 Buffer capacity

From (9.2.5) and (9.2.8), the probability that a particular codeword is delayed in the buffer for an interval γ and then the channel becomes available during dt is

$$p_\gamma = \sum_{w=1}^{\infty} p(w) \left(\frac{\gamma N_m f_c}{N_a} \right)^{w-1} \frac{1}{(w-1)!} e^{-\frac{\gamma N_m f_c}{N_a}} \frac{N_m f_c}{N_a} dt \quad (9.3.1)$$

For a total rate of selection of codewords of $N_m f_s/5$, we have from the recurrence relations of queueing theory (Molina⁽²⁷⁾)

$$p(w) = p(0) \left(\frac{f_s}{5} \cdot \frac{N_a}{f_c} \right)^w \quad (9.3.2)$$

For

$$\begin{aligned} \sum_{w=0}^{\infty} p(w) &= 1, & p(0) &= \frac{1}{\sum_{w=0}^{\infty} \left(\frac{f_s N_a}{5 f_c} \right)^w} \\ & & &= 1 - \frac{f_s N_a}{5 f_c} \end{aligned} \quad (9.3.3)$$

(Jolley⁽²⁸⁾)

Substituting in (9.3.1),

$$\begin{aligned} p_\gamma &= \left(1 - \frac{f_s N_a}{5 f_c} \right) \frac{N_m f_s}{5} e^{-\frac{\gamma N_m f_c}{N_a}} \sum_{w=1}^{\infty} \frac{\left(\frac{\gamma N_m f_s}{5} \right)^{w-1}}{(w-1)!} dt \\ &= \left(1 - \frac{f_s N_a}{5 f_c} \right) \frac{N_m f_s}{5} e^{-\left(1 - \frac{f_s N_a}{5 f_c} \right) \frac{\gamma N_m f_c}{N_a}} dt \end{aligned} \quad (9.3.4)$$

Hence the probability of a codeword being delayed

Average queue
 N_b codewords

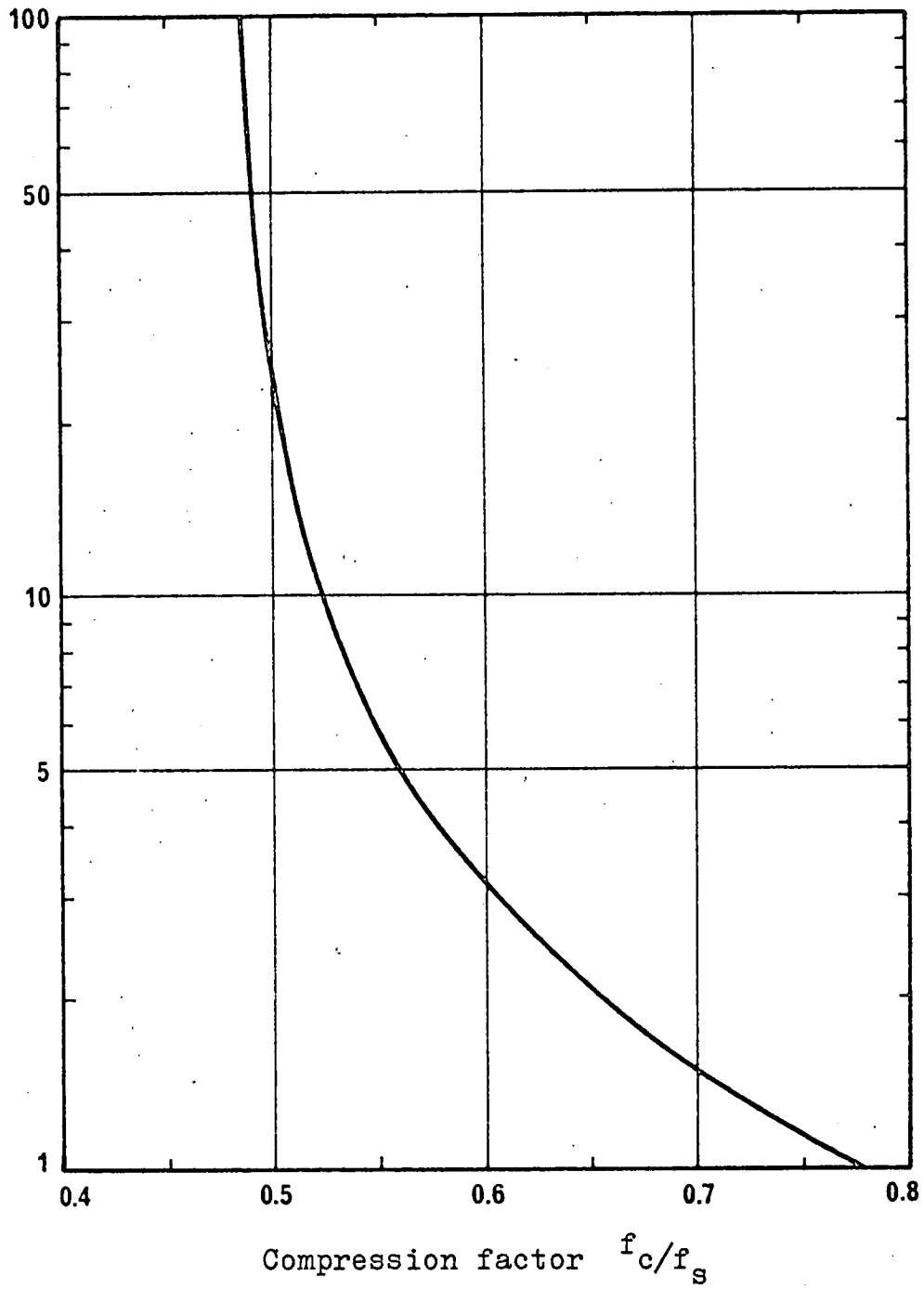


Fig. 9.2 Average queue length

greater than t before transmission

$$\begin{aligned} p(>t) &= \frac{N_m f_s}{5} \left(1 - \frac{f_s N_a}{5 f_c}\right) \int_t^{\infty} e^{-\frac{t N_m f_c}{N_a} \left(1 - \frac{f_s N_a}{5 f_c}\right)} dt \\ &= \frac{f_s N_a}{5 f_c} e^{-\frac{t N_m f_c}{N_a} \left(1 - \frac{f_s N_a}{5 f_c}\right)} \end{aligned} \quad (9.3.5)$$

The average number of codewords stored in the buffer is then

$$\begin{aligned} N_b &= \frac{N_m f_s}{5} \int_0^{\infty} t \frac{d}{dt} p(>t) dt \\ &= \frac{(f_s N_a)^2}{(5 f_c - f_s N_a) 5 f_c} \end{aligned} \quad (9.3.6)$$

which is independent of the number of sources multiplexed and is shown as a function of the compression factor f_c/f_s in Fig. 9.2. While queue length increases without limit as $(f_c/N_a)/(f_s/5) \rightarrow 1$, it falls rapidly to practical values as f_c is increased above the minimum permitted by TR_B .

From (9.3.5), the probability of buffer overflow becomes

$$P_{ov} = \frac{f_s N_a}{5 f_c} e^{-N_q \left(\frac{5 f_c}{f_s N_a} - 1\right)} \quad (9.3.7)$$

Fig. 9.3 gives representative channel buffer characteristics which allow the selection of an appropriate compromise between attainable compression factor and required buffer capacity for a range of overflow probabilities. For a 2 to 1 reduction in data rate, $P_{ov} < 10^{-5}$ is obtained with $N_q = 270$.

Overflow probability

P_{ov}

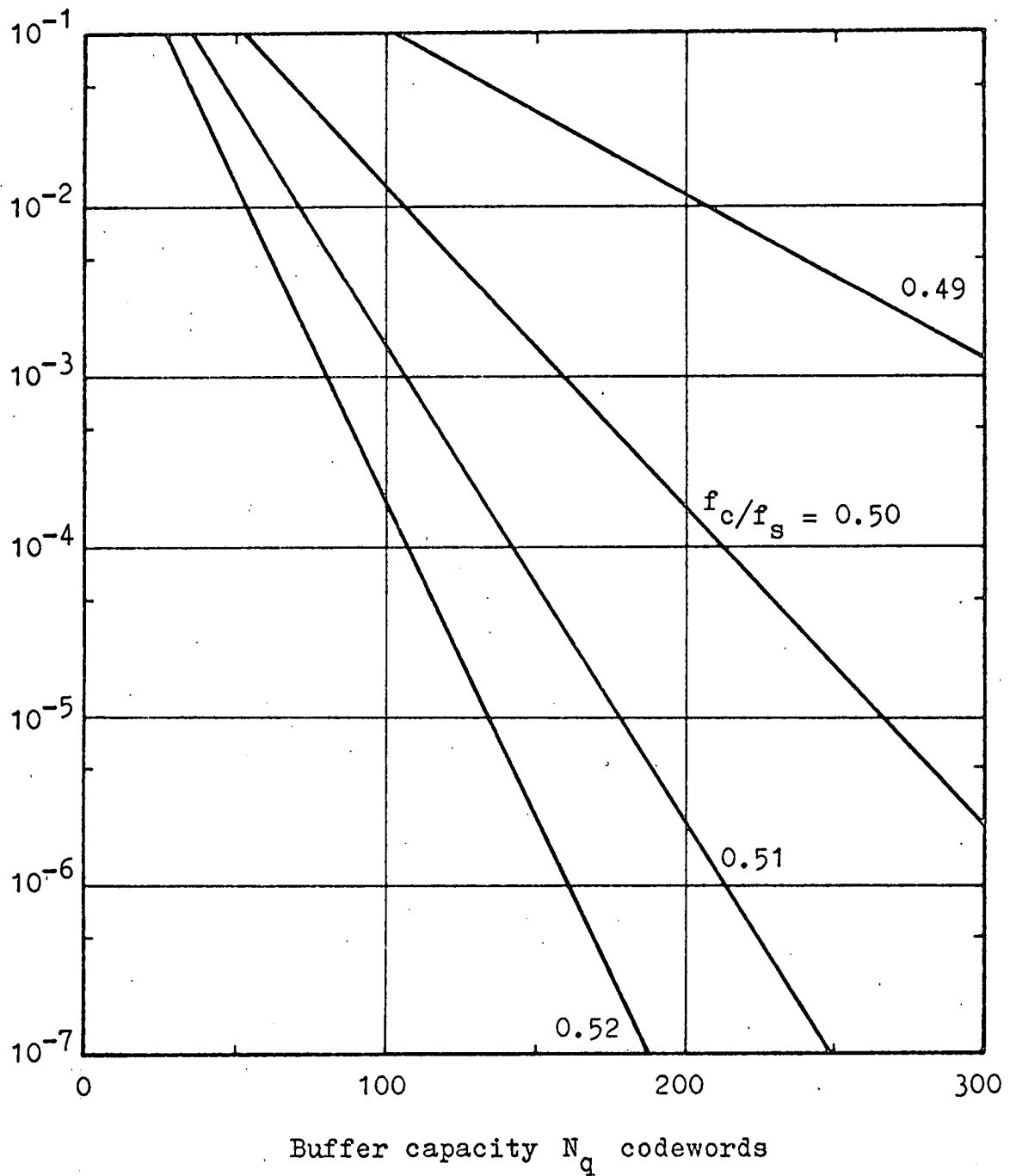


Fig. 9.3 Channel buffer characteristics

Chapter 10

DM signal detection

The previously considered applications of the relative entropy studies on delta-coded speech have been at the sending terminal of a communications link, to effect savings in required transmitter power or channel capacity. By an application of statistical decision theory it is also possible to exploit the knowledge of the message source information properties at a DM receiver to improve the signal detection performance. The gains attainable in this way are less than those for channel encoding, but the method can be very simply applied to an existing delta-coded speech circuit to secure a useful error rate reduction without any change of coding and signalling procedure.

A DM receiver improvement has been suggested by Tanaka et al⁽²⁹⁾, who show that for a sine wave signal an error rate reduction is achieved by replacing the channel signal by a 1 element prediction when the former is in the vicinity of the threshold. The receiver structure presented in this chapter employs switching of the decision threshold by the 6 element predictor described previously to achieve optimal (minimum error probability) detection for speech messages.

10.1 Optimal receiver structure

For a DM receiver performing bit-by-bit detection of signal elements from channel signals impaired by additive Gaussian noise, a Bayes' strategy⁽³⁰⁾ of minimizing the average risk is appropriate. Equal costs may reasonably be assigned to the errors occurring when the received signal x is judged to have been caused by transmitted signal θ_0 or θ_1 when the reverse is true and then the threshold K with which the likelihood ratio

$$\Lambda(x) = \frac{p(x | \theta_1)}{p(x | \theta_0)} \quad (10.1.1)$$

is to be compared becomes simply

$$K = \frac{p(\theta_0)}{p(\theta_1)} \quad (10.1.2)$$

Since in this case the total probability of error is minimized, the strategy is also that of Siegert's 'ideal observer'.⁽³¹⁾

In a typical optimum coherent discrete communications system, the signals with cross-correlation coefficient ρ representing the transmitted binary symbols are either orthogonal ($\rho = 0$) or antipodal ($\rho = -1$) and their replicas, either locally generated or stored as the impulse responses of two matched filters,^{*} are cross-correlated in the Bayes'

* For white noise, the filters have impulse responses of the form of the signals θ_0 , θ_1 run backwards in time from T .

receiver structure with the signal delivered by the channel. To the difference x_c between the correlator outputs at the end of the signal interval T is added the negative of a bias level b corresponding to the Bayes' test decision boundary and the sum is limited and sampled to generate the detector output sequence.

Fig. 10.1 indicates this structure for the $\rho = 0$ case of on-off pulse transmission, in which case only one correlator is required as signal $\theta_0 = 0$, and the probability density distributions $p(x_c | \theta_i)$, $i = 0, 1$, are shown in Fig. 10.2. For channel noise power δ^2 , average signal power M^* , $E[x_c]$ for θ_i transmitted is

$$\mu = 2M(1 - \rho) \quad (10.1.3)$$

and the conditional distributions, which remain Gaussian because of the linearity of the correlation detector, have

$$\delta_c = \delta \sqrt{2M(1 - \rho)} \quad (10.1.4)$$

10.2 Decision boundary loci

From (10.1.1) and (10.1.2), the decision boundary x_d is found by setting

* i.e. 'mark' power = $2M$. This definition is chosen so that the results are identical for the case of equi-energy orthogonal signalling (eg. coherent FSK) in which a second correlator is required for θ_0 and the distributions for x_c are translated for symmetry about the origin.

Synchronous crosscorrelator

Variable threshold detector

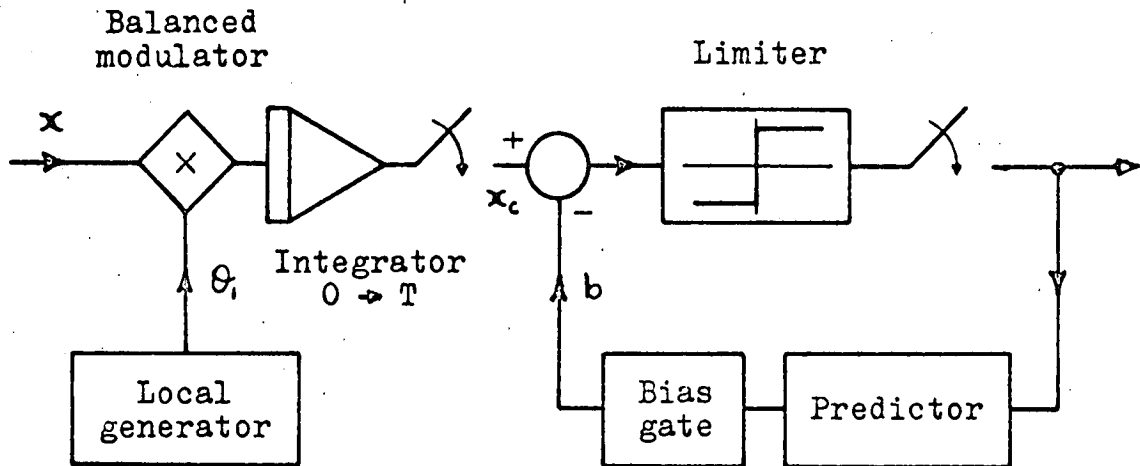


Fig. 10.1 Optimal receiver structure

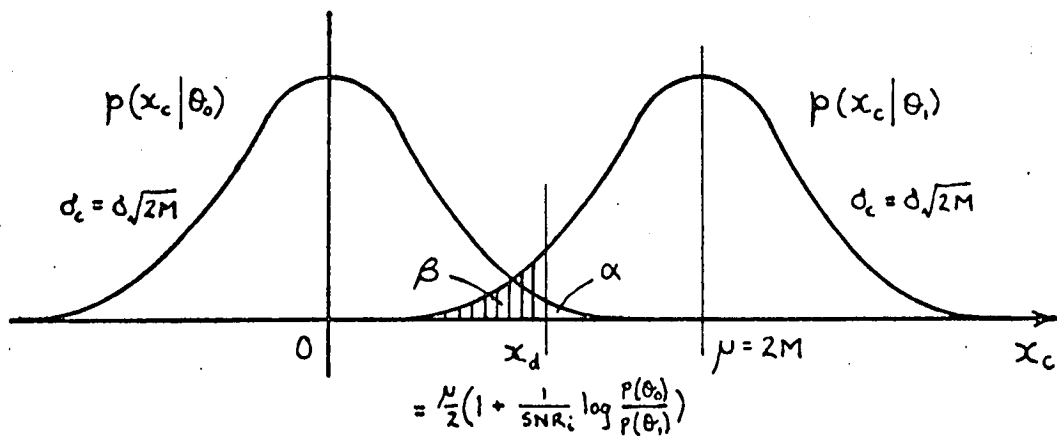


Fig. 10.2 Signal probability density distributions

$$\begin{aligned}
 K = \Lambda(x_d) &= \frac{p(x_d | \theta_1)}{p(x_d | \theta_0)} = \frac{\frac{1}{\sqrt{2\pi} \delta_c} e^{-\frac{(x_d - \mu)^2}{2\delta_c^2}}}{\frac{1}{\sqrt{2\pi} \delta_c} e^{-\frac{x_d^2}{2\delta_c^2}}} \\
 &= e^{\frac{\mu}{\delta_c^2} (x_d - \frac{\mu}{2})} \quad (10.2.1)
 \end{aligned}$$

from which

$$x_d = \frac{\mu}{2} + \frac{\delta_c^2}{\mu} \log_e K \quad (10.2.2)$$

Now it is possible from the results of chapter 5 to process groups of past detector output elements to generate predictions of $p(\theta_0)$, $p(\theta_1)$ for the following θ_i . Using this additional a priori information, the detector bias level can be switched so that the decision boundary location for each element corresponds to comparison of the likelihood ratio with the optimal threshold.

From (10.1.3), (10.1.4) and (10.2.2), the normalised boundary location for the orthogonal case is given by

$$\frac{x_d}{\mu} = \frac{1}{2} + \frac{1}{2 \text{SNR}_i} \log_e \frac{p(\theta_0)}{p(\theta_1)} \quad (10.2.3)$$

in which the input average signal - to - noise ratio

$$\text{SNR}_i = \frac{M}{\delta^2} \quad (10.2.4)$$

and decision boundary loci for a range of $p(\theta_0)$ and SNR_i are given in Fig. 10.3.

\emptyset symbol probability $p(\theta_0)$

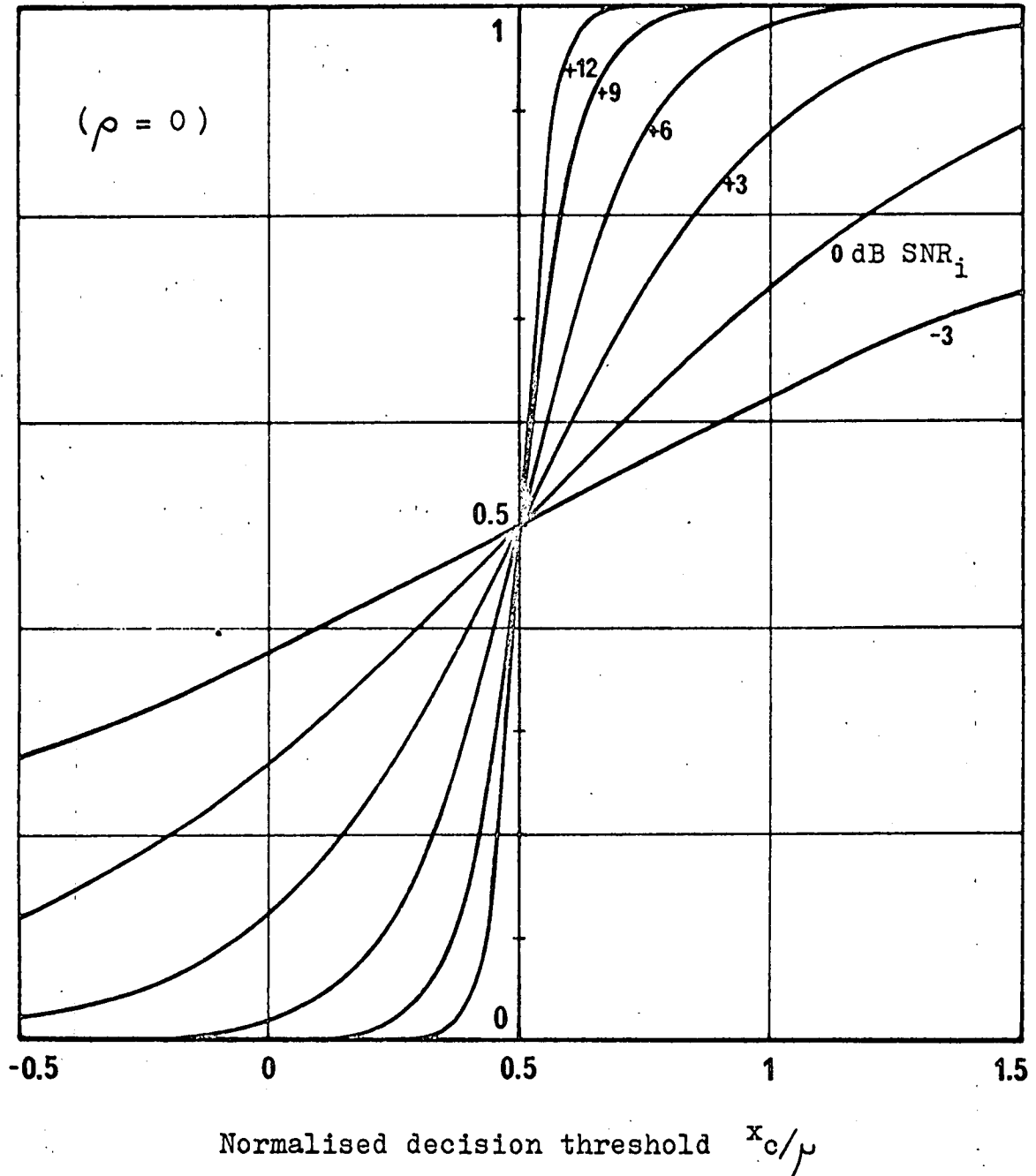


Fig. 10.3 Decision boundary loci

Restricting consideration to the practical case of the 6 element predictor described in chapter 7, which makes only a binary estimate of the more probable next symbol with average success probability P_s , the bias level is switched between values

$$\frac{b}{\mu} = \frac{1}{2} \pm \frac{1}{2 \text{SNR}_i} \log_e \frac{P_s}{1 - P_s} \quad (10.2.5)$$

with sign + or - according as a 0 or 1 symbol is predicted. The bias characteristics for $P_s = 0.898$ are shown in Fig. 10.4, in which the apparent rather critical dependence of the optimum levels on SNR_i is removed by considerations which follow.

10.3 Error rates

For transmitted signal θ_0 , signal detection errors occur when $x_c > x_d$, which occurs with probability

$$\begin{aligned} \alpha &= \int_{x_d}^{\infty} p(x_c | \theta_0) dx_c = \int_{\frac{N}{2} \left(1 + \frac{1}{\text{SNR}_i} \log_e \frac{p(\theta_0)}{p(\theta_1)} \right)}^{\infty} \frac{1}{\sqrt{2\pi} \sigma_c} e^{-\frac{x_c^2}{2\sigma_c^2}} dx_c \\ &= \frac{1}{2} \left[1 - \text{erf} \left(\frac{\sqrt{\text{SNR}_i}}{2} + \frac{1}{2\sqrt{\text{SNR}_i}} \log_e \frac{p(\theta_0)}{p(\theta_1)} \right) \right] \end{aligned} \quad (10.3.1)$$

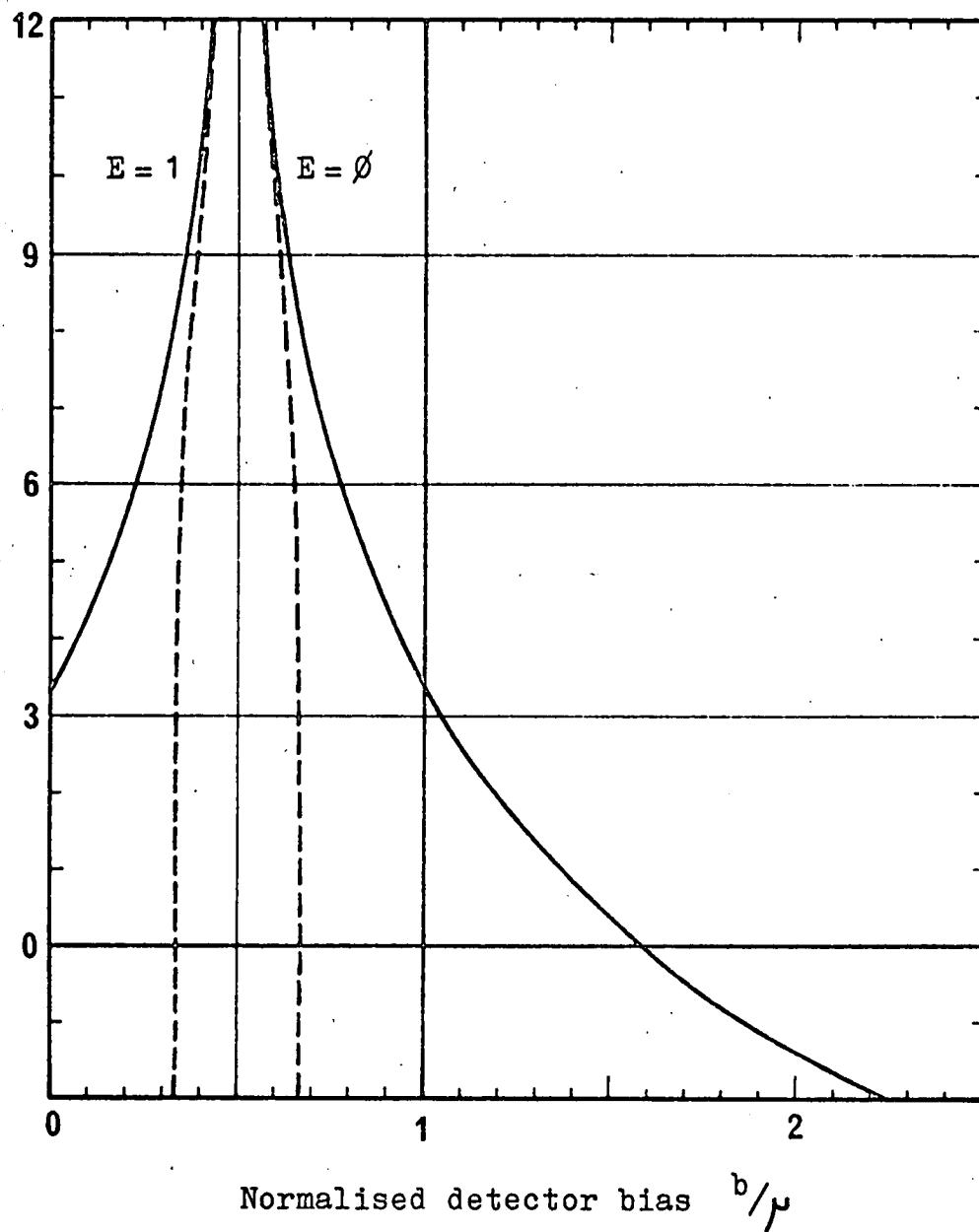
While for θ_1 , error probability

$$\beta = \frac{1}{2} \left[1 - \text{erf} \left(\frac{\sqrt{\text{SNR}_i}}{2} - \frac{1}{2\sqrt{\text{SNR}_i}} \log_e \frac{p(\theta_0)}{p(\theta_1)} \right) \right] \quad (10.3.2)$$

The total error probability is then

$$P_T = p(\theta_0)\alpha + p(\theta_1)\beta \quad (10.3.3)$$

SNR_i dB



————) $P_s = 0.898$

-----) $N = 6$ predictor

Fig. 10.4 Detector bias characteristics

For the case of fixed bias detection of a DM signal with

$p(\theta_0)/p(\theta_1) = 1$, (10.3.3) becomes

$$P_{TF} = \frac{1}{2} \left[1 - \operatorname{erf} \left(\frac{\sqrt{\text{SNR}_i}}{2} \right) \right] \quad (10.3.4)$$

which is shown in Fig. 10.5, together with the corresponding error characteristic for θ_1 antipodal ($\rho = -1$ in (10.1.3) and subsequently).

Employing bias switching by (10.2.5), the total error probability becomes

$$P_{TV} = \frac{1}{2} \left[1 - P_s \operatorname{erf} \left(\frac{\sqrt{\text{SNR}_i}}{2} + \frac{1}{2\sqrt{\text{SNR}_i}} \log_e \frac{P_s}{1-P_s} \right) + (P_s - 1) \operatorname{erf} \left(\frac{\sqrt{\text{SNR}_i}}{2} - \frac{1}{2\sqrt{\text{SNR}_i}} \log_e \frac{P_s}{1-P_s} \right) \right] \quad (10.3.5)$$

For the fixed 6th order predictor structure, P_s is a function of the data error rate which has been determined in Sec. 7.4. By a set of iterations for a range of channel SNR_i , bias levels and data error rates are computed from (10.2.5), (10.3.5) and the data of Fig. 7.4, and the results are shown in Figs. 10.4, 10.5.

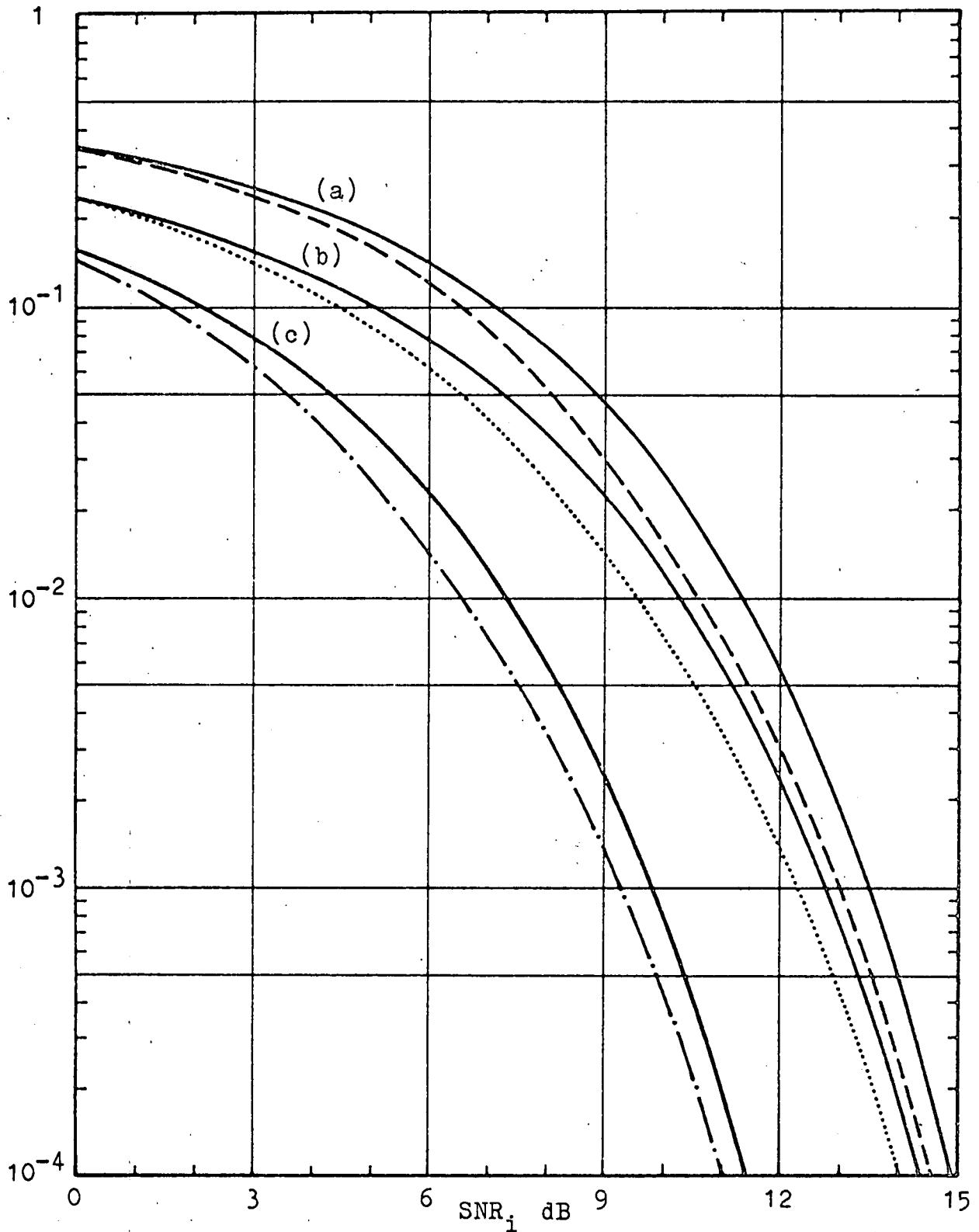
The effect of the degradation in P_s at low SNR_i is to make the normalised decision boundary locations near constant, and detector bias switching between levels

$$\frac{b}{\mu} = 0.34, 0.66 \quad (10.3.6)$$

is near optimal for a wide range of SNR_i . With these levels, an error rate reduction of 39 - 43% results over the typical

Error probability

P_{Tf} , P_{Tv}



(a) Noncoherent (b) Coherent orthogonal (c) Coherent antipodal
Continuous curves: fixed bias P_{Tf} . Broken curves: switched bias P_{Tv}

Fig. 10.5 Error probabilities

range in the case of both orthogonal and antipodal signalling.

10.4 Noncoherent signalling

In some digital communications situations noncoherent signalling is dictated by equipment instabilities or transmission path fluctuations. The optimal signal set is then restricted to an orthogonal pair, and typically on-off transmitter modulation is employed, while at the receiver bandpass filtering and envelope detection of the pulsed carrier is effected prior to the threshold comparator.

The probability density distribution for the envelope detector output x_n for a signal in noise has been studied by Rice⁽³²⁾ and

$$p(x_n | \theta_1) = \frac{x_n}{\delta^2} I_0 \left(\frac{\sqrt{2} x_n \sqrt{SNR_i}}{\delta} \right) e^{-\left(\frac{x_n^2}{2\delta^2} + SNR_i\right)} \quad (10.4.1)$$

while

$$p(x_n | \theta_0) = \frac{x_n}{\delta^2} e^{-\frac{x_n^2}{2\delta^2}} \quad (I_0(0) = 1) \quad (10.4.2)$$

Hence for the Bayes' criterion decision boundary x_{dn} ,

$$I_0 \left(\sqrt{2} \frac{x_{dn}}{\delta} \sqrt{SNR_i} \right) e^{-SNR_i} = \frac{p(\theta_0)}{p(\theta_1)} \quad (10.4.3)$$

from which x_{dn}/δ for switched bias detection may be determined by iterative solution of the approximation

$$\frac{e^v}{\sqrt{2\pi v}} \left(1 + \frac{1}{8v} + \frac{9}{2(8v)^2} \right) = \frac{1 \pm (2\rho_s - 1)}{1 \pm (1 - 2\rho_s)} e^{SNR_i} \quad (10.4.4)$$

in which v is the argument of the zero order modified Bessel

function of the first kind in (10.4.3) and signs + or - apply for a 0 or 1 prediction as before.

The conditional error probabilities are then

$$\alpha = \int_{\frac{x_{dn}}{\delta}}^{\infty} \frac{x_n}{\delta} e^{-\frac{x_n^2}{2\delta^2}} \frac{dx_n}{\delta} = e^{-\frac{1}{2} \left(\frac{x_{dn}}{\delta} \right)^2} \quad (10.4.5)$$

and

$$\beta = \int_0^{\frac{x_{dn}}{\delta}} \frac{x_n}{\delta} I_0 \left(\sqrt{2} \frac{x_n}{\delta} \sqrt{SNR_i} \right) e^{-\left(\frac{x_n^2}{2\delta^2} + SNR_i \right)} \frac{dx_n}{\delta} \quad (10.4.6)$$

in the computation of which the approximation $I_0(v) = e^{-\frac{v^2}{4}}$ may be used for the range of integration resulting in $v \leq 1$ and the expansion of (10.4.4) for the remainder.*

By repetitive application of a procedure by which, for decision boundary iterative solutions of (10.4.4) for trial values of P_s , total error probabilities are computed from (10.4.5) and (10.4.6) and used to revise the estimates by Fig. 7.4, the error characteristic for noncoherent signalling given in Fig. 10.5 is determined. The performance improvement is found to approach that attainable by coherent reception of the same transmitted signals, with less complexity than that necessary for a phase-locked demodulator and without imposing the equipment and path stability requirements of the latter.

$E[x_n | \Theta_i]$ in the noncoherent case is

* Both approximations incur an error of about 2% at $v = 1$.

$$\mu = \delta \sqrt{\frac{\pi}{2}} e^{-\frac{\text{SNR}_i}{2}} \left[(1 + \text{SNR}_i) I_0\left(\frac{\text{SNR}_i}{2}\right) + \text{SNR}_i I_1\left(\frac{\text{SNR}_i}{2}\right) \right], \quad (10.4.7)$$

and when the optimal x_{dn} are normalised to this level it is again found that the decision boundary locations are not a sensitive function of SNR_i , and remain close to

$$\frac{b}{\mu} = 0.50, 0.71 \quad E = 1, \emptyset \quad (10.4.8)$$

over the typical range. Unlike those of (10.3.6), the bias levels are not symmetrical about $\mu/2$ because the Rayleigh distribution of the detector output for Θ_0 has non-zero mean. To maintain minimum error probability reception during received signal strength fluctuations, the levels may readily be tapped in the ratios of (10.4.8) from a potential divider chain across which the mean detector output for Θ_i is developed by conventional gated AGC methods.

Chapter 11

Conclusion

In reviewing briefly the primary application areas of the knowledge gained by this study, the system performance data are selected from those presented in the thesis for representative characteristics and the most practically convenient procedures.

11.1 Transmitter applications

The information analysis of delta-coded speech by the data processing facility described has yielded central results for the entropies of this message source which indicate that the redundancy typically exceeds one half for process orders of practical interest. The efficacy of a predictive coding approach to the exploitation of this redundancy has been demonstrated by comparison of the entropy characteristics for Markov process approximations, for blocks of source elements and the corresponding optimal codes, and for the sequences generated by modulo-2 addition with the outputs of optimal predictors operating on past message elements.

IP transformations utilizing this property have been presented which may be employed at a sender to allow either a transmitter power saving or a reduction in required channel bandwidth without change to the message reconstructed by the

receiver. The common element of these techniques is a 6th order digital predictive coder with near-optimal structure, of form appropriate to economical monolithic fabrication, and exhibiting a typical predictor success probability of 0.9. The encoder performance has been shown to be superior to that for an optimal linear predictor processing many more message elements, and its use in a DM pack set application permits an extension of operational life by a factor of up to 10.

To achieve bandwidth compression in a channel encoder, the predictive coder is followed by optimal 5 element group encoding (or other schemes evaluated) of the error sequence, a combination which realises the attainable 2 to 1 reduction in data rate with considerably less hardware complexity than is required for the direct application of any known exact coding procedure. The channel buffer capacity necessary for uniform output data rate is 270 words, independent of the number of sources multiplexed, and this requirement decreases rapidly for compression factors slightly exceeding the minimum.

11.2 Receiver applications

It has further been shown that the practical predictor structure derived may alternatively be used in signal detection schemes to exploit the knowledge of the statistical properties of the message source at a receiver of delta-coded speech. In this case, the additional a priori information provided by the predictor is used to switch the decision threshold to

minimize the average error risk, and in noncoherent and coherent systems using orthogonal or antipodal signals error probabilities are reduced by 40% by this easily implemented procedure.

11.3 Further work

With the exception of printed English, detailed entropy studies of actual message sources are rarer than their conceptual and practical value merits. While the quantitative information approach is founded on Shannon's treatise of 1948, and the encoding and detection problems which it illuminates are classical, its extensive application to real source analysis has been restricted by message time - scaling and on - line computing requirements.

The combination of the falling availability - cost of these facilities with the increasing capital investment involved in establishing the major new communications links assures a profitable future return on research effort which may be stimulated by this study embracing the parallel application of its philosophy and technique to other information sources of engineering interest.

Appendix 1

Message power spectral density

The system function $H(s)$ (2.1.1) is defined by 12 zeros at the origin and 14 left half plane poles; the following 7 and their conjugates.

$$\begin{aligned} &-704.39 + j18774 \\ &-1903.8 + j15765 \\ &-2422.6 + j10692 \\ &-1742.3 + j5700.4 \\ &-717.36 + j3182.5 \\ &-268.00 + j2221.0 \\ &-70.936 + j1889.6 \end{aligned}$$

Normalising $\omega_n = \omega/10^4$, the denominator coefficient set of $\Phi_{mm}(\omega_n) = \frac{k^2 \omega_n^{12}}{\sum_{i=0}^{14} C_{2i} \omega_n^{2i}}$ ($A_{2i} = 10^{8i} \cdot C_{2i}$) is computed as

C0	5.1101	10^{-7}
C2	6.0907	10^{-5}
C4	3.0233	10^{-3}
C6	8.1291	10^{-2}
C8	1.2932	
C10	1.2547	10
C12	7.4548	10^2
C14	2.6778	10^2
C16	5.9052	10^2
C18	7.8729	10^2
C20	6.4275	10^2
C22	3.2005	10^2
C24	9.4289	10
C26	1.5047	10
C28	1.0	

with $k^2 = 1.7713 \cdot 10^{-5}$ for unit message power $\int_{-\infty}^{\infty} \Phi_{mm}(\omega) d\omega$.

Appendix 2

Analogue filter

With the computer variable scaling chosen, (3.2.3) is represented by the configuration of Fig. A2.1 in which the required gain between consecutive output taps of Q_{i-1}/Q_i is realized by the integrator time constants shown and the following potentiometer settings.

Q	0.2447
P0	0.3559
P1	0.9919
P2	0.4725
P3	0.2287
P4	0.6765
P5	0.4308
P6	0.1101
P7	0.7892
P8	0.2018
P9	0.1286
P10	0.3794
P11	0.1842
P12	0.8735

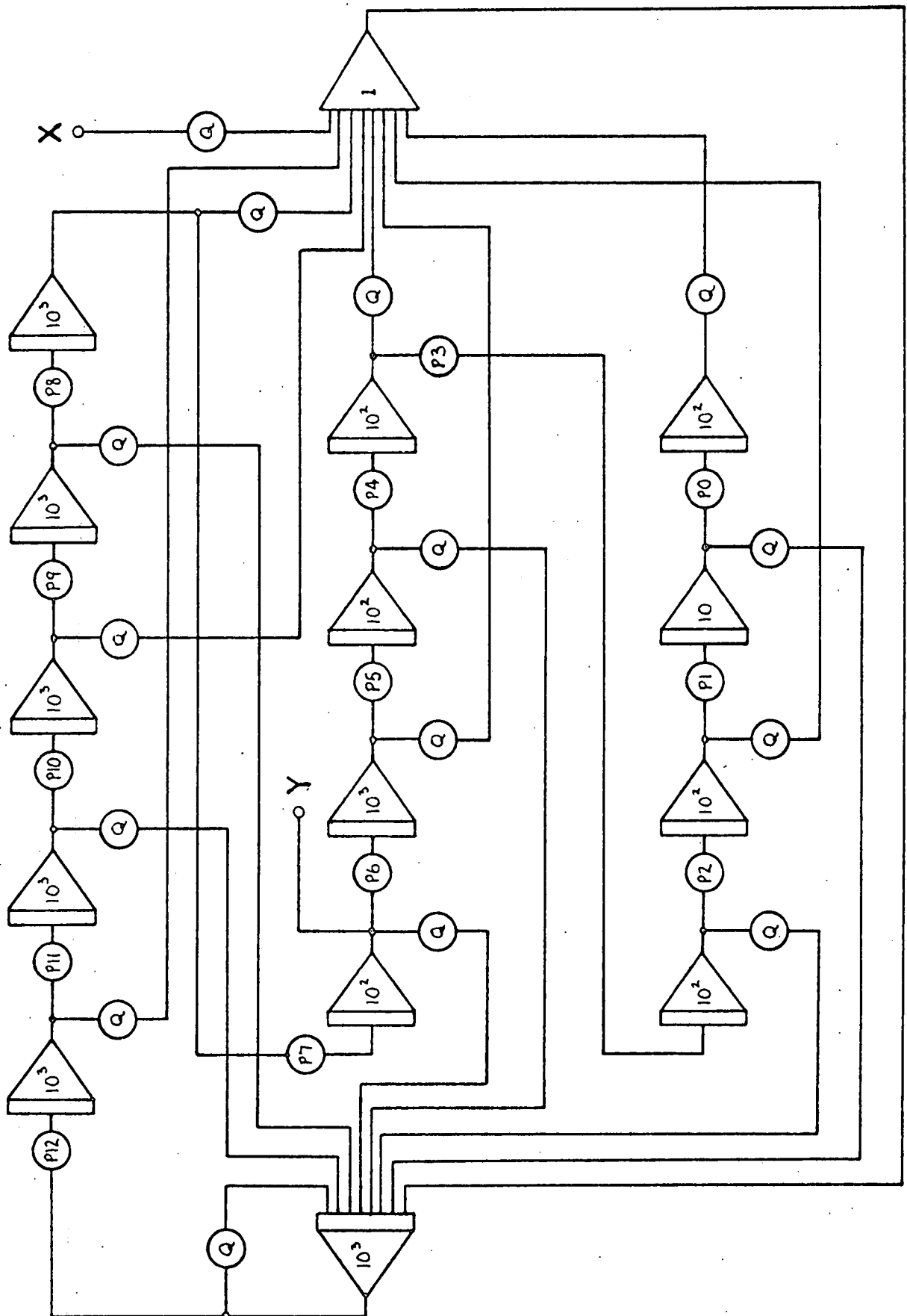


Fig. A2.1 Analogue message filter

Appendix 3

/STOCHASTIC MATRIX ASSEMBLER 06HR

PAGE 0

0000	0000	REG,	0	
0001	7300		CLA CLL	
0002	1525		TAD I CODAD	/LATEST 7 BIT TRANSFER
0003	7010		RAR	
0004	3127		DCA STATW	/6 BIT STATE
0005	7004		RAL	
0006	3130		DCA NUBIT	
0007	1127		TAD STATW	
0010	0377		AND (0017	/MASK SAVING 8-11
0011	7450		SNA	
0012	5045		JMP PRED0	/LAST FOUR 0
0013	1376		TAD (7761	
0014	7450		SNA	
0015	5050		JMP PRED1	/LAST FOUR 1
0016	7200		CLA	
0017	1127		TAD STATW	
0020	0375		AND (0037	/MASK SAVING 7-11
0021	1374		TAD (7776	
0022	7450		SNA	
0023	5045		JMP PRED0	/02 OR 42
0024	1373		TAD (7745	
0025	7450		SNA	
0026	5050		JMP PRED1	/35 OR 75
0027	7200		CLA	
0030	1127		TAD STATW	
0031	1372		TAD (7774	
0032	7450		SNA	
0033	5045		JMP PRED0	/04
0034	1371		TAD (7711	
0035	7450		SNA	
0036	5050		JMP PRED1	/73
0037	7200		CLA	/COMPLEMENT 11
0040	1127		TAD STATW	
0041	7010		RAR	
0042	7430		SZL	
0043	5045		JMP PRED0	
0044	5050		JMP PRED1	
0045	7200	PRED0,	CLA	/CL LINK FOR CORRECT PRED
0046	1130		TAD NUBIT	
0047	5053		JMP .+4	
0050	7200	PRED1,	CLA	
0051	1130		TAD NUBIT	
0052	7001		IAC	
0053	7010		RAR	

0054	7200	CLA	/FORM H-ADD OP SEQUENCE
0055	1124	TAD TEMDAT	
0056	7004	RAL	/L TO 11
0057	0370	AND (1777	
0060	3124	DCA TEMDAT	/STORE 10 BIT SEQ
0061	1124	TAD TEMDAT	
0062	7120	STL	
0063	7004	RAL	
0064	1367	TAD (3400	
0065	3126	DCA CNADD	/STORE LO ADD
0066	7100	CLL	/INCREMENT COUNT
0067	1526	TAD I CNADD	
0070	7001	IAC	
0071	3526	DCA I CNADD	/STORE LS BITS
0072	1126	TAD CNADD	
0073	1366	TAD (7777	
0074	3126	DCA CNADD	/STORE HI ADD
0075	7024	CML RAL	/DUBL COMP LINK TO BIT 11
0076	1526	TAD I CNADD	
0077	3526	DCA I CNADD	/STORE MS BITS
0100	1125	TAD CODAD	/INCREMENT CODAD
0101	1365	TAD (0201	
0102	7500	SMA	/TEST TO CYCLE
0103	1364	TAD (7600	
0104	1364	TAD (7600	
0105	3125	DCA CODAD	
0106	7604	LAS	/TEST SR FOR T ENABLE
0107	7012	RTR	
0110	7430	SZL	
0111	5763	JMP TERMIN	
0112	7200	CLA	
0113	6662	OPGND	
0114	4762	JMS RN	/GET RANDOM NO
0115	7100	CLL	
0116	1154	TAD ERRBND	
0117	7430	SZL	/L SET: BIT ERROR
0120	6664	OPNEG	
0121	7200	CLA	
0122	6001	HOLD, ION	/WAIT FOR DATA BREAK
0123	5122	JMP .-1	
0124	0000	TEMDAT, 0	/TEMPORARY REGISTERS
0125	7400	CODAD, 7400	
0126	0000	CNADD, 0	
0127	0000	STATW, 0	
0130	0000	NUBIT, 0	
0131	0000	STATEP, 0	
0132	0000	STATET, 0	
0133	0000	STATE0, 0	
0134	0000	STATE1, 0	
0135	0000	STATAP, 0	
0136	3400	STATAT, 3400	

0137 0000 C0H, 0
0140 0000 CN0HI, 0
0141 0000 CN0LO, 0
0142 0000 C0L, 0

0143 0000 C1H, 0
0144 0000 CN1HI, 0
0145 0000 CN1LO, 0
0146 0000 C1L, 0

0147 0000 SWITT, 0

0150 0000 TCNHI, 0
0151 0000 TCNLO, 0

0152 0000 TOTBHI, 0
0153 0000 TOTBLO, 0

0154 0000 ERRBND, 0

0155 0000 QUOTH, 0

OPGND=6662
OPNEG=6664

/CHANNEL ERROR PARAMETER ASSIGNMENT

PAGE 1

0200 7200 ENTER, CLA /ENTER PROGRAM. SET D ADDS
0201 1377 TAD (7400 /CLEAR REGISTERS AND FLAGS
0202 3125 DCA CODAD /INITIALIZE ROUTINES
0203 3124 DCA TEMDAT
0204 3152 DCA TOTBHI
0205 3153 DCA TOTBLO
0206 1376 TAD (T1
0207 4775 JMS TYPSTG
0210 1374 TAD (T4
0211 4775 JMS TYPSTG
0212 7200 CLA
0213 7402 HLT /((LOAD SR WITH ERROR RATE)

0214 7604 LAS
0215 3154 DCA ERRBND
0216 1373 TAD (T5
0217 4775 JMS TYPSTG
0220 7402 HLT /((CLEAR SR)

0221 4772 JMS INIT
0222 4771 JMS IR
0223 6662 OPGND
0224 6032 KCC
0225 6042 TCF
0226 6022 PCF
0227 7200 CLA

0230 6001 ION /WAIT FOR FIRST DATA BREAK
0231 5230 JMP --1

0232	0015	T1,	TEXT /@
		@	
0233	0012		
0234	2324	ST	
0235	1703	OC	
0236	1001	HA	
0237	2324	ST	
0240	1103	IC	
0241	4015	M	
0242	0124	AT	
0243	2211	RI	
0244	3040	X	
0245	0123	AS	
0246	2305	SE	
0247	1502	MB	
0250	1405	LE	
0251	2240	R	
0252	6066	06	
0253	1022	HR	
0254	0015	@	
		@	
0255	0012		
0256	0401	DA	
0257	2401	TA	
0260	4024	T	
0261	2201	RA	
0262	1623	NS	
0263	0605	FE	
0264	2240	R	
0265	2417	TO	
0266	4067	7	
0267	6460	40	
0270	6000	00	
0271	1500	@	
0272	1200	@	
0273	1200	@	
0274	0100	A/	
0275	2305	T4,	TEXT /SE
0276	2440	T	
0277	0522	ER	
0300	2217	RO	
0301	2240	R	
0302	2201	RA	
0303	2405	TE	
0304	0015	@	
		@	
0305	0012		
0306	0001	@A	
0307	0000	/	
0310	0314	T5,	TEXT /CL
0311	0501	EA	
0312	2240	R	
0313	2322	SR	
0314	0015	@	
		@	
0315	0012		
		@	

0316	0012	@	
0317	0012		
0320	0001	@A	
0321	0000	/	
0322	0000	LDRTRL, 0	/10 INS 0200
0323	7200	CLA	
0324	1370	TAD (7633	
0325	3341	DCA LENGTH	
0326	1367	TAD (0200	
0327	4333	JMS PRINTC	
0330	2341	ISZ LENGTH	
0331	5326	JMP LDRTRL+4	
0332	5722	JMP I LDRTRL	
0333	0000	PRINTC, 0	
0334	6026	PLS	
0335	6021	PSF	
0336	5335	JMP .-1	
0337	7200	CLA	
0340	5733	JMP I PRINTC	
0341	7633	LENGTH, 7633	
0367	0200	PAGE 2	
0370	7633		
0371	2200		
0372	1600		
0373	0310		
0374	0275		
0375	2400		
0376	0232		
0377	7400		
0400	7200	TERMIN, CLA	/TERMINATE RUN
0401	3147	DCA SWITT	
0402	3152	DCA TOTBHI	
0403	3153	DCA TOTBLO	
0404	1377	TAD (T3	
0405	4776	JMS TYPSTG	
0406	4775	JMS LDRTRL	
0407	4775	JMS LDRTRL	
0410	1374	TAD (MASKL	
0411	3306	DCA MASKA	/SET MASK POINTER
0412	1373	TAD (271	
0413	3307	DCA RUNDGT	/SET ORDER
0414	5234	JMP NEST-2	
0415	7200	INITZ, CLA	/SET STATEP LIMITS
0416	1706	TAD I MASKA	
0417	7041	CIA	
0420	3310	DCA LIMIT	
0421	1706	TAD I MASKA	
0422	7001	IAC	
0423	3311	DCA COLIM	
0424	4775	JMS LDRTRL	

0425	1372		TAD (T11	
0426	4776		JMS TYPSTG	
0427	1307		TAD RUNDGT	
0430	6026		PLS	
0431	6021		PSF	
0432	5231		JMP --1	
0433	4771		JMS TYCR	
0434	7200		CLA	
0435	3131		DCA STATEP	/CLEAR
0436	1131	NEST,	TAD STATEP	
0437	3132		DCA STATET	
0440	7200		CLA	/FORM PRESENT STATE ADDRESS
0441	1131		TAD STATEP	
0442	7006		RTL	
0443	0370		AND (3774	
0444	1367		TAD (3400	
0445	3135		DCA STATAP	
0446	1535		TAD I STATAP	/LOAD TEMP REGISTERS
0447	3140		DCA CN0HI	
0450	2135		ISZ STATAP	
0451	1535		TAD I STATAP	
0452	3141		DCA CN0LO	
0453	2135		ISZ STATAP	
0454	1535		TAD I STATAP	
0455	3144		DCA CN1HI	
0456	2135		ISZ STATAP	
0457	1535		TAD I STATAP	
0460	3145		DCA CN1LO	
0461	1147		TAD SWITT	
0462	7450		SNA	
0463	5766		JMP TBCN	
0464	7200	SEARCH,	CLA	
0465	2132		ISZ STATET	
0466	1132		TAD STATET	
0467	7004		RAL	
0470	7006		RTL	/BIT 2 TO LINK
0471	7430		SZL	
0472	5765		JMP OUTLNK	/STATES 000-777 SEARCHED
0473	7010		RAR	
0474	7012		RTR	
0475	0706		AND I MASKA	/MASK
0476	3312		DCA TRMST	/STORE TRIMMED STATE
0477	1131		TAD STATEP	
0500	0706		AND I MASKA	/MASK
0501	7041		CIA	
0502	1312		TAD TRMST	
0503	7450		SNA	/STATES SAME?
0504	4764		JMS TRANSF	/YES: TRANSFER COUNTS
0505	5264		JMP SEARCH	/NO: CONTINUE

0506	0000	MASKA,	0
0507	0271	RUNDGT,	271
0510	7001	LIMIT,	7001
0511	1000	COLIM,	1000
0512	0000	TRMST,	0

0564 0600 PAGE 3

0565	1000
0566	1024
0567	3400
0570	3774
0571	2617
0572	0720
0573	0271
0574	0642
0575	0322
0576	2400
0577	0654

0600	0000	TRANSF, 0	/FORM REP STATE ADDRESS
0601	7200	CLA	
0602	1132	TAD STATAT	
0603	7006	RTL	
0604	0377	AND (3774	
0605	1376	TAD (3400	
0606	3136	DCA STATAT	

0607	7300	CLA CLL	/ADD 0 COUNT
0610	2136	ISZ STATAT	
0611	1536	TAD I STATAT	
0612	1141	TAD CN0LO	
0613	3141	DCA CN0LO	
0614	1375	TAD (7777	
0615	1136	TAD STATAT	
0616	3136	DCA STATAT	
0617	7024	CML RAL	/DUBL COMP LINK TO A11
0620	1536	TAD I STATAT	
0621	1140	TAD CN0HI	
0622	3140	DCA CN0HI	

0623	1136	TAD STATAT	/ADD 1 COUNT
0624	1374	TAD (0003	
0625	3136	DCA STATAT	
0626	7300	CLA CLL	
0627	1536	TAD I STATAT	
0630	1145	TAD CN1LO	
0631	3145	DCA CN1LO	
0632	1375	TAD (7777	
0633	1136	TAD STATAT	
0634	3136	DCA STATAT	
0635	7024	CML RAL	/DUBL COMP LINK TO A11
0636	1536	TAD I STATAT	
0637	1144	TAD CN1HI	
0640	3144	DCA CN1HI	

0641	5600	JMP I TRANSF	
------	------	--------------	--

0642	0777	MASKL,	777
0643	0377		377
0644	0177		177
0645	0077		077
0646	0037		037
0647	0017		017
0650	0007		007
0651	0003		003
0652	0001		001
0653	0000		000

0654	0015	T3,	TEXT /@
		@	

0655	0012		
0656	2405	TE	
0657	2215	RM	
0660	1116	IN	
0661	0124	AT	
0662	0504	ED	
0663	0015	@	
		@	

0664	0012		
		@	

0665	0012		
		@	

0666	0012		
		@	

0667	0012		
0670	1723	OS	
0671	2440	T	
0672	4024	T	
0673	2201	RA	
0674	1623	NS	
0675	4060	0	
0676	4040		
0677	2422	TR	
0700	0116	AN	
0701	2340	S	
0702	6100	1@	
0703	1500	@	
0704	1200	@	

0705	1224	T	
0706	1724	OT	
0707	0114	AL	
0710	4002	B	
0711	1124	IT	
0712	4003	C	
0713	1725	OU	
0714	1624	NT	
0715	4040		
0716	4000	@	
0717	0100	A/	

0720	0015	T11,	TEXT /@
		@	

0721	0012		
------	------	--	--

0722 7160 90
0723 0001 @A
0724 0000 /

0774 0003 PAGE 4
0775 7777
0776 3400
0777 3774

1000	4777	OUTLNK,	JMS OUTPUT	/PRINT CYCLE
1001	1131		TAD STATEP	/TEST STATEP
1002	1776		TAD LIMIT	
1003	7450		SNA	/LIMIT REACHED?
1004	5210		JMP NURUN	/YES: REDUCE ORDER AND RERUN
1005	1775		TAD COLIM	/NO: INCR AND REPEAT
1006	3131		DCA STATEP	
1007	5774		JMP NEST	
1010	4773	NURUN,	JMS TYCR	
1011	2772		ISZ MASKA	
1012	7200		CLA	
1013	1771		TAD RUNDGT	
1014	1370		TAD (7520	
1015	7450		SNA	/RUNDGT 260? (0)
1016	5222		JMP CONCLD	/YES: EXIT
1017	1367		TAD (257	/NO: REDUCE BY 1 AND REPEAT
1020	3771		DCA RUNDGT	
1021	5766		JMP INITZ	
1022	4765	CONCLD,	JMS LDRTRL	
1023	7402		HLT	
1024	7300	TBCN,	CLA CLL	/FORM STATE ENTERED TOTAL
1025	1141		TAD CN0LO	
1026	1145		TAD CN1LO	
1027	3151		DCA TCNLO	
1030	7004		RAL	
1031	1140		TAD CN0HI	
1032	1144		TAD CN1HI	
1033	3150		DCA TCNHI	
1034	7300		CLA CLL	/INCREMENT TOTAL BIT COUNT
1035	1153		TAD TOTBLO	
1036	1151		TAD TCNLO	
1037	3153		DCA TOTBLO	
1040	7004		RAL	
1041	1152		TAD TOTBHI	
1042	1150		TAD TCNHI	
1043	3152		DCA TOTBHI	
1044	1131		TAD STATEP	/TEST STATEP
1045	1364		TAD (7001	
1046	7450		SNA	/IS IT 0777?
1047	5253		JMP TBOP	
1050	1363		TAD (1000	
1051	3131		DCA STATEP	
1052	5774		JMP NEST	

1053	1362	TBOP,	TAD (TOTBHI
1054	4761		JMS IDBBCD
1055	0153		TOTBLO
1056	4773		JMS TYCR
1057	2147		ISZ SWITT
1060	5766		JMP INITZ

1161	2000	PAGE 5
1162	0152	
1163	1000	
1164	7001	
1165	0322	
1166	0415	
1167	0257	
1170	7520	
1171	0507	
1172	0506	
1173	2617	
1174	0436	
1175	0511	
1176	0510	
1177	1200	

1200	0000	OUTPUT, 0	/ONE STATE OUTPUT SEQUENCE
1201	7200	CLA	
1202	4777	JMS TYCR	
1203	1131	TAD STATEP	/PRINT STATE OCTAL
1204	4776	JMS TYPOCT	
1205	4775	JMS TYSP	
1206	4775	JMS TYSP	
1207	1374	TAD (CN0HI	
1210	4773	JMS IDBBCD	/PRINT TOTAL TRANS TO STATE 0
1211	0141	CN0LO	
1212	4775	JMS TYSP	
1213	4775	JMS TYSP	
1214	1372	TAD (CN1HI	
1215	4773	JMS IDBBCD	/PRINT TOTAL TRANS TO STATE 1
1216	0145	CN1LO	
1217	7200	CLA	
1220	5600	JMP I OUTPUT	

1372	0144	PAGE 6
1373	2000	
1374	0140	
1375	2627	
1376	1400	
1377	2617	

1400	0000	TYPOCT, 0	/3D OCTAL STATE FORMATION
1401	7006	RTL	/7 LEFT
1402	7006	RTL	
1403	7006	RTL	
1404	7004	RAL	
1405	3225	DCA TEMOCT	
1406	1377	TAD (7775	
1407	3226	DCA CNOCT	/SET DIGIT COUNT

1410	1225		TAD	TEMOCT	
1411	0376		AND	(0007	/MASK, SAVE 9-11
1412	1375		TAD	(0260	/ASCII
1413	4227		JMS	PRINTN	
1414	1225		TAD	TEMOCT	
1415	2226		ISZ	CNOCT	/DONE 3?
1416	5221		JMP	MDIGIT	/NO: 3 LEFT AND REPEAT
1417	7200		CLA		/YES: EXIT
1420	5600		JMP	I TYPOCT	
1421	7006	MDIGIT,	RTL		
1422	7004		RAL		
1423	3225		DCA	TEMOCT	
1424	5210		JMP	TYPOCT+10	
1425	0000	TEMOCT,	0		
1426	0000	CNOCT,	0		
1427	0000	PRINTN,	0		/PUNCH DIGIT SR
1430	6026		PLS		
1431	6021		PSF		
1432	5231		JMP	--1	
1433	7200		CLA		
1434	5627		JMP	I PRINTN	
1575	0260	PAGE 7			
1576	0007				
1577	7775				
1600	0000	INIT,	0		/COUNT AND DATA REG INITIALIZATION
1601	7200		CLA		
1602	1377		TAD	(3400	
1603	3240		DCA	CTAD	
1604	3640		DCA	I CTAD	
1605	1240		TAD	CTAD	/TEST CTAD
1606	1376		TAD	(0401	
1607	7450		SNA		/IS IT 7377?
1610	5213		JMP	ALT	/YES: DO DATA REGISTER
1611	1375		TAD	(7400	/NO: INCREMENT CTAD 0001
1612	5203		JMP	INIT+3	
1613	7200	ALT,	CLA		
1614	1375		TAD	(7400	
1615	3241		DCA	DATAD	
1616	1374		TAD	(0125	
1617	3641		DCA	I DATAD	/LOAD 1010101
1620	1241		TAD	DATAD	
1621	7001		IAC		
1622	3241		DCA	DATAD	
1623	1373		TAD	(0052	
1624	3641		DCA	I DATAD	/LOAD 0101010
1625	1241		TAD	DATAD	/TEST DATAD
1626	1372		TAD	(0201	
1627	7450		SNA		/IS IT 7577?
1630	5233		JMP	FINI	/YES: EXIT
1631	1371		TAD	(7600	/NO: INCREMENT DATAD 0001
1632	5215		JMP	ALT+2	

1633	7200	FINI,	CLA
1634	1370		TAD (T2
1635	4767		JMS TYPSTG
1636	7200		CLA
1637	5600		JMP I INIT

1640	0000	CTAD,	0
1641	0000	DATAD,	0

1642	0015	T2,	TEXT /@
		@	

1643	0012		
1644	2324	ST	
1645	0124	AT	
1646	0540	E	
1647	0317	CO	
1650	2516	UN	
1651	2423	TS	
1652	4003	C	
1653	1405	LE	
1654	0122	AR	
1655	0015	@	
		@	

1656	0012		
1657	0401	DA	
1660	2401	TA	
1661	4020	P	
1662	0107	AG	
1663	0540	E	
1664	1417	LO	
1665	0104	AD	
1666	0504	ED	
1667	0015	@	
		@	

1670	0012		
		@	

1671	0012		
		@	

1672	0012		
1673	0001	@A	
1674	0000	/	

1767	2400	PAGE 10	
------	------	---------	--

1770	1642		
1771	7600		
1772	0201		
1773	0052		
1774	0125		
1775	7400		
1776	0401		
1777	3400		

2000	0000	IDBBCD, 0	/DUBL PREC INT BIN TO BCD
2001	3263	DCA VALUEH	/ADDR H ORDER IP
2002	1663	TAD I VALUEH	
2003	3265	DCA VALH	

2004	3271		DCA DIGIT	/CLEAR
2005	1600		TAD I IDBB CD	
2006	2200		ISZ IDBB CD	
2007	3262		DCA VALUEL	/ADDR L ORDER IP
2010	1662		TAD I VALUEL	
2011	3264		DCA VALL	
2012	1377		TAD (-7	/SET COUNTERS
2013	3270		DCA CNTR1	
2014	1376		TAD (TAD TENPH	/SET TABLE ARROWS
2015	3232		DCA ARROW1	
2016	1375		TAD (TAD TENPL	
2017	3226		DCA ARROW2	
2020	1264		TAD VALL	/COPY
2021	3266		DCA VL	
2022	1265		TAD VALH	
2023	3267		DCA VH	
2024	7300		CLA CLL	/DUBL PREC SUB PWR OF 10
2025	1266		TAD VL	
2026	1273	ARROW2,	TAD TENPL	
2027	3266		DCA VL	
2030	7004		RAL	
2031	1267		TAD VH	
2032	1272	ARROW1,	TAD TENPH	
2033	7004		RAL	
2034	7430		SZL	/RESULT STILL POSITIVE?
2035	5246		JMP READY	/NO: CANCEL
2036	7010		RAR	/YES: CONTINUE
2037	3267		DCA VH	
2040	2271		ISZ DIGIT	/DEVELOP BCD DIGIT
2041	1266		TAD VL	
2042	3264		DCA VALL	
2043	1267		TAD VH	
2044	3265		DCA VALH	
2045	5224		JMP ARROW2-2	/LOOP
2046	7200	READY,	CLA	/TYPE BCD DIGIT
2047	1271		TAD DIGIT	
2050	4774		JMS TDIG	
2051	7200		CLA	
2052	3271		DCA DIGIT	
2053	2232		ISZ ARROW1	/ADVANCE TABLE ARROWS
2054	2232		ISZ ARROW1	
2055	2226		ISZ ARROW2	
2056	2226		ISZ ARROW2	
2057	2270		ISZ CNTR1	/DONE EIGHT DIGITS?
2060	5220		JMP ARROW2-6	/NO: CONTINUE
2061	5600		JMP I IDBB CD	/YES: EXIT
2062	0000	VALUEL,	0	
2063	0000	VALUEH,	0	
2064	0000	VALL,	0	
2065	0000	VALH,	0	
2066	0000	VL,	0	
2067	0000	VH,	0	

2070	7771	CNTR1,	-7	
2071	0000	DIGIT,	0	
2072	7413	TENPH,	7413	/-1000000
2073	6700	TENPL,	6700	

2074	7747	DUBL	-0100000	
2075	4540			
2076	7775		-0010000	
2077	4360			
2100	7777		-0001000	
2101	6030			
2102	7777		-0000100	
2103	7634			
2104	7777		-0000010	
2105	7766			
2106	7777		-0000001	
2107	7777			
2110	7200	CLA		

2174	2645
2175	1273
2176	1272
2177	7771

/THE FOLLOWING SOFTWARE PACKAGES REQUIRE
/TO BE APPENDED TO THIS PROGRAM:

/PAGE 11
/DECUS NO 5-25 PSEUDO RANDOM NUMBER GENERATOR

/PAGE 12
/DIGITAL-8-20-U-SYM CHARACTER STRING TYPEOUT

/PAGE 13
/DIGITAL-8-19-U-SYM TELETYPE OUTPUT SUBROUTINES
/(MODIFIED FOR HS PUNCH)

/PAGE 14
/DIGITAL-8-6-U-SYM OCTAL MEMORY DUMP

/DOUBLE PRECISION STATE COUNTS OCCUPY PAGES 16 - 35

/DATA BREAK TRANSFERS ARE MADE DIRECT TO PAGE 36

/PAGE 37 HOLDS DIGITAL-8-1-U RIM LOADER AND
/DIGITAL-8-2-U BINARY LOADER

PAUSE

Appendix 4

4th order transition probability matrix for delta - coded speech

Sampling frequency = 96 KHz
pk - pk message amplitude = 128 Δ

Prediction Example ~ On occurrence of group 1001 (11)
predictor selects 0010 (02), the probability of
transition to which exceeds that to 0011 (03).

↓	00	01	02	03	04	05	06	07	10	<u>11</u>	12	13	14	15	16	17
00	0.895	0	0	0	0	0	0	0	0.468	0	0	0	0	0	0	0
01	0.105	0	0	0	0	0	0	0	0.532	0	0	0	0	0	0	0
<u>02</u>	0	0.963	0	0	0	0	0	0	0	<u>0.965</u>	0	0	0	0	0	0
03	0	0.037	0	0	0	0	0	0	0	0.035	0	0	0	0	0	0
04	0	0	0.437	0	0	0	0	0	0	0	0.077	0	0	0	0	0
05	0	0	0.563	0	0	0	0	0	0	0	0.923	0	0	0	0	0
06	0	0	0	0.832	0	0	0	0	0	0	0	0.813	0	0	0	0
07	0	0	0	0.168	0	0	0	0	0	0	0	0.187	0	0	0	0
10	0	0	0	0	0.198	0	0	0	0	0	0	0	0.149	0	0	0
11	0	0	0	0	0.802	0	0	0	0	0	0	0	0.851	0	0	0
12	0	0	0	0	0	0.923	0	0	0	0	0	0	0	0.579	0	0
13	0	0	0	0	0	0.077	0	0	0	0	0	0	0	0.421	0	0
14	0	0	0	0	0	0	0.036	0	0	0	0	0	0	0	0.037	0
15	0	0	0	0	0	0	0.964	0	0	0	0	0	0	0	0.963	0
16	0	0	0	0	0	0	0	0.523	0	0	0	0	0	0	0	0.094
17	0	0	0	0	0	0	0	0.477	0	0	0	0	0	0	0	0.906

Notes 1) States are octal, probabilities decimal.

2) In preference to the more common transpose, the conditional probabilities in the above format are for transitions from operand state columns to transform state rows. The source states are then column rather than row vectors, but the order of matrix multiplication is the natural

$$S_{i+1} = T S_i$$

in which operator precedes operand.

Acknowledgements

The author is indebted to Professor W.E.J. Farvis of the School of Engineering Science for proposing the study, accepting supervisory responsibility, and providing the facilities of the Computing and Communications Laboratories of the Department of Electrical Engineering for the work.

Valuable discussions with Professor S. Michaelson and colleagues of the Department of Computer Science on data processing and with W. Lawrence of the Phonetics Department on speech encoding are also acknowledged, and the study was aided by the co-operation of the staff of Edinburgh Regional Computing Centre and made possible by the financial support of the Science Research Council and Ferranti Ltd.

References

1. LIBOIS, L.J. : 'Un Nouveau Procédé de Modulation Codée - la Modulation en Δ ', L'écho des Recherches, Avril, 1951, pp. 8 - 15.
2. ABATE, J.E. : 'Linear and Adaptive Delta Modulation', D.Sc. Thesis, Newark College of Engineering, New Jersey, 1967.
3. ZETTERBERG, L.H. : 'A Comparison between Delta and Pulse Code Modulation', Ericsson Technics, 1955, Vol. 2, No. 1, pp. 95 - 154.
4. LENDER, A. and KOZUCH, M. : 'Single-bit Delta Modulating Systems', Electronics, 1961, Nov. 17, pp. 125 - 129.
5. BULLINGTON, K. and FRASER, J.M. : 'Engineering Aspects of TASI', Bell System Technical Journal, 1959, Vol. 38, pp. 353 - 364.
6. WIENER, N. : 'Extrapolation, Interpolation and Smoothing of Stationary Time Series', (M.I.T. Press, Cambridge, Massachusetts) 1949.
7. SHANNON, C.E. : 'The Mathematical Theory of Communication', Bell System Technical Journal, 1948, Vol. 27, July pp. 379 - 423 and October pp. 623 - 656.

8. DUNN, H.K. and WHITE, S.D. : 'Statistical Measurements on Conversational Speech', J. Acoust. Soc. Am., 1940, Vol. 11, pp. 278 - 288.
9. Reference 7. Section 20.5.
10. McDONALD, R.A. and SCHULTHEISS, P.M. : 'Information Rates of Gaussian Signals under Criteria Constraining the Error Spectrum', Proc. IEEE, 1964, April, pp. 415 - 416.
11. WATTS, D.G. : 'A study of Amplitude Quantization with Applications to Correlation Determination', Ph.D. Thesis, Imperial College of Science and Technology, London, January 1962.
12. JOLLEY, L.B.W. : 'Summation of Series', (Dover Publications Inc.) 1962. Series (1133).
13. BENNETT, W.R. : 'Spectra of Quantized Signals', Bell System Technical Journal, 1948, Vol. 27, July pp. 446 - 472.
14. DE JAGER, F. : 'Deltamodulation, a Method of PCM Transmission using the 1 - Unit Code', Philips Research Reports, 1952, Vol. 7, pp. 442 - 466.
15. VAN DE WEG, H. : 'Quantizing Noise of a Single Integration Delta Modulation System with an N - Digit Code', Philips Research Reports, 1953, Vol. 8, pp. 367 - 385.

16. HALIJAK, C.A. and TRIPP, J.S. : 'A Deterministic Study of Delta Modulation', IEEE Int. Convention Record, 1963, Part 8, pp. 247 - 259.
17. ELIAS, P. : 'Predictive Coding', Ph.D. Thesis, Harvard University, Massachusetts, May 1950.
18. Reference 6. Section 3.2
19. RALSTON, A. and WILF, H.S. : 'Mathematical Methods for Digital Computers', (John Wiley & Sons Inc., New York) 1960. Sec. 21.
20. LEE, Y.W. : 'Statistical Theory of Communication', (John Wiley & Sons Inc., New York) 1960.
21. FANO, R.M. : 'The Transmission of Information', (M.I.T. Press, Cambridge, Massachusetts) 1961.
22. HUFFMAN, D.A. : 'A Method for the Construction of Minimum Redundancy Codes', Proc. IRE, 1952, Vol. 40, pp. 1098 - 1101.
23. BRAUN, W. et al : 'Delta - Multiplex for Long Troposcatter Links', IEEE International Convention Record, 1965, Part 2, pp. 62 - 76.
24. GOLOMB, S.W. : 'Run-length Encodings', IEEE Transactions on Information Theory, 1966, Vol. IT-12, No. 3, July, pp. 399 - 401.
25. FRY, T.C. : 'Probability and its Engineering Uses', (D. Van Nostrand Co., New York) 2nd Edition, 1965, pp. 354 - 410.

26. BLASBALG, H. and VAN BLERKOM, R. : 'Message Compression',
IRE Transactions on Space Electronics and Telemetry,
1962, Vol. SET-8, September, pp. 228 - 238.
27. MOLINA, E.C. : 'Application of the Theory of Probability
to Telephone Trunking Problems', Bell System
Technical Journal, 1927, Vol. 6, July, pp. 461 - 494.
28. Reference 12. Series (39).
29. TANAKA, Y., YAMASHITA, K. and HOSOKAWA, S. : 'A New
Decoding Method of Delta Modulation Code, taking
the Redundancy of Codes into Consideration', Mem.
Fac. Engineering, Osaka City University, 1963,
Vol. 5, December, pp. 43 - 55.
30. HANCOCK, J.C. and WINTZ, P.A. : 'Signal Detection Theory',
(McGraw-Hill Book Co. Inc., New York) 1966.
31. LAWSON, J.L. and UHLENBECK, G.E. : 'Threshold Signals',
(M.I.T. Rad. Lab. Series, Vol. 24, McGraw-Hill
Book Co. Inc., New York) 1950.
32. RICE, S.O. : 'Mathematical Analysis of Random Noise, Pt. 3',
Bell System Technical Journal, 1945, Vol. 24,
January, pp. 46 - 108.